Structural and Functional Characterization of the SUMO Proteases SENP6 and SENP7

Kamela Olivya Alegre

Universitat Autonoma de Barcelona

"There are two ways you can live your life. One is as though nothing is a miracle. The other is as though everything is a miracle."

Albert Einstein

Structural and Fumctional Analysis of the SUMO Proteases SENP6 and SENP7

Doctoral thesis presented by Kamela Olivya Alegre for the degree of PhD in Biochemistry from the University Autonomous of Barcelona

Institute of Biotecnology and Biomedicine, Protein Structure laboratory. Thesis supervised by Dr. David Reverter.

Kamela Alegre David Reverter

INDEX

ABBREVIATIONS

AMP	adenosine mono-phosphate
ATP	adenosine triphosphate
BME	β-mercaptoethanol
C	concentration
CaCl2	calcium chloride
CD	Circular Dichroism
cDNA	complementary DNA
cm	centimeter
D20	deuterated water
Da	Dalton
DPN1	restriction enzyme used to cut circular DNA
DTT	dithioreital
E. coli	Escherichia coli
FTIR	Fourier Transform Infrared
g	gravitational acceleration factor
Gel-Doc	gel documentation system
GTP	guanosine triphosphate
h	hour
Hepes	4-(2-hydroxyethyl)-1-piperazineethanesulfonic acid
IPEGAL	octylphenoxypolyethoxyethanol
IPTG	isopropyl-β-D-thioga-lactopyranoside
kcat	catalytic constant
kDa	kilodalton
Km	Michaelis-Menten constant
LB	Luria-Bertani
MALDI-TOF	matrix assisted laser-desorption ionization time-of-flight
mg	milligram

mg/ml	milligram per milliliter
MgCl2	magnesium chloride
min	minute
ml	milliliter
mM	millimolar
mut/m	mutant
NaCl	sodium chloride
Ni-NTA agarose	nickel-charged affinity resin
nm	nanometer
nM	nanomolar
NMR	nuclear magnetic resonance
PCR	polymerase chain reaction
pH	hydrogen potential representative of acid/alkaline balance
PNK	polynucleotide kinase
PPi	a diphosphate molecule
SDS	sodium dodecyl sulfate
SDS-PAGE	sodium dodecyl sulfate polyacrylamide gel electrophoresis
TFA	trifluoroacetric acid
Tris	tris(hydroxymethyl)aminomethane
Tris-HCl	tris hydrochloric acid
Tween-20	Polysorbate 20
UV	ultraviolet
WT	wild type
µM	micromolar
µmol	micromole

General Introduction

The Ubiquitin System: Ubiquitin and Ubiquitin-like Proteins

Introduction to Ubiquitin

Ubiquitin, named thusly for its "ubiquitous" presence in all eukaryotic living organisms, is a post-translational modifier that was discovered in 1975 as an 8.5kDa protein of unknown function (Schlesinger *et al*, 1975). Two years later it was isolated as part of A24 protein found in chromatin in conjunction with histone (Hunt *et al*, 1977). Ubiquitin was linked to histone via an isopeptidic bond between the C-terminal tail of ubiquitin and the ε-amino lysine of Lys119 of histone and thus the first function of ubiquitin was elucidated – as a protein modifier (Goldknoph and Busch, 1977). In the following years, ubiquitin's role in intracellular proteolysis was uncovered and eventually it was identified as a protein tag that targets proteins for the proteasome, a large protein complex that degrades and recycles extraneous proteins (Ciechanover *et al* 1978; Herschko *et al* 1980). The Nobel Prize was awarded in 2004 to Aaron Ciechanover, Avram Hershko and Irwim Rose for their role in the "discovery of ubiquitin-mediated protein degradation" (www.nobelprize.org). Protein degradation was believed to occur in lysozomes but in 1977 non-lysozomal protein degradation was observed in rabbit reticulocytes, precursors of erythryocyes, which lack lysosomes (Etlinger and Goldberg, 1977). Further research revealed a cytosolic protein that, in an ATP-dependent manner, was responsible for the destruction

of abnormal rabbit reticulocytes and this protein was later revealed to be ubiquitin (Etlinger and Goldberg, 1997; Wilkinson *et al*, 1980). Glycine 67 in the C-terminal tail of ubiquitin was subsequently identified as the residue conjugated to substrate lysine residues (Chau *et al*, 1989)

Ubiquitin is a small protein consisting of 76 amino acids with a molecular mass of 8433 Da. Key characteristics of ubiquitin include a C-terminal tail and 7 lysine residues. It is highly conserved among eukaryotes, with yeast and human ubiquitin sharing 96% sequence identity. While ubiquitin and ubiquitin-associated machinery have not been found in prokaryotes it is believed to have been descended from prokaryotic proteins similar to ThiS (Wang *et al*, 2001). ThiS is a sulfur carrier protein involved in thiamine biosynthesis in *Escherichia coli* and while it shares only 14% sequence identity with ubiquitin, it contains the ubiquitin fold. In the case of ThiS, this fold is employed as a sulfur carrier in the ATP-dependent sulfurylation of cofactors while in ubiquitin it is employed as a covalent modification in ATP-dependent protein conjugation (Wang *et al*, 2001).

Ubiquitin is a very stable protein whose structure has been shown to withstand extreme values of pH, temperature and proteolysis (Ramage *et al*, 1975 Ibarr-Molero *et al*, 1999). Its globular structure contains no disulfide bonds, coordinated metal ions or binding cofactors lending its stability to mostly hydrogen bonds (Briggs and Roder, 1992; Khorasanizadeh *et al*, 1993). Ubiquitin has a compact secondary structure which contains three and one-half turns of α-helix, a 3_{10} helix (a helix with three residues per turn instead of 3.6 for α-helices),

a mixed β-sheet that contains five strands and seven reverse turns (Vijay-Kuman *et al*, 1987). This fold is commonly referred to as the ubiquitin-like fold.

Mechanism and enzyme cascade

Ubiquitination occurs when the C-terminal glycine of ubiquitin is conjugated to the recipient epsilon lysine of a substrate protein, resulting in an isopeptide bond. This enzymatic process involves a series of steps, the first of which is the ATP-driven activation of Gly76 to the active site cysteine residue of E1 enzyme, forming a high-energy thioester bond and releasing PP_i and AMP (Figure 1). Once activated, the ubiquitin is transferred to the sulphydryl cysteine residue of ubiquitin-conjugating enzyme E2, producing a thioester bond between E2 and ubiquitin and releasing E1 enzyme. The last step involves E3 enzyme, which is known as ubiquitin-ligase. It essentially modulates the interaction between ubiquitin and the substrate molecule by recognizing the target protein and facilitating the transfer of ubiquitin from the cysteine in E2 to the receptor lysine in the substrate. The end result of this cascade can result in either the proteasome-mediated degradation of the ubiquitinated protein or alteration of the proteins signaling pathway.

Ubiquitin conjugation machinery

The human genome comprises eight genes encoding ubiquitin E1 and ubiquitin-like activating enzymes. The E1 activity represents an essential step

during the ubiquitnation pathway and the reaction is well established due to early work with the ubiquitin-E1 or Ub-E1 complex (Hass and Rose, 1982; Hass *et al*, 1982; Herschko *et al*, 1983). The E1 for ubiquitin is a 110-120 kDa monomeric protein and Ub-E1 consists of four domains. There are crystal structures of the intact ubiquitin E1 catalytic domain, the individual domains and various complexes of the domains in complex with other proteins (Lee and Schindelin, 2008; Huang *et al*, 2004; Huang *et al*, 2005; Huang *et al*, 2007; Lake *et al*, 2001; Walden *et al*, 2003; Lois and Lima, 2005). While ubiquitin E1s do not have much variability due to the fact they only interact with ubiquitin, both E2 and E3 encompass large families of proteins, each enzyme specific to a different substrate protein.

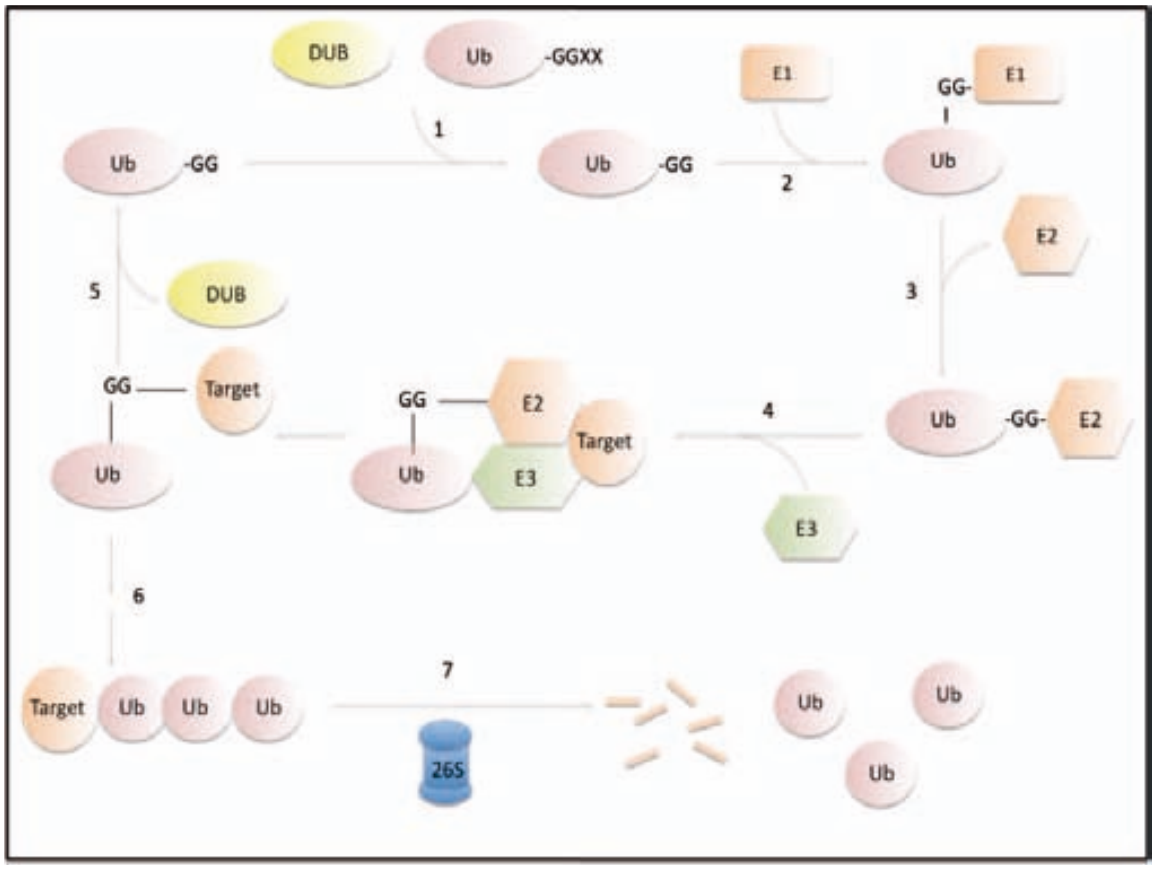

Figure 1. The ubiquitin conjugation pathway. Immature ubiquitin is activated by ubiquitin-specific proteases or *de-ubi*quitinating proteases to reveal a C-terminal double Gly-Gly motif (1). Once cleaved ubiquitin is activated by the adenylation of the C-terminal glycine residue by the E1 activating enzyme in an ATP•Mg^{2+}-dependent step. This results in the relaease of PP_i and ADP. The resultant E1-AMP is then attacked by an activated sulfhydryl residue on E1 and forms a high-energy thioester bond (2). Following activation ubiquitin is then transferred to a recipient cysteine residue on ubiquitin-conjugating enzyme or E2 (3). E2 then catalyzes ubiquitin conjugation in an E3-dependent manner through substrate recognition and conjugation to a receptor lysine residue (4). Ubiquitin can be removed from conjugated substrates through the action of DUBs (5). Alternatively a poly-ubiquitin chain can form through repeated ubiquitinations to form a multi-ubiquitin chain (6). Poly-ubiquitinated chains serve as a recognition signal for degradation by the 26S proteasome (7).

Once ubiquitin is covalently attached to an E1 active site cysteine, E2s are then recruited to transfer the E1-Ub thioester adduct to the conserved E2 cysteine to form an E2-Ub thioester adduct. The mammalian genome consists of 35

enzymes of this class and following conjugation to E2, ubiquitin can either be transferred directly to the epsilon lysine of an acceptor substrate or allocate an E3 ligase to faciliate transfer to the substrate protein. E2s share a conserved ~150 residue catalytic domain (UBC), which contains the main interfaces for E1 and E3 and the catalytic cleft, which accommodates the thioester bond with ubiquitin. There are currently ~100 structures of E2 enzymes in the PDB, over half of which are human E2s. While most of the structures are of the catalytic domain of E2, there are structures of E1-E2 complexes, E2-E3 complexes, E2 in complex with ubiquitin enzyme variants and E2 non-covalently bound to Ub proteins (Khorasanizadeh *et al*, 1993; Huang *et al*, 2004; Huang *et al*, 1999; Zheng *et al*, 2000; Moraes *et al*, 2001; Sundquist *et al*, 2004; Capili and Lima, 2007; Duda *et al*, 2007).

E3 ubiquitin ligase works in conjunction with E2 conjugating enzyme to direct ubiquitin to one or more lysines of a target protein. The overall chemical reaction of an ubiquitin-protein ligase is the following:

ATP + ubiquitin + protein lysine $\rightleftharpoons$ AMP + diphosphate + protein N-ubiquityllysine

The substrates in this reaction are ATP, ubiquitin and a substrate lysine while the products are AMP, a diphosphate molecule and an N-ubiquitinnated protein lysine.

The anaphase-promoting complex (APC) and the SCF complex (Skp1-Cullin-F-box protein complex) provide two examples of the common scaffold E3s

use to both recognize and ubiquitinate target proteins (Figure 2). Each complex contains an E2 binding domain and a substrate recognition and binding domain.

As E3s direct the specificity of the ubiquitination system, an organism would normally contain a large amount of E3s in comparison with E1s and E2s. The human genome, for example, is estimated to encode over 600 E3s (Li *et al*, 2008). Two types of E3s are commonly found: The RING (*R*eally *I*nteresting *N*ew *G*ene) type and the HECT type. Most human E3s are of the RING types (~95%), while only 28 belong to the HECT types (Li *et al*, 2008), though smaller families (U-box, plant homology domain and zinc finger) have been described.

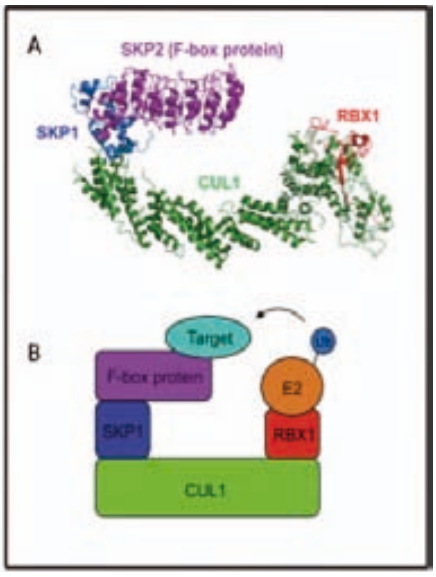

Figure 2. Structure of the SCF complex. Top panel, A, the crystal structure of the yeast SCF^{SKP2}complex (Zheng et al, 2002; Hao et al, 2005; assembled from Protein Data Bank files 1LKD and 2ASS). Bottom panel, B, cartoon of the SCF complex. The N-termianl half of the C-terminal half of CUL1 intersts with SKP1 and RBX1 respectively. RBX1 serves as a docking site for an E2 enzyme. An F-box protein interacts with SKp1 via its F-box domain and recruits the target protein to the ubiquitin ligase complex (Magori and Citovsky, 2011)

RING finger domains are protein structural domains of the zinc finger type containing a $Cys_3HisCys_4$ amino acid motif, which binds two zinc ions. This domain contains from 40-60 amino acids and contains the consensus sequence:

$$\mathbf{C}\text{-}X_2\text{-}\mathbf{C}\text{-}X_{[9\text{-}39]}\text{-}\mathbf{C}\text{-}X_{[1\text{-}3]}\text{-}\mathbf{H}\text{-}X_{[2\text{-}3]}\text{-}\mathbf{C}\text{-}X_2\text{-}\mathbf{C}\text{-}X_{[4\text{-}48]}\text{-}\mathbf{C}\text{-}X_2\text{-}\mathbf{C}$$

where C is a conserved cysteine residue involved in zinc coordination, H is a conserved histidine residue involved in zinc coordination, Zn is a zinc atom and X is any amino acid residue (Borden and Freemont, 1996). RING fingers are subcategorized into RING-HC and RING-H2 depending on whether a Cys or His occupies the fifth coordination site, respectively. In contrast to the tandem arrangement of zinc binding sites characteristic of zinc fingers, RING-HC fingers show interweaved zinc binding sites (Freemont, 2000). Some RING-type E3s are known to form heterodimers, such as BRCA1-BARD1, while others such as RNF4 act as homodimers (Brzovic *et al*, 2001; Liew *et al,* 2010). While the mechanism of RING-type E3 ligase activity is still under investigation due to the sheer numbers of RING-type E3s and E2s and all the possible chemical strategies, their ligase activity lies in their ability to directly bind E2s that are thioesterified with ubiquitin and activate these E2s to unload their ubiquitin cargo to substrate proteins.

A HECT or *H*omologous to the *E*6-AP *C*arboxyl *T*erminus domain, is a ~350 amino acid domain found at the C-terminal of proteins. This type of E3 ligase accepts ubiquitin from E2 conjugating enzyme in the form of a thioester bond to a conserved cysteine residue within the HECT domain. HECT E3s can

be divided into 3 groups based on the N-terminal architecture: the Nedd4 family (9 members), the HERC family (6 members) and the other HECTs (13 members)(Rotin and Kumar, 2009). The Nedd4 family members contain an N-terminal C2 domain, two to four WW domains and a C-terminal HECT domain. Members of the HERC family contain one or more regulator of chromosome condensation 1 (RCC1)-like domains plus a HECT domain. Members of the last group contain a HECT domain along with one or more of several architecturally distinct domains (Rotin and Kumar, 2009). Despite a common HECT domain, the various HECT family members are functionally distinct.

Introduction to SUMO

Since the discovery of ubiquitin in the mid-1970s an entire family of small ubiqiutin-related proteins have emerged, with new members still being added. These ubiquitin-like proteins (UBLs), while functionally distinct, all share the ubiquitin or β-grasp fold and target cellular targets in a pathway parallel to that of ubiquitin (Figure 3). These include, but are not limited to, small ubiquitin-like modifier (SUMO), neuronal-precursor-cell-expressed developmentally downregulated protein-8 (NEDD8), fau ubiquitin-like protein (FUB1) and ubiquitin-related modifier-1 (URM1). Of those protein systems, the SUMO pathway has been studied the most.

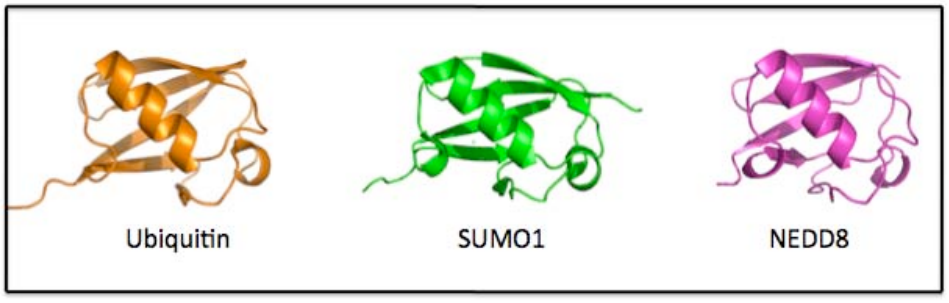

Figure 3. Structural comparison of Ub and Ubls. SUMO1 and NEDD8 share the hallmark β-grasp fold of ubiquitin-like proteins. Images modified from pdb1ubq, pdb2uyz and pdb1ndd taken from Protein Data Bank.

SUMO proteins are small, most around 100 amino acids in length and around 12 kDa in mass. SUMO shares only 18% sequence homology with ubiquitin and was discovered in mammals covalently linked to GTPase activating protein RanGAP1 (Matunis *et al*, 1996; Mahajan *et al*, 1997). The number of SUMO isoforms is species-specific, with lower eukaryotes such as yeast and insects encoding one SUMO gene while *Arabidopsis* contains genes encoding for eight SUMO isoforms (Kurepa *et al*, 2003). In humans there are four SUMO paralogs: SUMO1 (also known as Smt3c, PIC1, GMP1, sentrin and Ubl1), SUMO2 (also known as Smt3a and Sentrin3); SUMO3 (also known as Smt3b and Sentrin2); and SUMO4. SUMO2 and -3 share 95% sequence identity and are commonly referred to as SUMO2/3, while SUMO1 shares only 50% sequence identity with either of the two. SUMO4 shares 87% sequence identity with SUMO2 but it still remains unknown whether SUMO4 is processed or conjugated to cellular proteins (Owerbach *et al*, 2005).

As previously mentioned the SUMO pathway is analogous to that of ubiquitin, represented by an enzyme cascade resulting in the conjugation of SUMO to the epsilon lysine of a target protein (Johnson, 2004)(Figure 4). SUMO is first activated by a SUMO-specific protease to expose a C-terminal di-glycine residue. Once activated the mature SUMO is adenylated by SUMO E1 enzyme and the SUMO adenylate is then attacked by the E1 cysteine to form an E1-SUMO thioester. SUMO is then transferred to a conserved Cys on SUMO E2 enzyme generating an E2-SUMO thioester. This E2-SUMO moiety can interact

directly with the substrate or recruit an E3 ligase to facilitate transfer of SUMO to the substrate lysine. In contrast to ubiquitin, SUMO utilizes only one E1 enzyme, the heterodimer Sae1/Sae2 in humans, one E2 enzyme, Ubc9 in humans, and only a few E3 ligases. While the SUMO conjugation reactions can be replicated *in vitro* using only E1, Ubc9, SUMO and ATP, E3 is virtually indispensible in yeast SUMOylation reactions and SUMO E3 factors have been identified that facilitate conjugation *in vivo* and *in vitro* in humans (Johnson, 2004; Stelter and Ulrich, 2003; Tatham *et al* 2001).

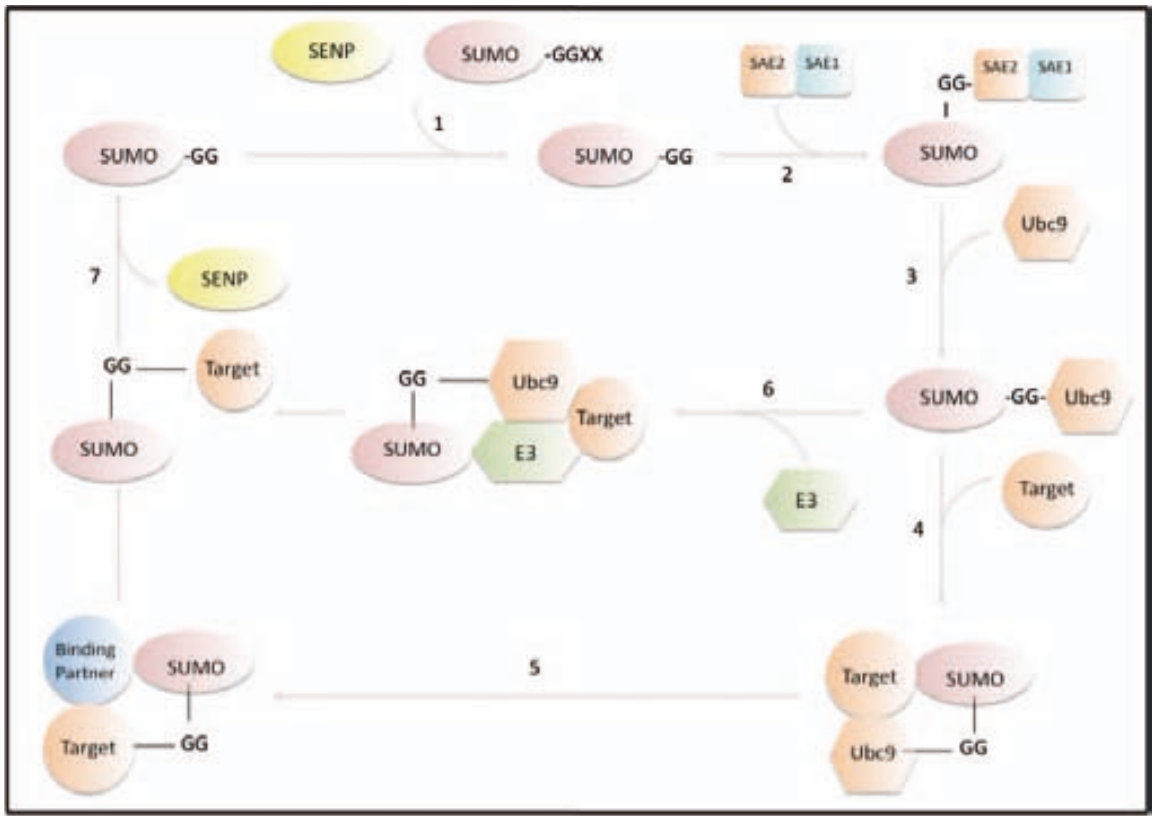

Figure 4. The SUMO conjugation pathway. Immature SUMO is activated by SUMO-specific proteases or SENP proteases to reveal a C-terminal double Gly-Gly motif (1). Once cleaved SUMO is activated by the adenylation of the C-terminal glycine residue by the SAE1 subunit of the SAE1/SAE2 heterodimer in an ATP•Mg^{2+}-dependent step. This results in the release of PP_i and ADP. The resultant E1-AMP is then attacked by an activated sulfhydryl residue on the SAE2 subunit of E1 and forms a high-energy thioester bond (2). Following activation SUMO is then transferred to a

recipient cysteine residue on SUMO-conjugating enzyme 9 (Ubc9) or E2 (3). E2 can then catalyze SUMO conjugation in an E3-independent manner through the recognition of the SUMO consensus motifs (ψKXE) that contain a receptor lysine residue (4). Substrates modified by SUMO can contact SUMO-binding partners through their interaction with *S*UMO-*I*nteracting-*M*otifs or SIMs (5). Alternatively the E2~SUMO thioester can interact with a SUMO E3 ligase which can coordinate SUMO conjugation to the target substrate either through indirect (as is the case for RanBP2) or direct (as is the case for Siz and PIAS E3 ligases) contact with the substrate (6). Deconjugation is performed by SENP proteases and free SUMO can then be recycled for another round of conjugation (7).

SUMO conjugation machinery

While ubiquitin E1 exists as a monomer, SUMO E1 exists is a heterodimer, though both individual components are related to the ubiquitin enzyme; the Sae1 subunit (also called Aos1) of SUMO E1 resembles the N-terminal of ubiquitin E1 while the Sae2 subunit (also called Uab2), where the catalytic cysteine is located, resembles the C-terminal (Azuma *et al* 2001). Structural analysis of E1 heterodimer revealed that SUMO interacts exclusively with subunit Sae2, and Ubl recognition may be dependent on conserved residues within this subunit (Tong *et al* 1997). Though SUMO1 E1 enzyme exists as two distinct subunits, the individual components are only found as part of the heterodimer within the cell.

The SUMO E2, Ubc9, also shares sequence similarity with its ubiquitin counterpart and the two enzymes share essentially the same folded structure (Rodriguez *et al*, 2001). Ubc9 also shows a strong, unique overall electrostatic

dipole, which might contribute to its ability to recognize and conjugate SUMO to its substrates without the help of E3 ligases. SUMO E2 specifically recognizes substrates containing the motif ψKxE/D, where ψ is a large hydrophobic residue, K is the acceptor lysine and x is any amino acid (Rodriguez *et al*, 2001). SUMO E2 makes direct contact with this motif and structural analyses of the E2 in complex with SUMO substrates have revealed a hydrophobic pocket on E2 that accommodates the acceptor lysine, with residues immediately flanking this lysine also facilitating substrate recognition via hydrogen bonding and electrostatic interactions with the surface of E2 (Bernier-Villamor *et al,* 2002; Sampson *et al*, 2001).

In general there are three types of E3 SUMO ligases: those belonging to the Siz/PIAS (protein inhibitor of activated STAT) family; those containing a domain in the large vertebrate nuclear protein RanBP2/Nup358; and the polycomb group protein Pc2 (Jackson, 2001; Hochstrasser, 2001; Shuai, 2000; Kagey *et al*, 2003; Kalman *et al*, 2002). The members PIAS family of proteins all share a ~400 residue N-terminal domain that contains smaller regions of similarity but more importantly it contains a SP-RING domain thought to function in a manner analogous to the ubiquitin RING E3 ligases by providing a scaffold for conjugation by bringing Ubc9 and the substrate together. This family includes Siz1, Siz2 and methyl methanesulphonate-sensivity protein 21 (Mms21) in yeast and PIASxα, PIASxβ, PIASy and Nse2 in humans (Kotaja *et al*, 2002; Andrews *et al,* 2005).

The RanBP2 ligase consists of a ~300 residue domain called the IR (internal repeat) and can be found in the core protein RanBP2 (Kalman *et al*, 2002). This domain contains two internal repeats of a ~50 residue sequence which not only function as SUMO ligases but are also responsible for localizing RanGAP1-SUMO to the nuclear pore (Matunis *et al*, 1998). While the RanBP2 and PIAS seem to have non-redundant cellular functions with some substrates are only SUMOylated exclusively by one ligase or the other there have been cases where SUMOylation can be induced by both (Kannouch *et al*, 2004, Sobko *et al,* 2002; Miyauchi *et al* , 2002).

The polycomb group (PcG) protein Pc2 is the last group of reported SUMO E3 enzymes. In humans, these proteins form large multimeric complexes (PcG bodies), which are involved in the stable maintenance of transcriptional repression and Pc2 has been shown to induce SUMOylation of various types of proteins within this pathway (Schuettengruber *et al*, 2007; Ringrose, 2007; Satijn *et al*, 1997; Jacobs *et al*, 2002). Moreover over expression of Pc2 in cells causes SUMO and Ubc9 to localize to PcG bodies, suggesting that PcG bodies may be major sites of SUMOylation.

In addition to the aforementioned SUMO consensus motifs, the SUMO conjugation machinery also makes use of SIMs or *S*umo *I*nteraction *M*otifs, to help recognize SUMO. SIMs are generally characterized by a hydrophobic core (V/I)X(V/I)(V/I), flanked at either its N or C terminus by acidic amino acids (Hecker *et al*, 2006). When in complex with SUMO, the SIM adopts a parallel or

anti-parallel β-strand conformation, which allows the hydrophobic side chains of the SIM to occupy a hydrophobic pocket on the SUMO surface (Reverter and Lima, 2005). SUMO E3s, such as those containing the Ran-binding protein 2 (RanBP2) domain and those belonging to the Siz/PIAS family of E3 ligases, are known to have both E3 ligase elements as well as SIMs (Rytinki *et al*, 2009; Pichler *et al*, 2004). Of the SIM-containing E3 ligases that have been characterized, some display substrate preferences, such as those mentioned above, while others show preference for specific SUMO isoforms, such as in the case of ubiquitin-specific protease 25 (USP25) and transcriptional regulator COREST1, which both exhibit a preference for SUMO2/3ylation (Meulmeester *et al*, 2008; Ouyang *et al*, 2009).

SUMO isoforms

Although SUMO1 and SUMO2/3 share the same overall structure and essentially the same conjugation machinery, the different SUMO isoforms seem functionally distinct; some substrates can be exclusively modified by SUMO1 or SUMO2/3 whereas others can be modified by both SUMO isoforms (Vertegaal *et al*, 2006; Ayaydin and Dasso, 2004). Another important difference between SUMO1 and SUMO2/3 is that SUMO2/3 has the ability to form polymeric chains

due to an N-terminal lysine residue while SUMO1 cannot (Tatham *et al*, 2001). SUMO4, on the other hand, is both structurally and functionally distinct than either SUMO1 or SUMO2/3. In contrast to SUMO1 and SUMO2/3, SUMO4 is only expressed in limited tissues, and SUMO4 mRNA was mainly detected in kidney and human embryonic kidney (HEK) cells (Kurt *et al*, 2004). In SUMO4 there is also a polymorphism, SUMO4-M55V, which is not reported in any other human SUMO member and has been shown to be associated with type-1 diabetes (Guo *et al*, 2004). This methionine is conserved not only within the SUMO family but also across species, so it could hypothesized that the M55V polymorphism, with an allelic frequency of 0.51 in a Caucasian test population, could provide a biologically relevant function in this molecule (Kurt *et al,* 2004).

Cellular Functions

In vertebrate cells SUMO localizes to the nucleus and concentrates at nuclear pore complexes and PMLs (Johnson, 2004). While the vast majority of SUMO1 exists in conjugated species, there is usually a free pool of SUMO2/3 species in cells (Saitoh and Hinchey, 2000). SUMO2/3 is strongly induced in response to *in vivo* heat shock and oxidative stress and is thought to provide cells with a SUMO reservoir in response to cellular stresses (Bossis and Melchior, 2006). Due to the fact that SUMOylation is both a dynamic and reversible process, it has been hard to follow *in vivo* and relies mostly on identification of SUMO substrates; since its discovery in 1996, more than three hundred SUMO

substrates have been identified and it has been implicated in a wide range of cellular processes including but not limited to: nuclear transport, DNA repair, DNA transcription and the cell-cycle.

SUMO was originally discovered as a post-translational modifier when it was isolated while conjugated to RanGAP1, the most abundant SUMO1 substrate in vertebrates (Matunis *et al*, 1996; Mahajan *et al*, 1997). Ran GTPase-activating protein RanGAP1 is highly associated near the nuclear pore complex (and, consequently, so is SUMO), where it associates with the 358kDa protein RanGTP-binding protein RanBP2. RanGAP1 modification by SUMO1 sequesters the cytosolic RanGAP1 to the filaments protruding from the nuclear pore complex. Here the RanGAP1-SUMO1 complex interacts with RanBP2, forming a complex that is essential for nuclear protein import (Mahajan *et al*, 1997). Aside RanGAP1, SUMO also modulates the nuclear trafficking of a proteins implicated in a variety of cellular processes such as transcriptional regulation (CREB, HIPK2), signaling transmission (IGF-1R, DdMER1) and tumor suppression (p53, VHL) (Comerford *et al*, 2003; Kim *et al*, 1999; Sehat *et al*, 2010; Sobko *et al*, 2002; Nakamura *et al,* 2002; Cia and Robertson, 2010).

In the context of DNA repair SUMO has been shown act antagonistically, able to both recruit and repel various binding factors. For example, SUMOylation of Lys 164 on proliferating cell nuclear antigen (PCNA) results in the recruitment of Srs2, a helicase-like enzyme, which prevents unwanted recombination at the replication fork (Papouli *et al*, 2005, Pfander *et al,* 2005).

When SUMO binds to Lys 127 on PCNA, which lies in the proteins PIP-box (PCNA interacting proteins-box), it occupies the binding pocket also reserved for other proteins, such as Eco1, a protein that establishes sister-chromatin cohesion in S-phase, and thus inhibits their binding (Hoege *et al*, 2002; Moldavan *et al*, 2006; Armstrong *et al,* 2011).

In regard to gene expression, the general trend for SUMO has been that it, in conjunction with various transcription factors, acts as an overall repressor of DNA transcription. Mutational analysis that prevents SUMO binding to such transcription factors as Sp3, to the androgen receptor and the co activator p300 show an overall increase in transcription, thus confirming the negative role of SUMO in gene transcription (Sapetschnig *et al*, 2002; Poukka *et al*, 2000; Girdwood *et al*, 2003). SUMO binding to Sp3 regulates transcription by establishing formation of localized heterochromatin-like silenced states through the recruitment of various heterochromatin-related proteins and the establishment of repressive histone modifications (Sapetschnig *et al*, 2002). SUMOylation of androgen receptor (AR), a ligand-activated transcription factor belonging to the steroid family receptor superfamily, at the N-terminal region, which is involved in interactions with the hormone-bound and ligand-binding domain, obstructs this domain and is thus likely to perturb the ability of AR to make intramoleculer interactions which might otherwise lead to DNA transcription (Poukka *et al*, 2000). P300 is a transcriptional coactivator which, when SUMO-bound, recruits histone deacetylase (HDAC) to set of promoters

that are susceptible to p300-mediated transcription and this subsequent deacetylation of core histones which strengthens the association of DNA with histones, making DNA less susceptible to transcription (Girdwood *et al*, 2003).

Another way SUMO effects transcription is through the formation of PML nuclear bodies. PML bodies or promyelocytic leukemia nuclear bodies are subnuclear structures that harbor both transient and permanent proteins, also referred to as "nuclear dots", "nuclear bodies" or "nuclear domains" due to the fact they were first identified as prominent interchromatin structures in the nuclei (Negorev and Maul, 2001; Brasch and Ohs, 1992). At the core of these nuclear bodies is the promyelocytic leukemia protein, a member of the TRIM family of proteins implicated in tumor suppression and DNA transcription (Salomoni and Pandolfi, 2002; Bernardi *et al*, 2006). PML is SUMOylated at three locations, Lys65, Lys 160 and Lys490 and nuclear body formation requires both the covalent conjugation of SUMO as well as interaction with SUMO through a SUMO binding domain (Shen *et al*, 2006). Patients with promyelocytic leukemia present a mutated version of this protein, a fusion protein with PML protein fused to retinoic-acid receptor α. Retinoic-acid receptor α obstructs the SUMOylation sites on PML and thus disrupts the normal formation of PML nuclear bodies (Duprez *et al*, 1999). SUMOyation is crucial to maintaining the structural and functional integrity of PML nuclear bodies and therefore is integral to the myriad of protein interactions that rely on stability of PML nuclear bodies.

SUMO also plays a role in the structural maintenance of higher-order cellular structures such as kinetechores. Kinetechores are proteinaceous structures located on chromatin which attach mitotic spindle fibers during mitosis and meiosis. Mitosis-dependent SUMOylation has been detected on outer kinetochore proteins, such as CENP-E, whose translocation to kinetechores is dependent on the non-covalent binding of SUMO2/3 (Azuma *et al*, 2003). SUMOylated proteins were also detected in the inner centromeric region, the region that lies between the centrome and the kinetechore. Topoisomerase II (TopII) is one such protein that's SUMO2/3ylation regulates its ability to attach to chromatin during the metaphase-anaphase transition (Zauma *et al*, 2003). *S. cerevisiae* strains lacking the SUMO isopeptidase Ulp2 exhibit premature separation of a section of the chromosome near the centromere prior to mitosis and mutation of the SUMOylation sites in TopII to prevent SUMOylation restore the normal separation phenotype, suggesting that excess SUMOylation is responsible for the erroneous phenotype.

Lysine-liked Chains

Mono-ubiquitination and –SUMOylation result in the formation of an isopeptide bond between a substrate lysine and the C-terminal tail of a single ubiquitin or SUMO moiety, respectively. The existence of multiple lysine residues in both ubiquitin and SUMO, however, gives way to the possibility of poly-ubiquitin and poly-SUMO chains. Ubiquitin has seven lysine residues,

which could potentially serve as polyubiquitination sites, K48, K63, K6, K11, K27, K29 and K33. While polyubiquitin chain formation leading to proteasomal degradradation mainly occurs at K48, polyubiquitin chain formation at the other lysine residues have various, non-proteolytic effects. K63-linked ubiquitin chains, the second most characterized of the ubiquitin-linked chains, have been implicated in four signaling pathways: DNA damage tolerance, the inflammatory response, proteins trafficking and ribosomal protein synthesis (Ulrich, 2002; Spench *et al*, 2000; Stelter and Ulrich, 2003; Kannouche *et al*, 2004). The proteasome has been shown to recognize K6-linked polyubiquitin chains but seem to process them differently from K48-linked chains; chains are dismantled but the conjugated protein is not degraded, as is the case for the breast and ovarian cancer-specific tumor suppressor BRCA1 (Nichikawa, 2004). K11-linked chains. While the other lysine-linked chains is less understood novel chain formation *in vitro* is shedding light on the structure and function of the poly-ubiquitin moieties (Saeki *et al*, 2004; Baboshina and Haas, 1996).

Aside from ubiquitin, SUMO is the most characterized Ubl known to participate in polychain formation. Interestingly the major SUMOylation site, Lys11, is located in the N-terminal extension of SUMO not present in ubiquitin (Tatham *et al*, 2001)(Figure 5). This lysine is only found in SUMO2 and -3 and is located within the SUMO consensus motif ψKxE, present in both human SUMO and the yeast SUMO paralog, Smt3, which has also exhibited chain formation *in vivo* (Bylebyl *et al*, 2003; Johnson and Gupta, 2001). Interestingly the Smt3

consensus site lysines are all flanked at their C-terminal by proline residues, suggesting substrate-binding interface unique to those of Smt3 family. SUMO1 is also able to form poly-SUMO chains *in vitro*, though much less efficiently than SUMO2/3, via N-terminal non-consensus SUMOylation sites (Pichler *et al*, 2002). *In vivo* poly-SUMO chains containing SUMO1 mixed with SUMO2 and/or -3 have been observed, with chain formation occurring at internal lysine residues (Matic *et al*, 2008).

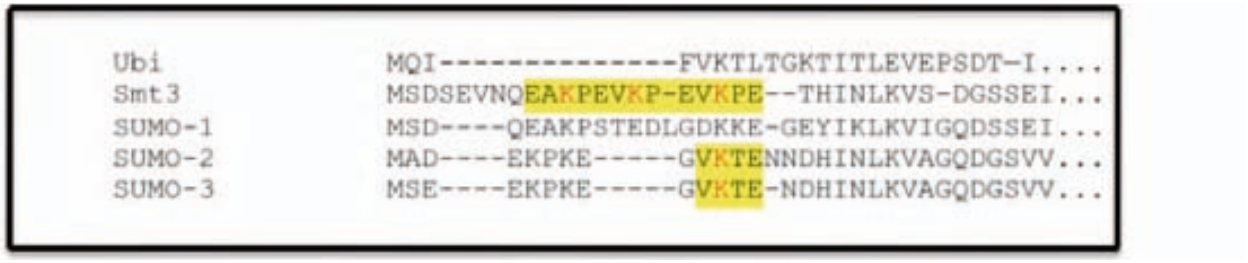

Figure 5. Sequence alignment of the ubiquitin, budding yeast Smt3 and the N-termini of human SUMO isoforms. Ubiquitin/SUMOylation motifs are *highlighted* and acceptor lysines are shown in *red*.

The mechanism for the formation of polySUMO chains has yet to be fully elucidated Capili and Lima have proposed a model suggesting that the formation of polySUMO chains relies in part on the ability of the E2-SUMO2 thioester to make non-covalent interactions with SIMs on incoming SUMOs (Capili and Lima, 2007). Mutation of Ubc9 surface residues that abrogated the ability of Ubs9 to interact through this non-covalent binding site showed stunted poly-SUMO chain growth, though it should be noted this could be attributed to disruptions between E1-SUMO2 binding interface due to the fact that the non-

covalent binding site partially overlaps with their tentative SUMO1 E1 interaction surface. The non-covalent SUMO binding interface is too far from the E2 active site to facilitate diSUMO formation through the N-terminal extension of SUMO2/3 but once formed the binding interface could serve as a dock for additional E2s thus permitting chain elongation.

SUMO E3s have an overall tendency to enhance polySUMO chains *in vivo,* but their promiscuity has been shown to lead to SUMOylation of non-consensus lysines (Bylebyl *et al*, 2003). Reactions containing a mutated version of Smt3 where the three N-terminal consensus lysines (K11, K15 and K19) were changed to arginine still resulted in the accumulation of high molecular weight species corresponding with polySUMO chains, meaning SUMOylation occurred at one or multiple non-consensus lysines. Under these reaction conditions, the *S. Cereviseia* E3 Siz1 was required for chain formation, but other groups have demonstrated that polySUMOylation can also occur when only E1 and E2 are present (Kalman *et al*, 2002; Takahashi *et al*, 2003).

Previously it was difficult to identify endogenous polySUMOylated substrates due to the inability to distinguish between polySUMO chains and multi-mono-SUMOylated substrates or to unanchored SUMO chains. So far transcriptional regulator HIF1α, PARP1, Top2, proliferating cell nuclear antigen (PCNA) and PML protein have been identified as polySUMO conjugates (Matic *et al*, 2008; Martin *et al*, 2009; Takahashi *et al*, 2003; Yeh *et al*, 2000). Recently however Bruderer and associates developed a method involving an inactive form

of the E3 ligase RNF4 to identify potential polySUMO substrates (Bruderer *et al*, 2011). An RNF4 fragment (residues 32-133) containing four SIMs that show low affinity for mono-SUMOylated substrates but high affinity for polySUMO chains was used as bait in an affinity chromatography column (Bruderer *et al*, 2011). Using this truncated version RNF4 they were able trap over 300 putative heat shock-induced polySUMOylated substrates. Their results indicate that proteins involved in the transcription and transcription regulation do no seem to be polySUMOylated upon heat shock whereas proteins involved in checkpoint response and DNA repair do.

Interestingly recent papers have suggested a role for polySUMO chains in the ubiquitin-mediated degradation pathway. *SLX5* (synthetic lethal of unknown function) and *SLX8* are genes in yeast that code for Slx5 and Slx8, respectively, two proteins that form a heterodimer and together function as an ubiquitin E3 ligase of the RING-type (Li *et al*, 2007). Inactivation of the genes associated with these proteins or blocking of ubiquitin-mediated proteolysis led to cells with an accumulation of SUMOylated proteins that corresponded to high molecular weight SUMO conjugates (Uzunova *et al*, 2007; Xie *et al*, 2007; Wang *et al*, 2006). These theories purport that this accumulation occurs due to the inability of these SUMO-substrate specific E3 ligases to ubiquitinate target proteins and hence target them for ubiquitin-mediated proteolysis. This theory is further exemplified by the fact that in their N-terminal domains they contain at least one SIM, which could modulate interactions between SUMO and Slx5-Slx8

(Prudde *et al*, 2007). RNF4 is the vertebrate homologue of Slx5 and Slx8 cells depleted of RNF4 show similar accumulations of high molecular weight SUMO conjugates (Bruderer *et al*, 2011). As mentioned before it contains multiple SIMs and *in vitro* studies show that it can ubiquitylate SUMO chains in a SIM-dependent manner thus proving it is a ubiquitin E3 ligase with a specificity for SUMO chains.

Introduction to Ubiquitin and SUMO Isopeptidases

The challenge of identifying polyUb or -Ubl substrates is exacerbated by the action of endogenous isopeptidases, which perpetually recycle the chains into their constituent molecules. These isopeptidases include but are not limited to DUBs (*DeUB*iquitinating) proteases, Ulps (*U*biquitin-*L*ike *P*rotein) proteases and SENPs (*SEN*trin *P*roteases). Each isopeptidase has two functions within the cell: the first is the activation of the Ub or Ubl through cleavage of its C-terminal tail to expose a di-glycine motif. It is this mature version of the protein that can then be conjugated to the acceptor lysine of a substrate protein; the second is the deconjugation of Ub or Ubl from conjugated substrate.

Deubiquitinating enzymes present the largest group of these enzymes, with over a hundred known proteases involved in regulation of ubiquitin-dependent pathways in humans and roughly twenty in *S. cerevisiae* (Amerik *et al*, 2004; Nijman *et al*, 2005). These proteases can be subdivided into two classes, cysteine proteases and metalloproteases. Within the class of cysteine proteases

there are four main superfamilies including: the ubiquitin-specific processing protease (USP/UBP) superfamily; the C-terminal hydrolyase (UCH superfamily); the ovarian tumor (OUT) superfamily; and the Machado-Josephin domain (MJD) superfamily.

The activity of cysteine proteases is dependent on the reactivity of an active site thiol group of a cysteine, together with histidine and aspartate, form the catalytic triad characteristic of cysteine proteases. Proteolysis is initiated when the aspartate residue polarizes an adjacent histidine, causing deprotonation of the active site cysteine. This activated thiol can then perform a nucleophilic attack on the carbonyl bond between a target and ubiquitin. This results in the release of the target and the formation an intermediate covalent bond between the protease and ubiquitin, which, when reacted with water, leaves free protease and ubiquitin. Ubiquitin-specific metalloproteases, the second class of DUBs, rely on active site coordination of conserved hisitdine and aspartate residues with a zinc ion. These proteases belong to the JAMM domain superfamily of proteins, bear a characteristic MPN+/JAMM motif and are associated with the 26S proteasome (Yao and Cohe, 2002; Guterman and Glickman, 2004).

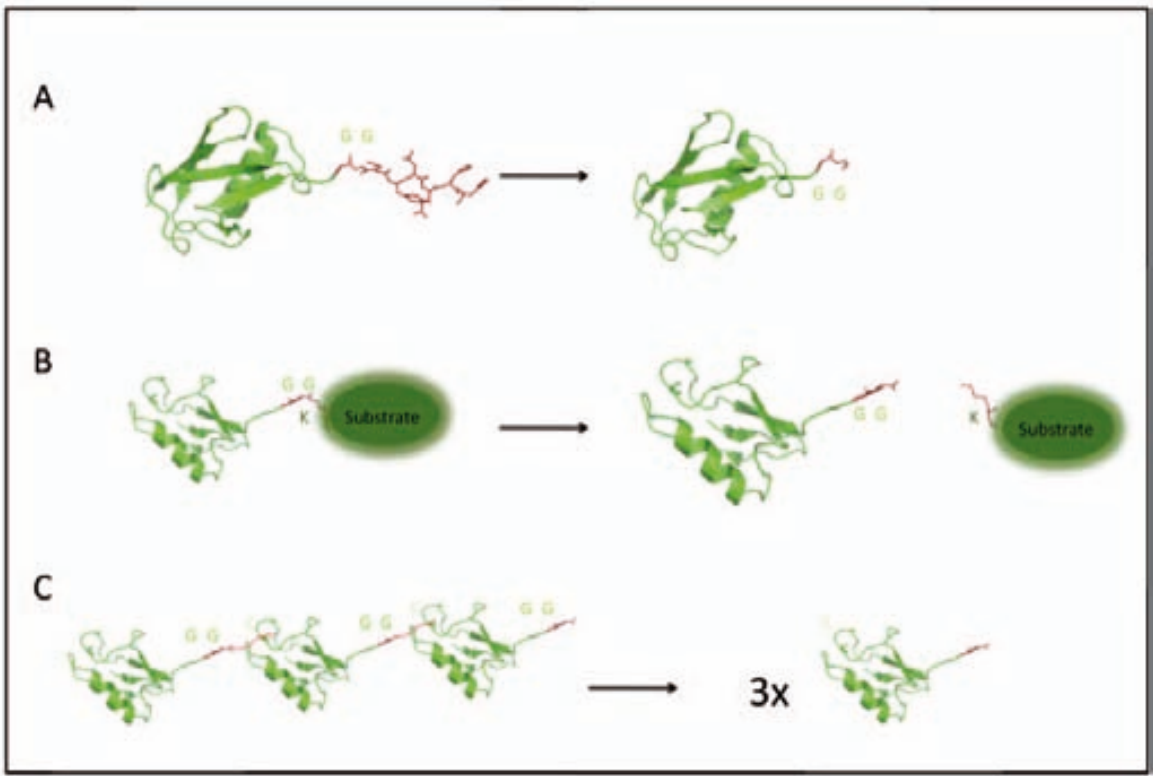

Figure 6. Catalytic functions of SENPs. Top panel, A, SUMO activation by removal of C-terminal tail to reveal di-glycine motif by SENP isopeptidase activity. Top panel, B, SUMO deconjugation from target by SENP endopeptidase activity. Bottom panel, C, model of SENP dismantling of polySUMO chains to constituent SUMO molecules. SUMO is shown in *green* in *cartoon* representation. Recipient lysine and C-terminal glycine residues and are shown in *red* and *stick* configuration and *labeled*. Images were modified and modeled by PyMOL structure PDB2IY1.

The enzymes associated with SUMO activation and deconjugation are called SENPs in humans and Ulps in yeast (Figure 6). There are only six human deSUMOylating enzymes, SENP1, SENP2, SENP3, SENP5, SENP6 and SENP7. Originally there were believed to be seven SENPs in humans, labeled according to their sequences in a database search but it was later discovered that SENP3 and SENP4 shared the same sequence (Yeh *et al*, 2000). SENP8 was originally thought to be a SUMO protease until it was subsequently discovered that it

showed a unique specificity for NEDD8, the closest Ubl related to ubiquitin (Wu *et al*, 2003; Mukhopadhyay and Dass, 2007; Gan-Erdene *et al*, 2008). Human SENPs, as well as yeast Ulps, share a ~220 amino acid protease fold, the defining characteristic of C48 cysteine proteases and within this core lies the characteristic His-Asp-Cys catalytic triad (Mukhopadhyay and Dasso, 2007). SENPs and Upls both belong to the CE clan of cysteine proteases while their mechanistic relatives, the deubiquitylating enzymes (DUBs) belong to the CA clan of proteases (Drag and Salvesen, 2008). Interestingly a new class of protease has recently been identified which is specific for SUMOylated but not ubiquitylated substrates that bears the papain-like fold characteristic of the DUBs (Mukhopadhyay *et al*, 2006). The protein, called DeSI-1, belongs to the PPPDE superfamily and, unlike the SENPs, seems to show little to no processing ability and restricted deconjugation ability. The fact that it is unable to deconjugate known SENP substrates suggests that the two types proteases likely have non-re dundant cellular functions in regard to SUMO deconjugation from substrates.

Figure 7. Evolutionary relationship of Ulp/SENP family members. An early branch separates the Den1-like (NEDD8-specific) proteases. The SUMO proteases have diverged into two main branches, Ulp1-like (SENP1, SENP2, SENP3 and SENP5) and Ulp2-like, (SENP6 and SENP7). Image taken from (121).

Sequence comparisons of the SENPs/Ulps reveal that they diverged from DUBs early in evolution (Barrett and Rawlings, 2001). Presently the six human SENPs can be divided into two groups: one containing Ulp1 (SENP1, SENP2, SENP3 and SENP5); and one containing Ulp2 (SENP6 and SENP7)(Xu and Au, 2005; Gong *et al*, 2000) (Figure 7). In most cases the catalytic domain is localized to the C-terminal of the protein but there have been cases, such as in Ulp2 and two Ulp2-like proteins (NP_195088 and NP_17444), where the catalytic domain lies within the center of the protein (Li and Hochstrasser, 2003; Novatchkova *et al*, 2004). It is interesting to note that within the catalytic domain of SENP6 and SENP7 there are inserts of 150 and 50 residues, respectively (Figure 8). *In vitro* deconjugation assays with both wild type and SENP6 and -7 constructs lacking these inserts show functional protease activity, leaving the relevance of these

large insertions to be elucidated (Lima and Reverter, 2008; Alegre and Reverter, 2011). While the C-48 catalytic domain persists through all of the SENP/Ulps the N-termini are non-conserved and vary between each protease. The N-terminal domains of both Ulps and SENPs have been shown to direct sub-cellular localization and substrate specificity but their full function within the cell has yet to be determined (Mukhopadhyay *et al*, 2006; Li and Hochstrasser, 2003).

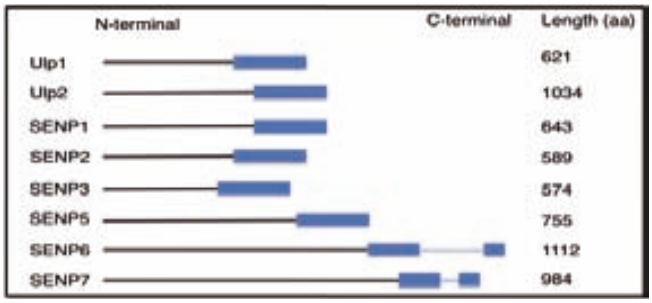

Figure 8. Primary structure of the SENPs. Non-conserved catalytic domains are shown in *black*. Conserved catalytic domains are blocked in *blue*. Loop3 insertions in SENP6 and SENP7 are shown in *light blue.*

Ulp1 and Ulp2 have distinct substrates and non-redundant functions. Over-expression of processed Smt3p weakly rescues Δ*ulp1* cells, but full-length Smt3p does not, indicating that Ulp1 plays a role in Smt3p processing. The Ubl1-like proteases SENP1, SENP2, SENP3 and SENP5 show similar processing activity but act more specifically; each SENP seems to have a SUMO isoform preference. SENP1 processes SUMO1 precursor more efficiently than SUMO2, SENP2 processes SUMO2 precursor better than SUMO1 but neither SENP1 nor SENP2 show appreciable activity toward SUMO3 (Reverter and Lima, 2004; Xu and Au, 2005). SENP3 and SENP5 show isoform specificity toward SUMO2/3 but essentially no activity against SUMO1, in contrast to SENP1 and SENP2

which have been shown to be able to deconjugate all three all isoforms *in vivo* (Gong *et al*, 2000; Zhang *et al*, 2002; Hang and Dasso, 2002).

In regard to deconjugation, over expression of Ulp1 showed strong activity against a wide range of substrates and over expression of both catalytically active and inactive forms of the enzyme can, at least partially, suppress the temperature-sensitive growth defects some of the Δ*ulp1* cells, suggesting an overlap between Ulp1 and Ulp2 substrates, which is consistent with *in vitro* studies (Li and Hochstrasser, 2003). SENP1 is able to efficiently deconjugate substrates with isoform preferences reminiscent of the processing reaction; it can cleave SUMO1 and SUMO2 more efficiently than SUMO3 from target substrates (Yukita *et al*, 2004). SENP2 is able to deconjugate all three SUMO isoforms with similar efficiency and SENP3 and SENP5 both show isopeptidase activity against SUMO2 and -3 conjugated substrates but not ones conjugated to SUMO1 (Lima and Reverter, 2008; Gong and Yeh, 2006; Di Bacco *et al*, 2006).

In contrast to Ulp1 Ulp2 may mainly be implicated in the deconjugation of Smt3p from conjugated substrates and from polySmt3 chains. Ulp2 can dismantle polySmt3 chains *in vitro* and Δ*ulp2* strains have been shown to accumulate high molecular weight polySmt3 species (Takahashi and Strunnikov, 2008). Furthermore expression of Smt3 branch site mutants which aren't capable of forming polymeric chains were able to suppress several of the Δ*ulp2* phenotypes, further suggesting that said defects were due to high molecular

weight chain accumulation (Takahashi and Strunnikov, 2008). Similar to Ulp2, SENP6 and SENP7 show little to no activity in processing SUMO precursors (Lima and Reverter, 2008; Alegre and Reverter, 2011). Both enzymes, however, have demonstrated activity in deconjugating SUMO conjugated substrates, more specifically polySUMO chains and show isoform specificity for SUMO2/3 over SUMO1 (Lima and Reverter, 2008; Alegre and Reverter, 2011; Nagamalleswari *et al*, 2010).

Table 1. Ulp/SENP localization and substrate specificity

Name	Subcellular localization	Processing	Deconjugation	Chain editing
Saccharomyces cerevisiae				
Ulp1	Nuclear periphery	Yes	Yes	No
Ulp2	Nucleoplasm	No	No	Yes
Humans				
SENP1	Nuclear speckled foci, nuclear pore	SUMO1>SUMO2> SUMO3	SUMO1/2/3	No
SENP2	Nuclear Pore	SUMO2>SUMO1> SUMO3	SUMO1/2/3	No
SENP3	Nucleolus	SUMO2/3	SUMO2/3>SUMO1 (very low)	No
SENP5	Nucleolus, cytosolic	SUMO2/3	SUMO2/3>SUMO1 (very low)	No
SENP6	Nucleoplasm	No (very low)	SUMO2/3>SUMO1 (very low)	SUMO2/3
SENP7	Nucleoplasm	No (very low)	SUMO2/3>SUMO1 (very low)	SUMO2/3

The SENPs

SENP1 and SENP2

Each human SENP contains a non-conserved N-terminal extension thought to be involved in sub-cellular localization and substrate specificity of each enzyme. SENP1 contains as nuclear export signal (NES) in its C-terminal as well as a nuclear localization signal (NLS) in its N-terminal but it is mainly localized in the nucleoplasm (Gong *et al*, 2000; Nagamalleswari *et al*, 2010; Bailey

and O'Hare, 2004). Human SENP1 is expressed in a tissue-specific manner with increased expression in the testis and detectable expression levels in the thymus, pancreas, spleen, liver, ovary and small intestine (Xu and Au, 2005). *Xenopus laevis* SENP1 (xSENP1) is also regulated during development in a stage- and tissue-specific manner but in this case it shows prominent expression patterns in the central nervous system (Yukita *et al*, 2004). SENP1 activity has been shown to regulate transcription through interaction with histone deacetylase 1 (HDAC1); SUMO deconjugation by SENP1 reduces the deacetylase activity of HDAC1 thereby allowing increased transcription of the androgen receptor (AR) (Cheng *et al*, 2004). Aberrant SENP1 expression has also been implicated in prostate cancer through disruption of the positive feedback loop with AR transcriptional activity, which causes androgen-driven prostate cell proliferation (Bawa-Khalfe *et al*, 2007). SENP1 has been shown to regulate another deacetylase, the mammalian NAD+-dependent histone deacetylase SIRT1, but in this case deSUMOylation results in loss of deacetylase activity and subsequent activation of apoptotic proteins (Yang *et al*, 2007). Additioanlly SENP1 knockout mice show developemental abnormalities as a result of deficient production of Epo protein, which is essential for the growth and survival of erythroid progentiors during differentiation into red cells (Cheng *et al*, 2007; Wu *et al* 1995).

Similar to SENP1, SENP2 is a nucleoplasmic shuttling protein, but SENP2 is predominantly found associated with the nuclear pore complex (NPC) though cases of its dispersion into nuclear bodies have been reported (Zhang *et al*, 2002;

Hang and Dasso, 2002; Ross *et al*, 2002). SENP2 also contains non-conserved nuclear export and nuclear localization signals and akin to SENP1 its nuclear export signal functions through the CRM1-dependent nuclear pathway (Kim *et al*, 2005; Itahana *et al*, 2006). Cytoplasmic SENP2 is polyubiquitinated and degraded through the 26S proteolysis pathway and mRNA splice variants have produced SENP2 isoforms with distinct cellular localization thus highlighting the importance of sub cellular localization in protease regulation and substrate specificity (Zhang *et al*, 2002; Itahana *et al*, 2006; Nishida *et al*, 2001; Best *et al*, 2002). SENP2 is mainly expressed in tissues of epithelial origin and previous works have shown that SENP2 is essential in the embryonic development of mice (Kang *et al*, 2010). Like SENP1 SENP2 isopeptidase activity plays a role in transcriptional regulation. SUMO1-bound Sp3 represses transcriptional activity but removal of SUMO1 by SENP2 results in augmented activity as well as relocation of the Sp3 protein. SENP2 has also been implicated in p53-depenedent stress responses as a negative regulator; deSUMOylation of Mdm2, a ubiquitin E3 ligase, permits Mdm2 binding to p53 thereby initiating proteosomal degradation, suggesting a role for SENP2 in regulating genome integrity (Jiang *et al*, 2011). It is also a negative regulator of NF-κB-dependent cell survival responses; deSUMOylation of NEMO (NF-κB essential modulator) blunts DNA damage-induced NF-κB activation thus suggesting a role for the SENP2/NF-κB feedback mechanism in oncogenesis and cancer resistance (Lee *et al*, 2011).

The catalytic domains of SENP1 and SENP2 have been characterized alone and in complex with pre-SUMO1 and -2 and RanGAP1-SUMO1 (Lima and Reverter, 2008; Reverter and Lima, 2004; Shen *et al*, 2006; Zheng *et al*, 2006; Shen *et al*, 2006; Reverter and Lima, 2006). Additionally SENP2 has been crystallized in complex with pre-SUMO3 and RanGAP-SUMO2 (Lima and Reverter, 2008). Both proteases adopt a fold that identifies them as part of the cysteine protease superfamily and they harbor the characteristic catalytic triad, Cys602, His 533 and Asp 550 for SENP1 and Cys 548, His 478 and Asp495 for SENP2, within their C-terminal domains (Reverter and Lima, 2004; Shen *et al*, 2006). The structures of SENP1 and SENP2 can be subdivided into two domains; a predominantly α-helical N-terminal domain containing the catalytic cysteine (Cys602 for SENP1 and Cys548 for SENP2) and a C-terminal region with a five-stranded mixed β-sheet ensconced by two α-helices and the other two residues of the catalytic triad (Reverter and Lima, 2004; Shen *et al*, 2006)(Figure 9 and 10). Their catalytic domains share 60% sequence similarity and their structures can be aligned with an r.m.s.d. of 0.8Å over 224 residues (Reverter and Lima, 2004).

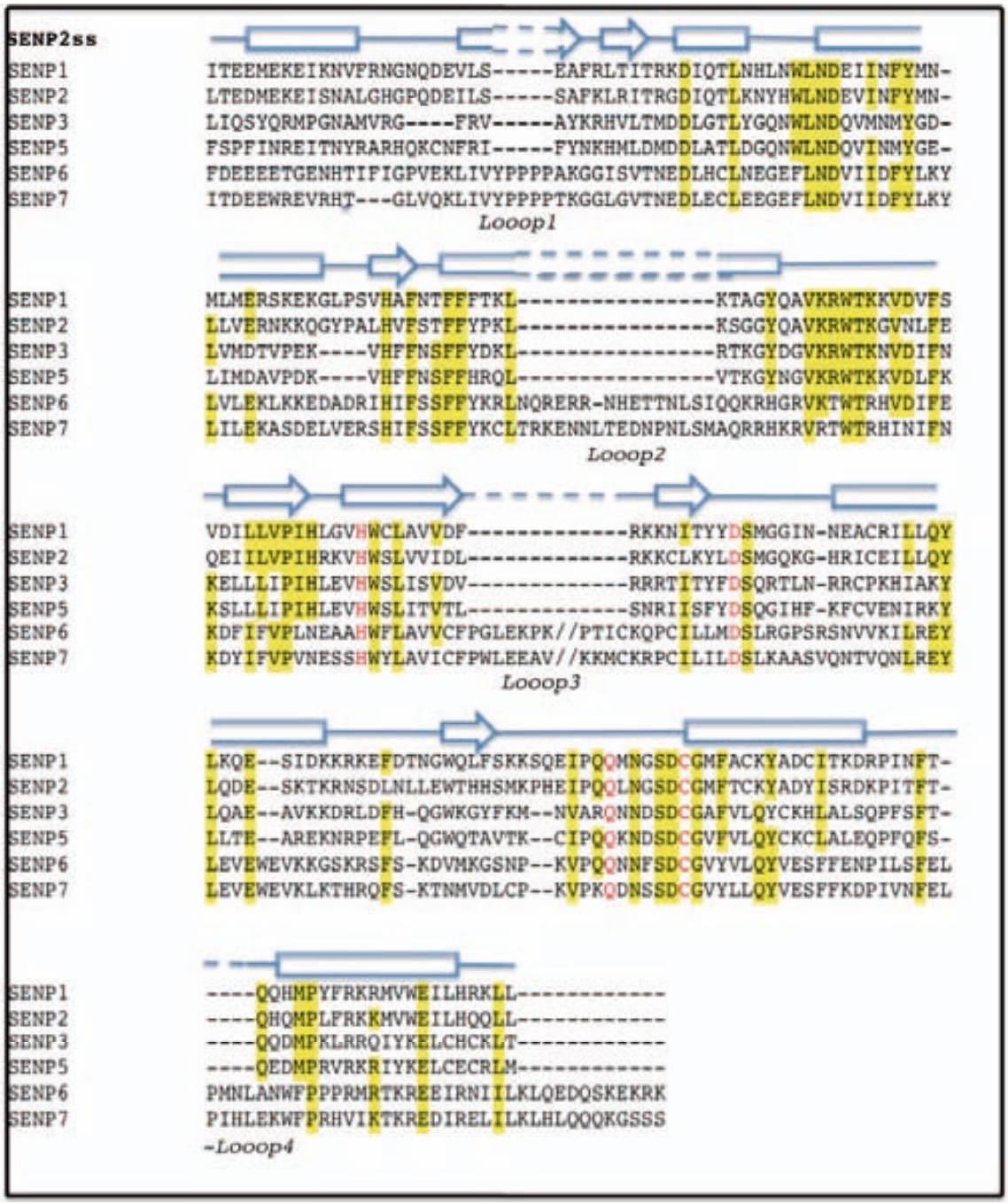

Figure 9. Sequence alignments of SENP1, -2, -3, -5, -6 and -7. Alignment is based on structure of SENP2 and SENP6 and -7 loop insertions are indicated *below* sequences. Gaps are shown as *dots* and Loop3 of SENP6 and SENP7 is denoted by // to denote that the sequence is missing from the alignment. For SENP2 α-helices are represented by *arrows,* β-sheets by *blocks*, conserved residues are *highlighted*, and catalytic residues are *red.*

Figure 10.Sequence of SENP2 and SENP2-SUMO1. Top panel, A, secondary structure of the human SENP2 catalytic domain shown in *ribbon* represenation. Catalytic residues are *numbered* and shown in *bond* representation. Bottom panel, B, secondary structure of the human SENP2 catalytic domain shown in *ribbon* representation and *dark blue* with human SUMO1, shown in *brown*). β strands are *numbered* and α helices are *lettered*. (Reverter and Lima, 2004)

The SENP1 and SENP2 complexes have provided insights into the mechanisms by which these proteases cleave SUMO isopeptides and SUMO-conjugated species (Lima and Reverter, 2008; Reverter and Lima, 2004; Shen *et al*, 2006; Reverter and Lima, 2006). For example both SENP1 and SENP2 have conserved surface residues essential for SUMO recognition. Both enzymes also tunnel SUMO precursors through a hydrophobic core and undergo local structural rearrangements upon binding the inactive SUMO. Individually active site characterization reveals different modes of substrate recognition, which can be attributed to different interactions between the C-terminal tails of SUMO and the residues harbored in the active site of each protease. The active site of SENP1

for example is stabilized through an aspartic acid forming a hydrogen bond with a water molecule, which in turn forms a hydrogen bond with a serine residue immediately flanking the Gly-Gly motif of SUMO1 (Shen *et al*, 2006). The SENP1/SUMO1 interaction is additionally reinforced by an active site glycine forming a hydrogen bond with a histidine residue just C-terminal to the SUMO1 Gly-Gly motif. This histidine is not present in SUMO2/3 and the SENP1 isoform preference for SUMO1 might be attributable to stabilization by this histidine. C-terminal residues also contribute substrate specificity for SENP2; in fact Reverter and Lima studied the effects of switching the C-terminal tails of SUMO1, SUMO2 and SUMO3 and showed that the activity (both iso- and endopeptidase) of SENP2 was dependent upon the C-terminal tail present on each SUMO (Reverter and Lima, 2004). By swapping the residues just C-terminal to the Gly-Gly motif of SUMO1 for those of SUMO2 or SUMO3, the enzyme was able to process the SUMO precursor more or less efficiently, respectively.

In regard to deconjugation, the SENP1/RanGAP1SUMO1 complex reveals a lack of specific active site interactions, thus providing an explanation as to why SENP1 is rather promiscuous in deconjugation SUMO isoforms from conjugated substrates (Shen *et al*, 2006). The SENP2/RanGAP1SUMO2 complex sheds light onto why SENP2 shows poor processing activity in comparison to the deconjugation activity; less sterical hindrance near the active site lysine in conjugated substrates allows for more efficient catalysis (Reverter and Lima, 2006). In both cases there was minimal interaction of the protease with RanGAP1

apart, from the region near the active site which functions as a substrate exit tunnel which, as is the case with the processing reaction, could serve as a means for substrate recognition.

SENP3 and SENP5

Both SENP3 and SENP are nucleolar Ulp1-like proteases that are more or less expressed throughout the human body (Mukhopadhyay and Dasso, 2007; Gong and Yeh, 2006; Di Bacco *et al*, 2006). Localization signals have been mapped in the N-termini of both SENP3 and SENP5 in mice but the mechanism for their localization in the nucleolus has yet to be determined (Gong and Yeh, 2006; Nishida *et al*, 2000). Ulp1 localizes to nuclear pores and has been implicated in ribosome biogenesis and its human counterparts SENP3 and SENP5 have also been found to interact with B23/nucleophosmin, a 37-kD shuttling phosphoprotein involved in ribosome biogenesis and export (Di Bacco *et al*, 2006; Borer *et al*, 1989; Yun *et al*, 2008). In a work done by Yun and associates co-depletion of both proteases resulted in SUMO protein accumulation within nucleoli and defects in ribosome biogenesis. Elevated SUMO2/3 levels were only found when both species were depleted, suggesting at least somewhat non-redundant functions for SENP3 and SENP5 in this context. Individually depletion of SENP3 interferes with ribosomal RNA processing and prevents maturation of 32S rRNA into the mature 28S form while depletion of SENP5 results in failure of cells to pass through the cell cycle which is consistent with defective ribosome biogenesis (Di Bacco *et al*, 2006; Haindl *et al*, 2008). While

SENP3 and SENP5 have predominantly behaved as dedicated SUMO2/3 proteases, *in vivo* and *in vitro* studies have shown minimal activity toward SUMO1ylated substrates so further investigation is required to show the true endogenous substrates of these proteases (Gong and Yeh, 2006; Nishida *et al*, 2000).

As previously mentioned, SENP3 is predominantly located within nucleoli but in response to cellular stresses nucleoplasmic redistribution has been observed (Huang *et al*, 2009). SENP3 is another SUMO protease that is a target for ubiquitin-mediated proteosomal degradation but cellular exposure to reactive oxygen species (ROS) H2O2 inhibits SENP3 degradation and causes relocation of SENP3 to the nucleoplasm where the protease is exposed to a different set of SUMO substrates (Huang *et al*, 2009; Kuo *et al*, 2008). Increased reactive oxygen species have been detected in human prostate tumors and not surprisingly elevated SENP3 levels have been detected in prostate cancer as well as ovarian, lung, rectum and colon carcinomas (Lim *et al*, 2005).

Similar to SENP1 and SENP2, SENP3 has been implicated in transcription, though its cellular interactions have been studied with less scrutiny. While SENP1 has been known to interact directly with HIF1α through deSUMOylation resulting in subsequent up regulation of HIF1α-dependent genes, SENP3 indirectly influences HIF1α transcription through interaction with the coregulator p300, whose deSUMOyation by SENP3 results in enhanced binding

of p300 to HIF1α and similar up regulation of HIF1α-dependent genes (Huang *et al*, 2009).

SENP5 sub-cellular redistribution is cell cycle dependent and results in migration of nucleolytic and cytosolic SENP5 to the surface of mitochondriae at G2/M transition prior to the breakdown of the nuclear envelope (Zunino *et al*, 2009). This transition and subsequent deSUMOylation leads to an increase in free DRP1, a protein involved in mitochondrial division, and subsequent polymerization of DRP1, which, in turn, promotes mitochondrial fission during mitosis. SENP5-silenced cells showed an increase in free radicals and fragmented mitochondria, implicating a role for SENP5 in metabolism and mitochondrial morphology. Knockdown of SENP5 also leads to an increase in SUMOylated proteins and a dramatic decrease in cell proliferation, with cells displaying abnormal nuclear morphology (Di Bacco *et al*, 2006). SENP5 could therefore be instigated in more than one pathway in cell division.

SENP6 and SENP7

SENP6, also called known as *SU*mo-1-*S*pecific *P*rotease or SUSP1, is the largest of SENP proteases, with the entire protein encompassing 1112 amino acids and a C-terminal domain of 447 amino acids. It is highly expressed in reproductive organs, primarily the testis, ovary and prostate (Kim *et al*, 2000). Originally thought to be localized to the cytoplasm, it was later designated a nuclear protein, with an N-terminal localization signal between residues 84 and

448 (Mukhopadhyay *et al*, 2006; Kim *et al*, 2000; Cheng *et al*, 2006). SENP6 also contains four putative SUMO binding domains, dispersed throughout the entire length of the protein, though the utility of these domains has yet to be elucidated. SENP6 is involved in dismantling high molecular weight SUMO2/3 moieties and depletion of SENP6 results in redistribution of SUMO2/3 into PML nuclear bodies and a subsequent increase in PML NB size (Mukhopadhyay *et al*, 2006; Lima and Reverter, 2008; Alegre and Reverter, 2011; Hattersley *et al*, 2011). A SENP6 cysteine to serine active site mutant shows an accumulation at PML NBs, in contrast to wild-type SENP6, which shows no accumulation due to its likely dissociation from these structures following its protealytic role (Hattersley *et al*, 2011). Though it has mainly been implicated in the deconjugation of SUMO2/3ylated species, SENP6 has demonstrated deconjugation activity toward monoSUMO1ylated nuclear receptor RXRalpha and polySUMO2/3ylated chains terminating in SUMO1 (Choi *et al*, 2006; Hattersley *et al*, 2011). Depletion of SENP6 also causes spindle assembly deformations as well as defects in mitotic progression, with some cells persisting in interphase and some showing prolonged mitotic delays and chromosome misalignment (Mukhopadhyay *et al*, 2010). This phenotype has also been demonstrated in cells lacking outer kinetechore components CENP-H/I/K and SENP6-depleted cells resulted in an RNF4-dependent proteasome-mediated proteolysis.

SENP7, like SENP6, is a nuclear protein though the mechanism of this sub-cellular localization remains unknown (Mukhopadhyay *et al*, 2006; Cheng *et*

al, 2006). siRNA-mediated depletion of SENP7 results in accumulation of high molecular weight SUMO2/3ylated but not SUMO1ylated species within PML nuclear bodies and SENP7 has been shown to dismantle polySUMO2/3 chains *in vitro* (Lima and Reverter, 2008; Alegre and Reverter, 2011; Shen *et al*, 2006). Thus SENP7, like SENP6, is probably a modulator of polySUMO2/3ylated species *in vivo.* Very recently it was discovered that both wild type and a C979S active site mutant SENP7 co-immunoprepcipitated with heterochromatin protein alpha (HP1α) and that it co localized with HP1α at pericentric heterochromatin (Maison *et al*, 2012). It was also shown that SENP7 was able to deconjugate SUMO1-modified HP1α *in vivo*, altogether proving that SUMO1ylated HP1α in an endogenous substrate of SENP7.

In 2008 Lima and Reverter characterized the catalytic domain of SENP7 (Lima and Reverter, 2008). In this structure the relationship between SENP7 and other Cys-48 cysteine family proteases as well as the other characterized SENP family members could be seen (Figure 11). While SENP7 doesn't align well with either SENP1 (r.m.s.d. of 2.0 Å over 182 residues) or SENP2 (r.ms.d. of 2.0 Å over 187 residues) several similar structural elements can be seen in the overlay of SENP2 and SENP7, such as an N-terminal rich with α-helices and a C-terminal domain containing a mixed β-sheet. The arrangement of the active site residues is also similar in both structures, with the catalytic cysteine (Cys926) residing in the N-terminal and the catalytic histidine (His794) and aspartic acid (Asp873) located in the C-terminal. Notable differences between the structures of SENP2

and SENP7 are the lack of an N-terminal helix within SENP7 which is in the structures of both SENP1 and SENP2 and four loop insertions (Loop1, -2, -3 and -4) in the structure of SENP7 that are not present in either SENP1 or SENP2.

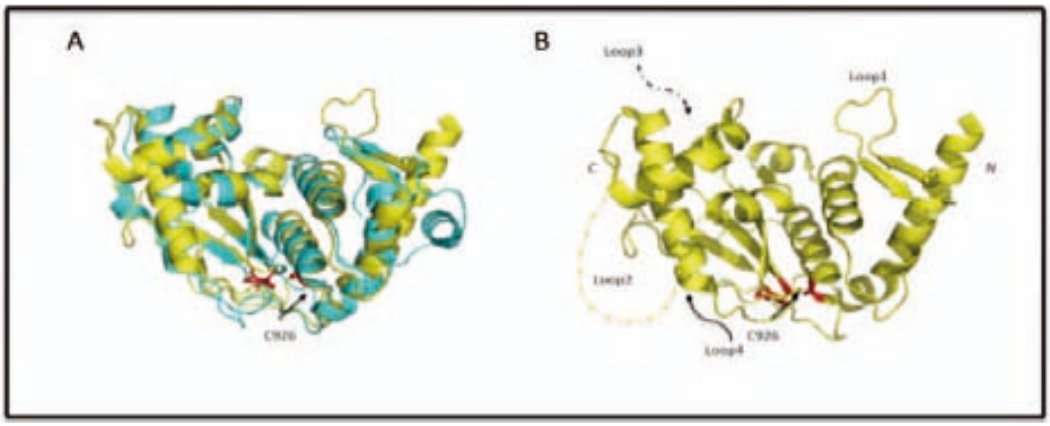

Figure 11. Structure of the catalytic domain of SENP7. *A,* superposition of the structures of SENP7 (PDB3eay) and SENP2 (PDB1TH0) in *ribbon* representation with SENP7 shown in *yellow* and SENP2 shown in *cyan*. Catalytic residues are shown in *stick* and colored *red* and the catalytic cysteine is labeled C926. *B*, SENP7 catalytic domain shown in *ribbon* representation. Loop insertions are labeled Loop1, Loop2, Loop3 and Loop4 and *dashed* lines represent elements that were unstructured within the crystal and not characterized. Graphics were prepared with PYMOL.

Objectives

Objectives I

- Use known complex structures to model SENP7 interactions and identify and characterize putative SUMO interaction surfaces
- Obtain SUMO1 and SUMO2 mutants to characterize putative interactions with SENP6 and SENP7 Loop1
- Obtain SENP6 loop deletions and characterize activity against SUMO substrates

Objectives II

- Identify key SENP7 Loop1 residues in putative SUMO interacting site
- Obtain and characterize SENP7 Loop1 mutants to reinforce putative characterization of SENP7 with SUMO1 and SUMO2
- Insert SENP6 Loop1 into SENP2 and determine functionality in context of diSUMO2 conjugation

Objectives III

- Obtain and purify wild type and active site mutant catalytic domains of SENP6 and SENP7
- Obtain and purify SUMO substrates for use in complex formation

- Identify substrates that form stable complexes with SENP6 and SENP7

Experimental Procedures

Experimental Procedures

Protein Purification

Proteins were amplified by PCR and cloned into pET28b vecotor to encode a polypeptide fused to a thrombin-cleavable N-terminal hexa-histidine tag. Expression constructs were used to transform Escherichia coli BL21(DE3) codon plus cells (Novagen). Bacterial cultures were grown by fermentation at 37 °C to A600=0.8, and isopropyl-β-D-thioga-lactopyranoside (IPTG) was added to a final concentration of 0.5 mM. Cultures were incubated for 3– 4 h at 30 °C and harvested by centrifugation (6500 g), and the supernatant was discarded. Cell suspensions were equilibrated in 20% sucrose, 20 mM Tris-HCl (pH 8.0), 1 mM β-mercaptoethanol, 350 mM NaCl, 20 mM imidazole, 0.1% IGEPAL CA-630 and 10mM MgCl2, and cells were disrupted by sonication. Cell debris was removed by centrifugation (40,000g). Protein was separated from lysate by metal affinity chromatography using nickel-nitrilotriacetic acid-agarose resin (Qiagen) and eluted with 25 mM Tris-HCl (pH 8.0), 350 mM NaCl, 300 mM imidazole, and 2 mM β-mercaptoethanol and dialyzed against buffer containing 25 mM Tris-HCl (pH 8.0), 100 mM NaCl, and 2 mM β-mercaptoethanol with thrombin (Sigma) at a 1:1000 ratio. After thrombin cleavage, fractions containing SENP6 and SENP7 were separated by gel filtration (Superdex 200; GE Healthcare). Fractions containing the protein of interest were pooled, diluted to 50 mM NaCl, applied to anion exchange resin (Mono Q; GE Healthcare), and eluted with a NaCl gradient from 0 to 50% of a buffer containing 25 mM Tris-HCl (pH 8.0), 1 M NaCl, and 2

mM β-mercaptoethanol in 12 column volumes. Fractions containing the protein of interest were pooled, concentrated to 10 mg/ml, and snap-frozen in liquid nitrogen prior to storage at 80 °C.

Protein Constructs

SENP7

SENP7 catalytic domain- SENP7-(662-982) was amplified by PCR using human lung and brain PCR-ready cDNA (Ambion) and subsequently cloned into pET28b vector. SENP7 catalytic domain was produced in *E. coli* and purified by the procedure mentioned above.

SENP7 mutants- Single point mutations were introduced into the SENP7 (K691E, K691A) coding regions using QuikChange mutagenesis kit (Stratagene). The SENP7 four mutant construct P686G/P687G/P688G/P689G was constructed by PCR, treated with DPN1, purified by agarose gel and subsequently left with PNK and T4 DNA ligase to produce the circular plasmid (Table 1). SENP7Δ1 was constructed by David Reverter at the Sloan-Kettering Institute in New York and was made by fusing amino acids 680-692 (Loop1 SENP7-Δ681-691)(Lima and Reverter, 2008). All SENP7 isoforms were produced in *E. coli* and purified by the procedure mentioned above.

SENP2

SENP2 catalytic domain- The catalytic domain of SENP2 was amplified from human testes cDNA library (Clontech) by PCR and the sequence was found to be identical to the reported sequence for SENP2 (GenBank number AF151679). SENP2-(364-489) was amplified and cloned into pET28b vector with a hexa-histadine tag fused at the N-terminal (Reverter and Lima, 2004). SENP2 catalytic domain was produced in *E. coli* and purified by the procedure mentioned above.

SENP2 ative site mutant- pET28b- SENP2-(364-489) was amplified by PCR using primers introducing a cysteine to serine mutant at position 548 in the SENP6 catalytic domain and the DNA was subsequently transformed in XL1-Blu super competent cells. SENP6C548S was produced in *E. coli* and purified by the procedure mentioned above.

SENP2ins- SENP6 Loop1 residues 658-666 (PPPPAKGG) were inserted into SENP2 by inserting PPPP C-terminal to residue 392 of SENP2 and AKGG N-terminal to residue 395 of SENP2 to give the following sequence: EILSSAPPPPAKGGLRIT, where inserted amino acids are *underlined.* The mutant was amplified by PCR, treated with DPN1, purified by agarose gel and subsequently left with PNK and T4 DNA ligase to produce the circular plasmid (Table 1). SENP2ins was produced in *E. coli* and purified similarly to the native proteins.

SENP6

SENP6 catalytic domain- SENP6-(637-1112) was amplified by PCR using human lung and brain PCR-ready cDNA (Ambion) and subsequently cloned into pET28b vector. SENP6 catalytic domain was produced in *E. coli* and purified by the procedure mentioned above.

SENP6 ative site mutant- pET28b-SENP6-(637-1112) was amplified by PCR using primers introducing a cysteine to serine mutant at position 1030 in the SENP6 catalytic domain and the DNA was subsequently transformed in XL1-Blu super competent cells. SENP6C1030S was produced in *E. coli* and purified by the procedure mentioned above.

SENP6Δ1, SENP6Δ2, SENP6Δ3, SENP6Δ2Δ3- PCR was used to construct SENP6 deletion mutants by fusing amino acids 656-664 (Loop1 SENP6-Δ657-663), by substituting two glycine residues for the loop between residues 720 and 735 (Loop2 SENP6-Δ721–734), and by fusing amino acids 874 to 973 (Loop3 SENP6-Δ875–972)(Table1). The deletion mutant DNA was subsequently left with DPN1 at 37°C for 3 hours to remove circular mother DNA, purified from 0.8% agarose gel using *Real* Clean Spin Kit, left with PNK for 30 minutes at 37°C then ligated at room temperature for two hours. Circular DNA was then transformed into XL1-Blue super competent cells. Colonies were grown 4ml cultures overnight and

DNA was purified using FastPlasmid Mini Kit (Fermentas), checked via restriction enzyme analysis and sent for sequencing. Plasmids bearing the correct deletion sequences were then transformed into BL21(DE3) codon plus cells (Novagen). Active site mutants were introduced into the SENP6(C1030) coding region using Quick-Change mutagenesis kit (Stratagene). DNA was treated with DPN1 for 3 hours at 37°C then transformed into XL1-Blue super competent cells. Colonies were checked via restriction enzyme and sent for sequencing. Positive clones were sent for sequencing and plasmids bearing the correct mutation were transferred into BL21(DE3) codon plus cells (Novagen). SENP6Δ2Δ3 was produced by PCR with pET28b-SENP6Δ3CS as template DNA and a substitution of two glycine residues for the loop between residues 720 and 735 (Loop-2 SENP6-Δ721–734). All mutant SENP6 isoforms were produced in *E. coli* and purified by the method mentioned above.

SUMO

SUMO constructs- Plasmids containing full-length SUMO1, SUMO2, SUMOG_iG_i and SUMO2G_iG_i,with an insertion of two additional glycine residues after the Gly-Gly motif were constructed at the Sloan-Kettering Institute in New York by David Reverter (Reverter and Lima, 2006). Plasmids were expressed from pET28b in *E. coli* Bl21(DE3) codon plus cells (Novagen) and purified by excluding the native stop codon and fusing a C-terminal hexa-hisitidine tag C-terminal to the native polypeptide. SUMO1 and SUMO2 were purified by Ni-

NTA-affinity chromatography (Qiagen) and separated by gel filtration (Superdex 200; GE Healthcare). Fractions containing the protein of interest were pooled, concentrated to 10 mg/ml, and snap-frozen in liquid nitrogen prior to storage at 80 °C.

SUMO Loop1 interacting mutants- Single point mutations were introduced into the SUMO1 (A68N, H71D), SUMO1 G_iG_i (A68N, H71D), SUMO2 (N68A, D71H) and SUMO2 G_iG_i (N68A, D71H) coding regions using the Quick-Change mutagenesis kit (Stratagene). Insertion of two additional glycine residues after the Gly-Gly motif of SUMO1 and SUMO2 were generated by PCR using the QuikChange Sit-Directed Mutagenesis Kit (Stratagene).

SUMO N-terminal deletion mutants- Δ18SUMO1 was made by PCR by amplifying between residues 18 and 101 of full-length SUMO1. Δ14SUMO2 was made by PCR by amplifying between residues 15 and 95 of full-length SUMO2. Δ18SUMO1 and Δ14 SUMO2 proteins were activated by cleavage with SENP2 to expose two C-terminal glycine residues. Proteins were purified in the same manner as wild type proteins but in addition were dialyzed and further purified by anion exchange to removal residual SENP2.

SUMO C-terminal deletion mutants- SUMO2ΔGG was made by PCR by amplifying between residues 1 and 91 of full length SUMO2 and cloning this

region into pET28b vector with an N-terminal hexa-histidine tag. The protein was purified by Ni-NTA-agarose resin (Qiagen) and dialyzed in a buffer containing 25 mM Tris-HCl (pH 8.0), 100 mM NaCl, and 2 mM β-mercaptoethanol in the presence of thrombin (Sigma) at a 1:1000 ratio. SUMO2□GG was then purified by gel filtration, concentrated to 10mg/ml and snap-frozen in liquid nitrogen prior to storage at 80 °C.

RanGAP1

RanGAP1- RanGAP1 residues 418-587 ($RanGAP1_{418-587}$) were subcloned into pET28b, expressed in *E. coli* BL21 (DE3) and subsequently purified by the methods mentioned above (Shen et al, 2006).

Table 1. Primers used in SENP6 and SENP7 – SUMO interaction studies

Name	Sequence (5'-3')
SENP6loop1for	GGAGGCATCTCTGTTACCAATGAG
SENP6loop2rev	ATATACTATCAACTTTTCTACTGG
SENP6loop2for	GGGGGACATGGGAGAGTAAAAACATGGACC
SENP6loop2rev	CTGATTAAGGCGTTTATAGAAAAA
SENP6loop3for	CCTACTATCTGTAAACAACCTTGT
SENP6loop3rev	TTCATACTTTGGTTTTTCCAAACC
SENP6C1030Sfor	CAAAACAACTTCAGTGACTCTGGTGTATATGTATTGCAG
SENP6C1030Srev	CTGCAATACATATACACCAGAGTCACTGAAGTTGTTTTG
SENP7K691Afor	CCTCCACCACCTACTGCGGGGGGATTAGGAGTAAC
SENP7K691Arev	GTTACTCCTAATCCCCCCGCAGTAGGTGGTGGAGG
SENP7K691Efor	CCTCCACCACCTACTGAGGGGGGATTAGGAGTAAC
SENP7K691Erev	GTTACTCCTAATCCCCCCTCAGTAGGTGGTGGAGG
SENP74P_Gfor	GGAGGTACTAAGGGGGGATTAGGAGTAAC
SENP2ins_for	GCTAAGGGAGGCTTGCGAATTACTCGAAGG
SENP2ins_rev	TGGAGGTGGTGGAGCACTACTTAGGATTTC
SENP74P-Grev	TCCACCATATACAATCAACTTCTGAACAAGTCC

SENP6Loop3for	AACAGGATCCCATTACCATGAAAATGCTGTC
SENP6Loop3rev	AACTCTCGAGTTACTTTAAATGCCACTGTCCTATTTC
SUMO1_A72N_H75D_for	GAGGGTCAGAGAATTAATGATAATGATACTCCAAAAGAACTG
SUMO1_A72N_H75D_rev	CAGTTCTTTTGGAGTATCATTATCATTAATTCTCTGACCCTC
SUMO2_N68A_D71H_for	GACGGGCAACCAATCGCTGAAACACACACACCTGCACAGTTG
SUMO2_N68A_D71H_rev	CAACTGTGCAGGTGTGTGTGTTTCAGCCATTGGTTGCCCGTC

Conjugation Reaction

RanGAP1-SUMO

RanGAP1-SUMO1 and RanGAP1-SUMO2- RanGAP1-SUMO1 and RanGAP-SUMO2 were formed in a reaction mixture containing 20mM Hepes pH7.5, 5mM MgCl2, 0.1% Tween, 50mM NaCl, 1mM dithiothreitol, 2mM ATP, 150nM SAE1/SAE2 (E1)), 100nM Ubc9 (E2), 16mM N□419RanGAP1 and 32mM □14SUMO2 or □18SUMO1 in MilliQ water.

diSUMO

diSUMO2 and diSUMO1/2- DiSUMO2 was formed in a reaction mixture containing 20mM Hepes pH7.5, 5mM MgCl2, 0.1% Tween, 50mM NaCl, 1mM dithiothreitol, 2mM ATP, 150nM SAE1/SAE2 (E1)), 100nM Ubc9 (E2), IR1 (E3), 32mM □14SUMO2 and 16mM SUMO2□GG in MilliQ water. DiSUMO1/2 chimera was produced using □18SUMO1 and SUMO2□GG in the same reaction conditions as the diSUMO2 reaction above. Products were verified by SDS-page, purified by gel filtration (Superdex 200 or 75), concentrated to 10mg/ml and and snap-frozen in liquid nitrogen prior to storage at 80 °C.

Biochemical Assays

Processing

Activity Assays- Titration of carboxyl-terminal hydrolase activity (processing) was measured by incubating preSUMO1GGG$_i$G$_i$-X, preSUMO1GGG$_i$G$_i$-X (A72N/H75D), preSUMO2GGG$_i$G$_i$-X and preSUMO2GGG$_i$G$_i$-X (N68A/D71H) (-X represents the natural C-terminal tail sequence for each SUMO isoform and G$_i$ represents the glycine insertions) precursor proteins (5μM) with purified SENP6, SENP7 and SENP2 at three different enzyme concentrations (0.5, 5, and 50 nM) at 37 °C in a buffer containing 25 mM Tris-HCl (pH 8.0), 150 mM NaCl, 0.1% Tween 20, and 2 mM dithiothreitol. Reactions were stopped after 25 min with SDS loading buffer and analyzed by gel electrophoresis (PAGE). Proteins were detected by staining with SYPRO (Bio-Rad).

Time course assays- SENPWT, SENP6□1 and SENP6□ were run against preSUMO1GGG$_i$G$_i$-X, preSUMO1GGG$_i$G$_i$-X (A72N/H75D), preSUMO2GGG$_i$G$_i$-X and preSUMO2GGG$_i$G$_i$-X (N68A/D71H) at substrates at 3 μM. Reactions were run at 37 C and stopped at 5, 20, 40 and 80 minutes with SDS loading buffer and analyzed by PAGE. The same buffer conditions were used for the time course reactions using di-SUMO2 and di-SUMO2 (N68A/D71H) mutant with SENP2, SENP6 and SENP7 at 0.5nM and diSUMO2 and diSUMO2(D71K) with SENP7, SENP7-ΔLoop1, SENP7(K691E), SENP7(K691A) and SENP7(P686to689G) at 0.5nM with reactions stopped at 15, 30, 60 and 120 minutes.

Deconjugation

Activity Assays- SENP2, SENP6 wild type and deletion mutants, and SENP7 at 0.5, 5, 50 nM were run against RanGAP1SUMO1, RanGAP1SUMO1 (A72N/H75D), RanGAP1SUMO2, and RanGAP1SUMO2 (N68A/D71H) substrates at 3mM in a buffer containing 25 mM Tris-HCl (pH 8.0), 150 mM NaCl, 0.1% Tween 20, and 2 mM dithiothreitol. Deconjugation activities using di-SUMO2 substrates at 3 μM were performed using enzyme concentrations at 0.05, 0.5 and 50 nM. The reactions were stopped after 25 min with SDS loading buffer and analyzed by PAGE. Proteins were detected by staining with SYPRO (Bio-Rad). Products were quantified by detecting fluorescence under UV illumination using a Gel-Doc apparatus with associated integration software (Quantity-One; Bio-Rad).

Time course assays- SENP6 and SENP2, at 5 nM and 1 nM respectively, were incubated with RanGAP1SUMO1, RanGAP1SUMO1 (A72N/H75D), RanGAP1SUMO2, and RanGAP1SUMO2 (N68A/D71H) substrates at 3 μM. Reactions were run at 37 C and stopped at 5, 20, 40 and 80 minutes with SDS loading buffer and analyzed by PAGE. The same buffer conditions were used for the time course reactions using di-SUMO2 and di-SUMO2 (N68A/D71H) mutant with SENP2, SENP6 and SENP7 at 0.5nM and diSUMO2 and diSUMO2(D71K) with SENP7, SENP7-ΔLoop1, SENP7(K691E), SENP7(K691A) and

SENP7(P686to689G) at 0.5nM with reactions stopped at 15, 30, 60 and 120 minutes.

Kinetic Analysis

Initial rate velocities- Initial reaction velocities were measured for SENP6-Δloop3 at 1nM and SENP7 and associated mutants at 0.5nM in a buffer containing 25 mM Tris-HCl (pH 8.0), 150 mM NaCl, 0.1% Tween-20, and 2 mM dithiothreitol at 37 C. Substrates used for the processing and deconjugation reactions were prepared at 5 μM. Reactions were stopped at indicated time intervals with SDS loading buffer and analyzed by PAGE. Products were quantified by detecting fluorescence using a Gel-Doc apparatus with associated integration software (Quantity-One; Bio-Rad). All data points were fitted to a hyperbolic curve. All assays were conducted in triplicate. Error bars indicate ±1 standard deviation.

Steady=state kinetics- Michaelis-Menten steady-state kinetics was performed for SENP6 by introduction of S9C and C52A point mutants into SUMO1 and SUMO1 (A68NH71D) to allow for fluorophore addition. SUMO1(S9C/C52C) and SUMO1 (S9C/C52C/A68N/H71D) were used for labeling with Alexa-Fluor-488 fluorophore (Invitrogen), and were subsequently conjugated to RanGAP1. Initial deconjugation velocities were measured at eight different substrate-labeled concentrations (0, 0.25, 1, 2, 6, 20, 50 and 100□M) for a SENP6 concentration at 25nM. Reactions were stopped after 0, 5, 15, 40 and 80 minutes with SDS loading

buffer and analyzed by SDS gel electrophoresis. Fluorescence signal was followed and measured by using Versadoc apparatus with associated integration software (Quantity One, Bio-Rad). Kinetic constants were obtained from the graph representation substrate concentration (□M) vs. initial velocity (□Mmin-1). All assays were conducted in triplicate.

Loop3 Characterization

1H 1D NMR

1mg of SENP6 Loop3 was dissolved in 600□l of TrisHCl at pH 7. The sample was run on 1D-1H NMR on a complete scale and expanded vertically 512 times and the spectrum was measured. The sample was additionally run on 1D-1H NMR at 300K, heated to 350K and again at 300K. Analysis was performed at the Servei de Ressonància Magnètica Nuclear at the Universidad Autonoma de Barcelona.

Cicular dichroism

Samples for CD spectroscopy were prepared by dissolving SENP6 Loop3 to a final concentration of 0.2 mg/ml in 20mM sodium phosphate buffer at pH 7.4. CD analyses were conducted in a JASCO J-715 spectrometer at 20, 60 and 90°C using a cell of 0.5mm path length. Analysis was performed at the Servicio de Analysis Quimico at the Universidad Autonoma de Barcelona.

Fourier Transform Inrared Spectrum

Protein samples for FTIR analysis were prepared by lyophilizing a sample of protein in a buffer containing 20mM Tris, pH 8.0 and 1 mM β-mercaptoethanol to obtain 2mg. The dried protein was then dissolved in D20 and the sample sent for analysis. Analysis was performed at the Servicio de Analysis Quimico at the Universidad Autonoma de Barcelona.

Limited Proteolysis

Samples for limited proteolysis were prepared by diluting SENP6 Loop3 in a buffer containing 150mM NaCl, 20mM Tris, pH 8.0 and 20mM CaCl2 with prepared dilutions of trypsin, chymotrypsin and elastase at concentrations of 10-1 to 10-5. The reactions mixture were run at 37°C for one hour and subsequently analyzed by SDS-page. Once a stable fraction was established (chymotrypsin, C=10-3), the gel was transferred to a nitrocellulose membrane, excised and sent for N-terminal sequencing.

Mass spectrometry

The reaction mixtures for mass spectrometry were incubated at the same enzyme concentration for time intervals T=0, 10, 20, 40 and 60 minutes at 37°C and one half of the sample was stopped using SDS loading buffer and the other half with TFA. The samples with SDS were then analyzed by gel electrophoresis (PAGE)

for determination of fragment size and the samples containing TFA were sent for Mass Spectrometry (MALDI-TOF) analysis. Analysis was performed at the Servei de Proteomica I Bioinformatica (SePBio) at the Institut de Biomedicina i de Biotecnologia.

Complex Preparation

Complex Preparation

The catalytic domain of SENP2 (SENP2C548S) and SENP6 (C1030S) along with deletion mutants Δ2-, Δ3- and Δ2Δ3SENP6CS were concentrated to >10mg/ml and added to a reaction mixture containing 5mM NaCl, 20mM Tris, pH 8.0 and 1mM β-mercaptoethanol. Complexes were attempted by adding a 2:1 dilution of protease to substrate, using the following substrates: preSUMO2GG, RanGAP1-SUMO1, RamGAP1-SUMO2 and diSUMO2. The mixtures were purified by gel filtration (Superdex 200; GE Healthcare) and fractions containing the complex were verified by SDS-PAGE and pooled to a final protein concentration of >10mg/ml.

Crystallization

Both individual protease and protease-substrate complexes (100nl-200nl) were sprayed into 96-well sitting drop plates using an Art Robbing Instruments Phoenix protein crystallization robot, mixed with purchased screen conditions (100nl-200nl) and stored at either 4 or at 18°C in a Crystal Motion crystal farm.

Optimized plates were made by mixing 0.5-1 L of protein/complex with corresponding buffer and adding to either sitting or hanging drop plates and stored at either 4 or 18°C.

Results

Swapping the SUMO Isoform Specificity of SENP6/7

SENP6 is SUMO2/3 specific and inefficient at SUMO processing

SENP2 was previously shown, via biochemical studies and structural characterization, to have an isoformal bias toward the processing of SUMO1, -2 and -3 (Reverter and Lima; 2004 and 2006). This bias was first based on the resolved structure of SENP2 with SUMO1, which shed light on the fact that the amino acid tails C-terminal to the conserved Gly-Gly motifs determined processing efficacy. This study was corroborated with the resolution of the structure of SENP2 in complex with pre-SUMO3, and additional biochemical studies rendering SENP2 more protealytically active toward substrates bearing an ε-linkage or an ε-like linkage just C-terminal to the Gly-Gly (ε-like linkage referring to the insertion of an additional two glycines directly adjacent to the conserved Gly-Gly, which mimics the ε-linkage found between SUMO and the

lysine of a given SUMO conjugate). Most recently, similar experiments were carried out with SENP6 and SENP7 against identical substrates and the same trends were noticed; more specifically both proteases showed more activity toward SUMO-conjugated substrates than toward SUMO precursors, but in either case there was an overwhelming tendency for SENP6 and -7 to act against SUMO2/3 substrates (Reverter and Lima; 2008, Alegre and Reverter, 2011). As previously mentioned, both of these proteases contain loop insertions not present in any of the other SENPs.

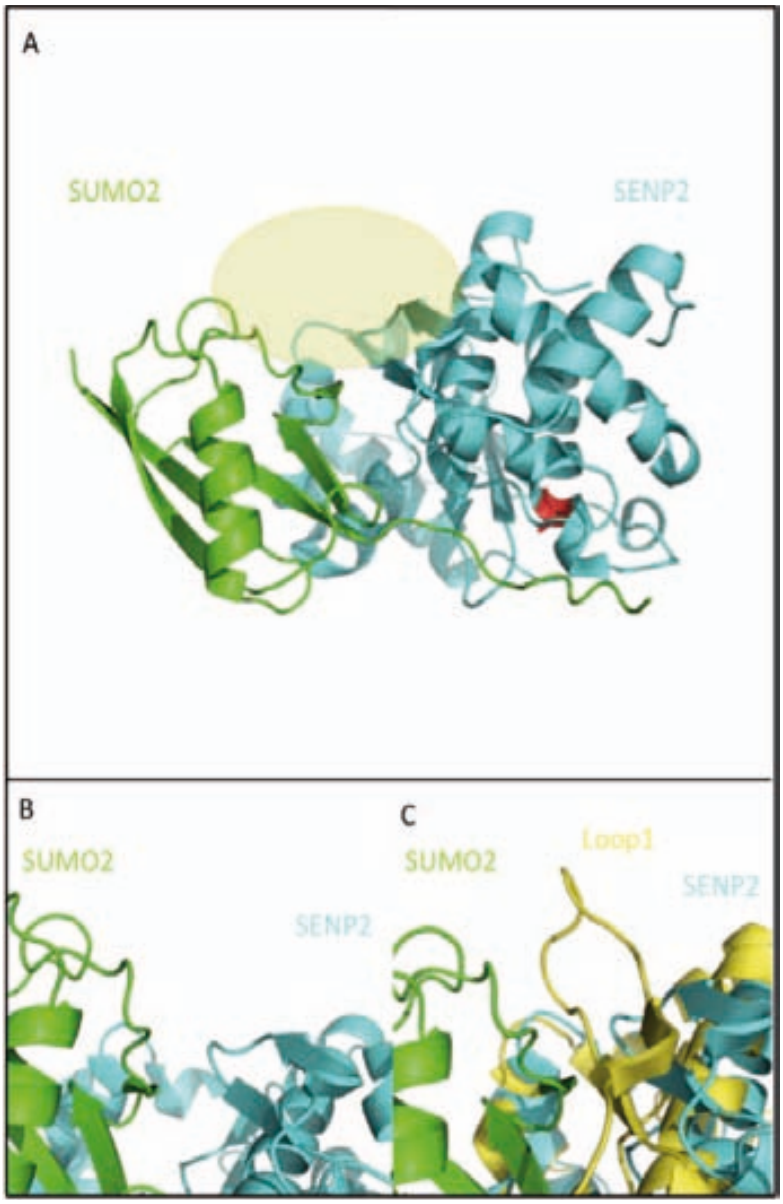

Figure 1. Structural models for interactions between SENP7 and SUMO. Top panel, A, structure of SENP2 in complex with SUMO2 with tentative SENP7 Loop1 interface site shown as a *yellow circle* (PDB2io0). Lower panels, B and C, close-up of tentative SENP7 Loop1-SUMO interaction site shown by superposition of SENP7 catalytic domain structure with SENP2-SUMO2 complex (PDB3eay). SENP2 is shown in *cyan*, SUMO2 is shown in *green* and SENP7 is shown in *yellow*. SENP7 Loop1 is shown in *stick* configuration. The location of the catalytic cysteine (in this complex serine) is shown in *red*. All images were modified and represented using the respective PDB files in PyMOL (DeLano, W.L., 2002).

In previous biochemical experiments, loop deletions were performed on SENP7 and subsequently run in both processing and deconjugation reactions. Loss of Loop1 reduced rates not only in the processing reactions compared to wild-type SENP7 but also dramatically reduced the ability of SENP7 to deconjugate both diSUMO and polySUMO substrates (Reverter and Lima; 2008).

Model for SENP6/7 Interaction with SUMO2/3 and Identification of Interface Residues

Using this information, similar deletions were performed on SENP6 and in addition residues were shown to interact with Loop1 in the overlay of SUMO1/2-SENP2 and SENP7 were identified and targeted for mutagenesis. The first of these residues, His 71 on SUMO1, produces a net positive charge, which would theoretically not be conducive in the polar, slightly positive cleft formed by Loop1 on SENP6/7. The corresponding residue on SUMO2 is an aspartic acid and the negative charge on this residue would be more suitable in the given environment. The second residue is Ala68 on SUMO1 and Asn68 on SUMO2, and the advantage of SUMO2 here is that the polar asparagine, as opposed to nonpolar alanine group, would be more accommodated polarly in the Loop1 environment.

Figure 2. Structural models for interactions between SENP7 Loop1 and SUMO1/2 interface residues. Top panel, A, overlay of SENP2-SUMO1 and SENP7 to show tentative interaction between N68 and H71 of SUMO1 and SENP7 Loop1 (PDB1tgz and PDB3eay). Top panel, B, electrostatic potential surface representation of SUMO1 with key residues *labeled*. Bottom panel, C, overlay of SENP2-SUMO2 and SENP7 to show tentative interaction between A68 and N71 of SUMO2 and SENP7 Loop1 (PDB2io0 and PDB3eay) Bottom panel, D, electrostatic potential surface representation of SUMO2 with key residues *labeled.* All proteins are shown in *cartoon* representation and SENP2 is shown in *cyan*, SUMO2 is shown in *green* and SENP7 is shown in *yellow*. SENP7 Loop1 and SUMO1/2 interface residues are shown in *stick* configuration. All images were modified and represented using the respective PDB files in PyMOL (DeLano, W.L., 2002).

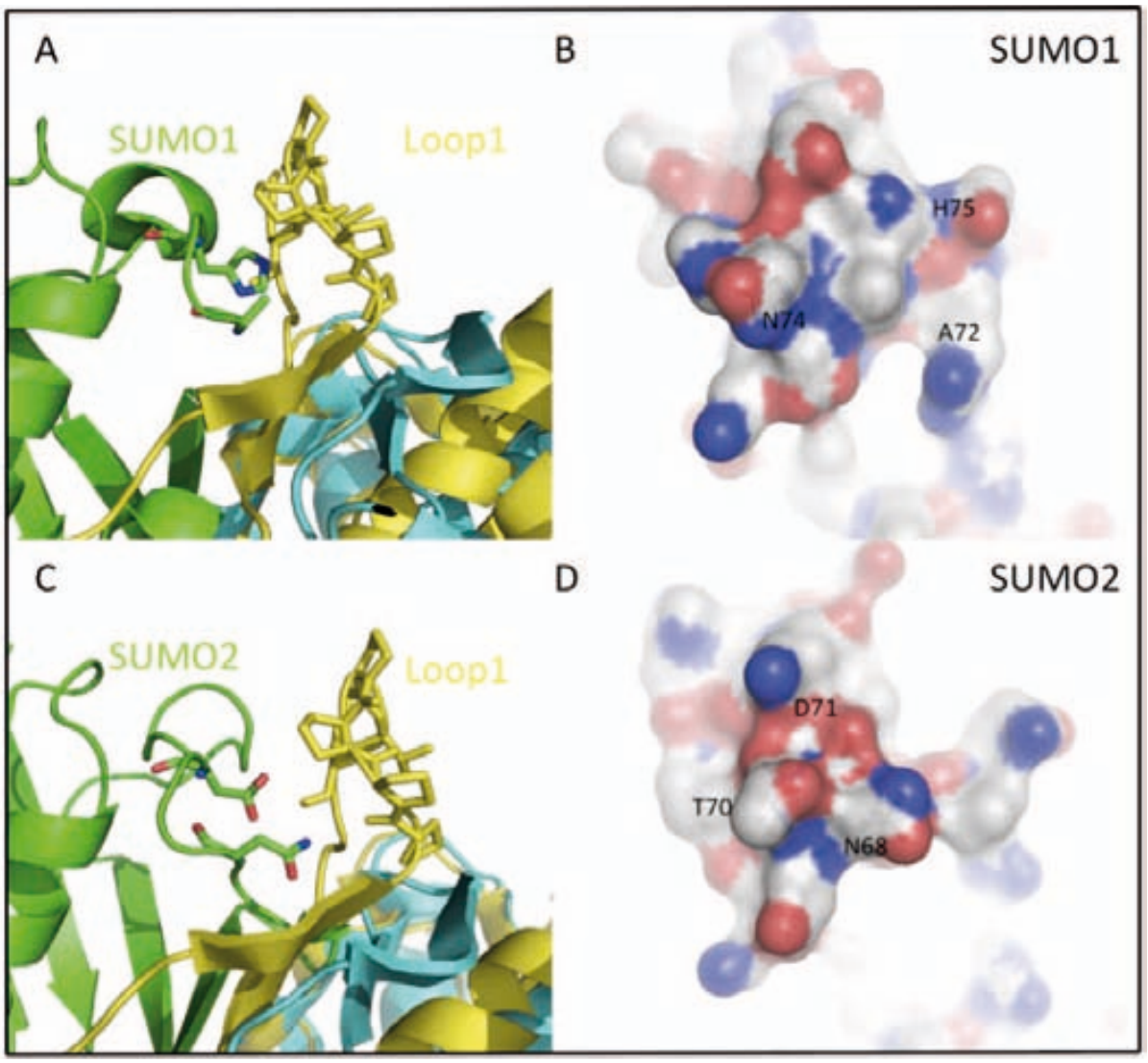

Swapping SUMO1/SUMO2 in the Processing Reaction

Two mutant SUMOs were produced, SUMO1A68NH71D-GG and SUMO2N68AD71H-GG that exchanged the identified residues of SUMO1 for those of SUMO2 and vice versus (Fig 3). As expected, the processing of both wild-type SUMOs by SENP6 and SENP7 was lower than that of SENP2, but they

did show a slight preference for SUMO2. The SUMO1mutant (SUMO2-like) was processed at a higher rate than SUMO1 by SENP6 and SENP7 and the SUMO2mutant (SUMO1-like) was processed at a lower rate, confirming our hypothesis that residues A68 and H71 are at least somewhat responsible for the isoform specificity of SENP6 and -7 (Fig 3, A). In order to look at the more gradual changes involved in the processing reaction, a time course assay was run with SENP6, Δ1 and Δ3 (which shows similar activity to Δ2) at 5nM and substrates at 5μM. The same trend was seen here as in the titration assay; processing of SUMO1 enhances with the mutant form and that of SUMO2 diminishes with the SUMO-1 like form (Fig 3, C). In this assay however, the preference of SENP6 for SUMO2 over SUMO1 is more distinguishable.

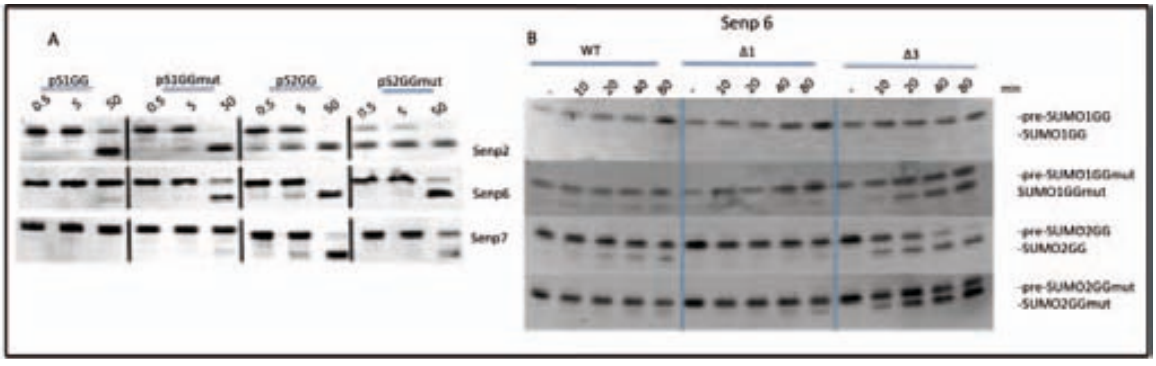

Figure 3. Processing of SUMO1/2 and associated mutants by SENP2/6. Top panel, A, activity assay of SENP2 and -6 wild type against pSUMO1GG, pSUMO1GGN68AH71D, pSUMO2GG and pSUMO2GGA68ND71H. Assays were run at 0.5, 5 and 50nM enzyme concentrations and 5μM substrate concentration at 37°C and stopped after 15 minutes with SDS

loading buffer and analyzed with PAGE. Top panel, B, time course assays using SENP6 wild type and SENP6Δ1 and -Δ3 against pSUMO1GG, pSUMO1GGN68AH71D, pSUMO2GG and pSUMO2GGA68ND71H. Reactions were run at 0.5nM enzyme concentration and time intervals are indicated above each lane in minutes. Reactions were stopped at each respective interval with SDS loading buffer and analyzed by PAGE. Proteins in both assays were detected by staining with SYPRO (Bio-Rad).

Swapping RanGAP1-SUMO1/SUMO2 in the Deconjugation Reaction

The mammalian guanosine triphosphate (GTP)-ase-activating protein RanGAP1 was the first example of a protein covalently linked to SUMO-1 and its modification results in the transfer of the protein from the cytoplasm to the nuclear pore complex (Mahajan *et al*; 1997 and 1998). RanGAP-SUMO moieties were previously used to test the deconjugation activities of SENP2, -6 and -7 by Reverter and Lima (2008). In these experiments it was shown that SENP6 and -7 were able to deconjugate RanGAP1 from SUMO2 at rates comparable to that of SENP2 but as expected, were less proficient at deconjugating RanGAP1 from SUMO1. We constructed novel substrates using SUMO1A68NH71D and SUMON68AD71H conjugated to RanGAP1 to determine whether the mutated amino acids had an effect on the deconjugation abilities SENP6. Wild type SENP2 and SENP6 were run in activity assays against RanGAP-SUMO1, RanGAP-SUMO1 mutant, RanGAP-SUMO2 and RanGAP-SUMO2 mutant (Fig. 4, A). SENP2 was universally active against all conjugates and as expected SENP6 was almost inactive against the RanGAP-SUMO1 moiety and considerably more active against the RanGAP-SUMO2 substrate. SENP6 showed the same increase and decrease against the mutant substrates (Fig 4, A and B). A

time course reaction was run with SENP2, -6 and Δ3Senp6 and in this assay the comparable activities of the loop deletion mutant and SENP2 become more apparent (Fig 4, C). SENP6 wild type followed the same trend seen in the activity assay and interestingly the protease was able to achieve the same activity against RanGAP1-SUMO2 at a concentration only five times less than that of SENP2.

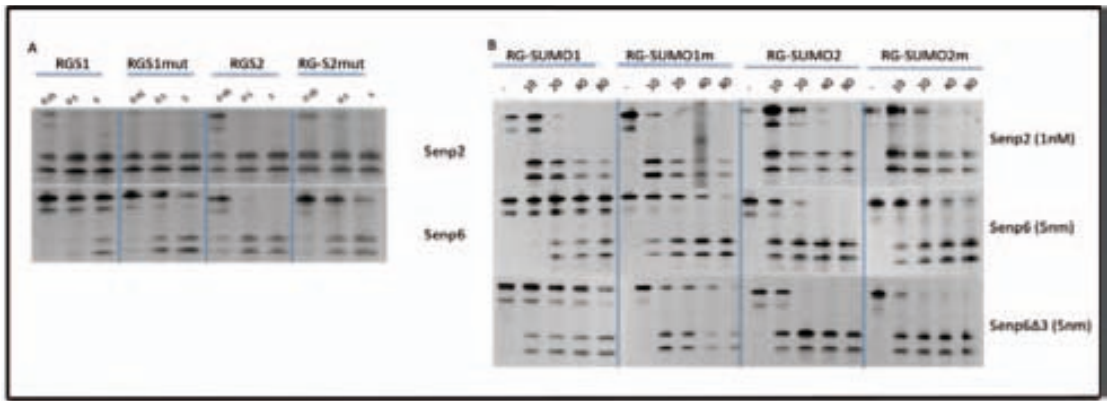

Figure 4. Deconjugation of SUMO1/2 and associated mutants from RanGAP1 by SENP2/6. Top panel, A, activity assay of SENP2 and -6 wild type against RanGAP-SUMO1, RanGAP-SUMO1N68AH71D, RanGAP-SUMO2 and RanGAP-SUMO2GGA68ND71H. Assays were run at 0.05, 0.5 and 5nM enzyme concentrations and 5μM substrate concentration at 37°C and stopped after 15 minutes with SDS loading buffer and analyzed with PAGE. Top panel, B, time course assays using SENP2 and -6 wild type and Δ3 against RanGAP-SUMO1, RanGAP-SUMO1A68NH71D, RanGAP-SUMO2 and RanGAP-SUMO2GGN68AD71H. Reactions were run at enzyme concentrations indicated next to each enzyme and time intervals are indicated above each lane in minutes. Reactions were stopped at each respective interval with SDS loading buffer and analyzed by PAGE. Protein in both assays were detected by staining with SYPRO (Bio-Rad)

Swapping SUMO1/SUMO2 in diSUMO Deconjugation Reaction

In an experiment run by Mukhopadhyay *et al.*, a tagged construct of RanGAP1 was incubated with E1 and E2 enzymes and SUMO and subsequent high molecular weight SUMO species were run in activity assays to test whether

SENP6 (SUSP1 using their nomenclature) was more active in the deconjugation of mono- versus multiple-SUMOylated species (Mukhopadhyay et al.; 2006). By immunoprecipiation of the SENP6 fraction, it was found that SENP6 was in fact able to deconjugate species containing multiple SUMO2s more than those containing single SUMO2 or any SUMO1-containing substrates. Reverter and Lima further demonstrated this phenomenon in a similar experiment implementing diSUMO2 or -3 and poly-SUMOylated constructs (2008).

Two mutant SUMO substrates were constructed to confirm not only the preferential substrate cleavage of SENP6 but also the proficiency of SENP6 at dismantling substrates containing two or more SUMO moieties. The first substrate was a chimera of SUMO1 and SUMO2 and was formed by using Δ18SUMO1 as the donor (or species containing the exposed C-terminal –GG) and SUMO2ΔGG as the acceptor (which contains the internal Lys11). For the second mutant we created a merged diSUMO2 hybrid using Δ14SUMO2 as the donor and SUMO1-like SUMO2D71HN68A as the acceptor. Deconjugation assays were run against both mutants as well as diSUMO2 at protease concentrations of 0.05, 0.5 and 5nm (Fig 5, A, B and C). In the deconjugation of SUMO2 from diSUMO2 we see for the first time comparable activities between SENP2 and SENP6 and again we see the greatest activity from the SENP6 Loop3 deletion mutant. When the SUMO1-SUMO2 chimera is used as a substrate the activity of all SENP2, SENP6 and SENP6 Δ3 is substantially reduced to levels comparable to when RanGAP1-SUMO1 was used as a substrate and when the SUMO2-SUMO1-like

substrate was implemented an activity immediately between those of the diSUMO2 and diSUMO1/2 was observed.

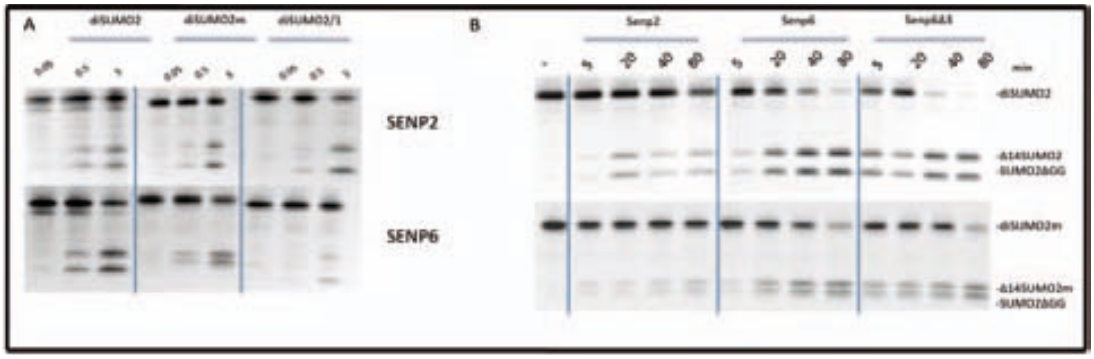

Figure 5. Deconjugation of multi-SUMOylated, isoform-specific moieties by SENP2/7/6. Top panel, A, activity assay of SENP2 and -6 wild type and SENP6Δ3 against diSUMO2, diSUMO2/1 and diSUMO2/2A68ND71H(m). Assays were run at 0.05, 0.5 and 5nM enzyme concentrations and 0.5μM substrate concentration at 37°C and stopped after 15 minutes with SDS loading buffer and analyzed with PAGE. Top panel, B, time course assays using SENP2 and -6 wild type and Δ3 against diSUMO2 and diSUMO2m. Reactions were run at enzyme concentrations indicated next to each enzyme and time intervals are indicated above each lane in minutes. Reactions were stopped at each respective interval with SDS loading buffer and analyzed by PAGE. Protein in both assays were detected by staining with SYPRO (Bio-Rad)

SENP6 Loop Deletion Mutants

Mutational analysis of SENP7 by Reverter and Lima (2008) revealed residues critical to the dismantling of diSUMO2 and poly-SUMO chains. Loop deletions of SENP7 provided further insight into key characteristics of the protease; over the assayed one hundred and twenty minutes, Loop1 removal resulted in significant rate reductions both in the deconjugation of diSUMO2 and of poly-SUMO chains. While removal of Loop2 and -3 didn't produce noticeable differences in the initial rate kinetics, over the one hundred and twenty minute assay, the ΔLoop2 mutant did show slightly decreased activity compared to the

wild type and the ΔLoop3 mutant showed a slight increase in activity. In order to see if SENP6 loop deletions shared the same change in activity, we constructed a Δ1, Δ2 and Δ3SENP6 and ran assays against diSUMO2 and associated mutants (Figure 6). As expected, removal of Loop1 resulted in the diminishment of all activity against diSUMO2 (as anticipated Δ1SENP6 activity did not vary over any of the mutated substrates given that the mutations made were on the SUMO-Loop1 interface) and removal of Loop2 was comparable to wild-type SENP6. Interestingly removal of Loop3 resulted in an increase in the activity of the protease against all substrates. Overall SENP6Δ3 activity shows no deviation from the trends observed for SENP6 and a summary of reaction kinetics is shown in Figure 7 (deconjugation vs. processing; SUMO2 vs. SUMO1). It was formerly postulated that this loop (due to its location and size) might play a role in recognition or serve a scaffold for interaction with di- or poly-SUMOs. Given that there is an increase in the activity of enzyme once this loop is removed, it is more likely that this loop insertion is hindering the interaction of SENP6 and multi-SUMO conjugates, rather than encouraging it

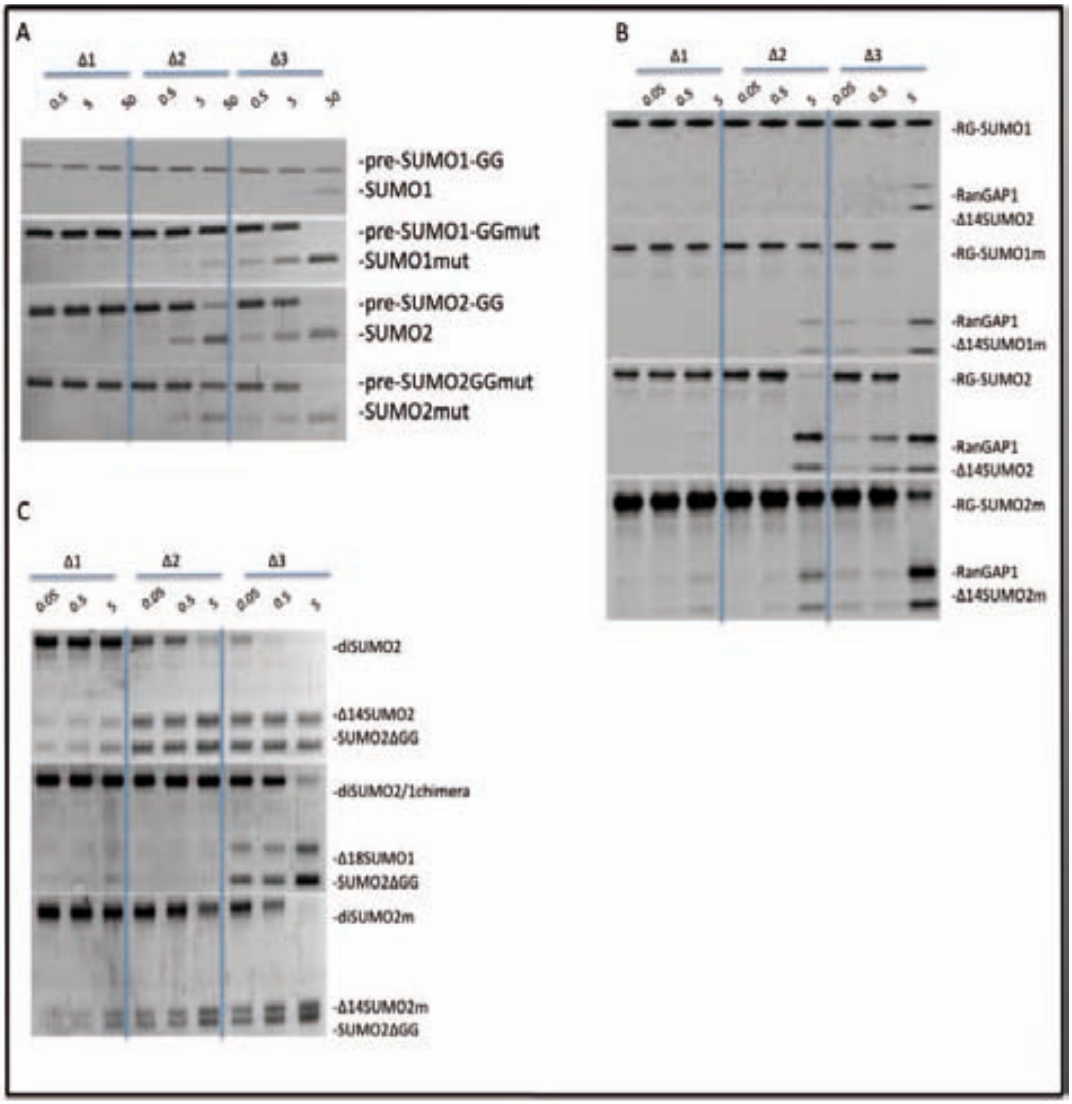

Figure 6. Processing and deconjugation of deletion mutants SENP6-1, --2 and --3. Top panel, A, activity assay of SENP6-1, --2 and --3 against pSUMO1GG, pSUMO1GGN68AH71D, pSUMO2GG and pSUMO2GGA68ND71H. Top panel, B, activity assay of SENP6-1, --2 and --3 against RanGAP-SUMO1, RanGAP-SUMO1N68AH71D, RanGAP-SUMO2 and RanGAP-SUMO2GGA68ND71H . Bottom panel, C, activity assay of SENP6-1, --2 and --3 against diSUMO2, diSUMO2/1 and diSUMO2/2A68ND71H(m). All assays were run at 0.05, 0.5 and 5nM enzyme concentrations and 0.5M substrate concentration at 37°C and stopped after 15 minutes with SDS loading buffer and analyzed with PAGE. Protein in all assays were detected by staining with SYPRO (Bio-Rad)

Figure 7. Kinetic analysis for processing and deconjugation of 3SENP6. Top panel, A and B, processing and deconjugation activities of 3SENP6, respectively taken at T=0, 10, 20, 40 and 80min. Middle panel, C and D, processing and deconjugation initial rate activities of 3SENP6 taken at T=0, 5, 10, 15 and 20min. Bottom panel, E and F, bar representation for initial rate velocities for processing and deconjugation of 3SENP6 determined within a linear range from data obtained from C and D. Axes are labeled, and error bars were obtained by conducting assays in triplicate.

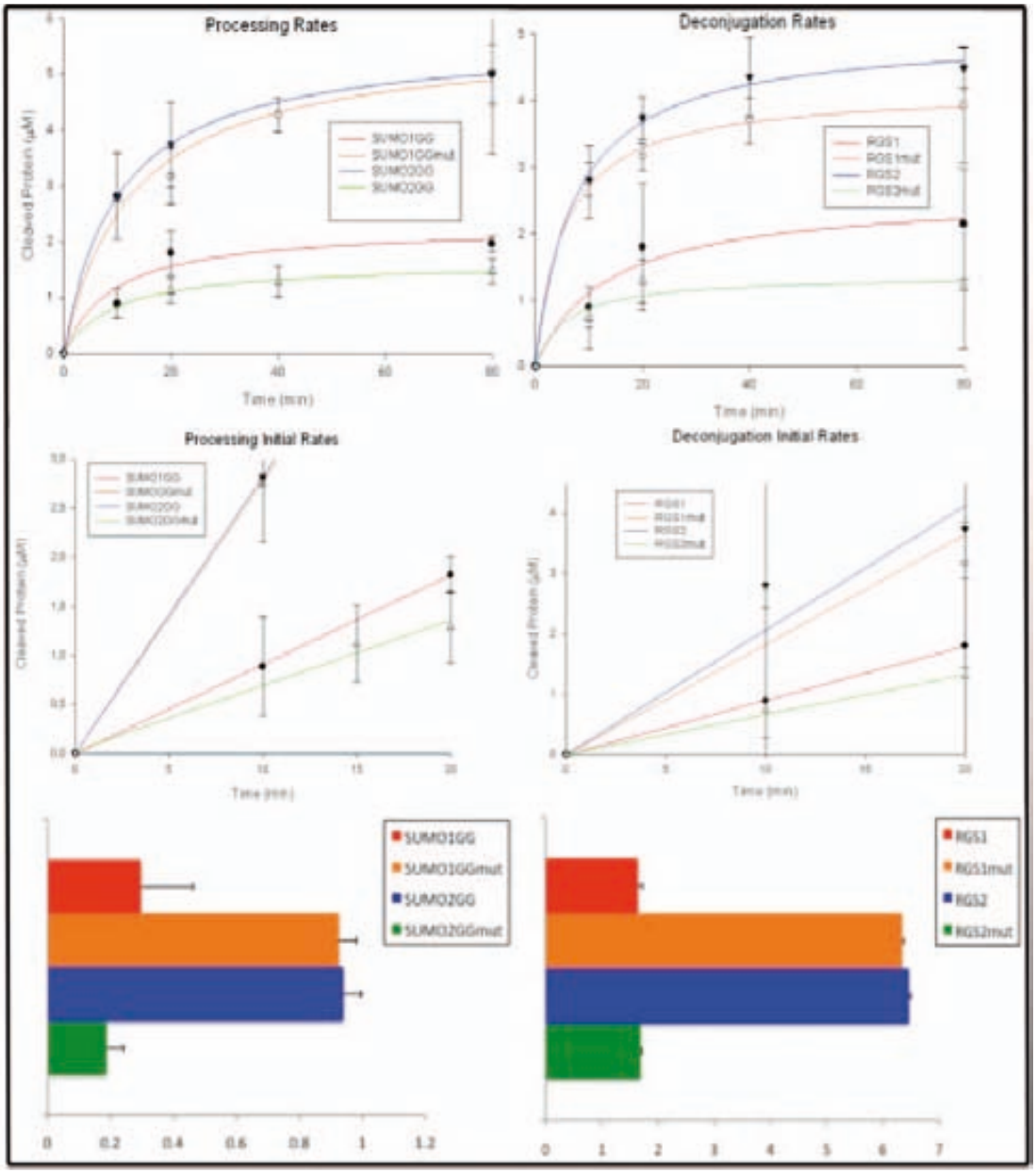

Steady-State Kinetic Analysis of SUMO1 Mutants

To estimate the kinetic parameters of the contribution of this novel surface of SUMO to the proteolytic activity of SENP6 and SENP7 subclass, we have developed a more quantitative activity assay using deconjugation substrates that are chemically modified with a fluorophore (Alexa Fluor-488). The maleimide group of Alexa-fluor-488 reacts covalently with cysteine residues. To develop this reagent we have produced a double mutant of SUMO1 with the substitutions of Ser9 for cysteine and Cys52 for alanine. SUMO1 (S9C/C52A) is modified with the fluorophore at the flexible N-terminal tail at position 9, which is not essential for activity. Although SUMO1 contains a cysteine residue buried in the hydrophobic core (Cys52), it has been replaced by alanine to avoid a potential modification by the fluorophore that could affect the catalytic properties of the SUMO proteases. SUMO1 (S9C/C52A) was tested in conjugation assays and compared with SUMO1 wild type to assess that they both have similar catalytic properties (data not shown).

Deconjugation time-course reactions were run using fluorogenic RanGAP1-SUMO1 and RanGAP1-SUMO1 (A72N/H75D) substrates with SENP2 and SENP6 at 1nM and 25 nM, respectively (Figure 8). As shown in previous results (Figures3, 4 and 5), there is a clear gain of proteolytic activity for SUMO1 (A72N/H75D) double point mutant compared to SUMO1 wild type for SENP6, in contrast to SENP2 where both substrates display almost similar catalytic

properties. Michaelis-Menten representation of the initial velocities measured for a range of substrate concentration varying from 0.25 μM to 100 μM, displayed hyperbolic curves that allowed us to estimate the catalytic constants of the reaction (figures 7B & 7C). Michaelis-Menten constants K_m were 41.6 and 13.16 μM for SUMO1 and SUMO1 (A72N/H75D) substrates, respectively; whereas the catalytic constant k_{cat} were 0.075 and 0.294 s^{-1} for SUMO1 and SUMO1 (A72N/H75D) substrates, respectively. The total gain of proteolytic activity by the SUMO1 double point mutant is approximately 12.5-fold, as estimated by the k_{cat}/K_m catalytic efficiency of the enzyme. Based on these results, this novel interface between Loop1 of SENP6 and SENP7 and SUMO affects both the binding and the catalytic properties of the enzyme.

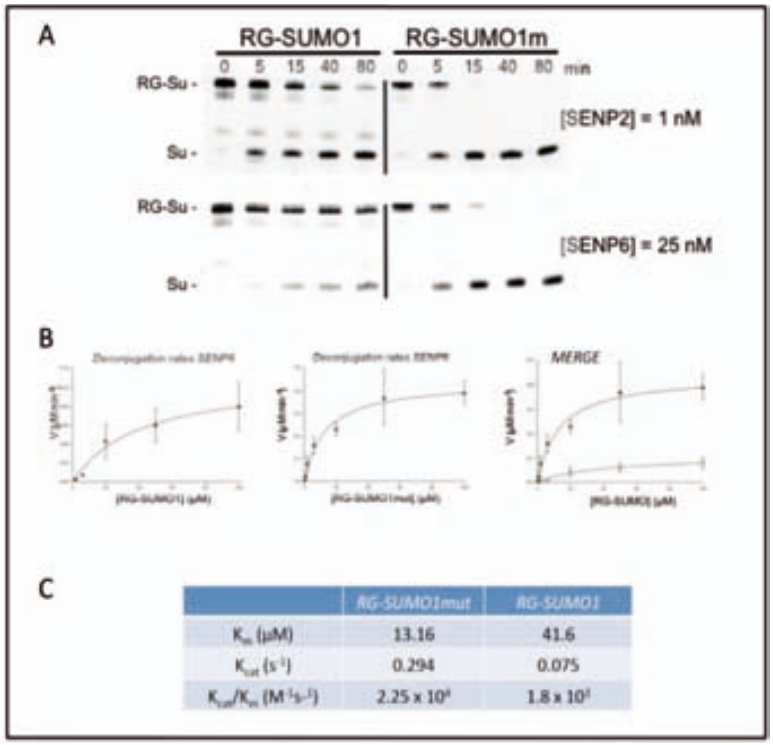

Fig 8. Steady-state kinetics of the deconjugation reaction for RanGAP1-SUMO1 and SUMO1mut by SENP6. Top panel, a, deconjugation activity of SENP6 against RGS1 and RGS1A68NH71D. S9C and C52S were introduced in SUMO1 and

SUMO1A68NH71D to allow for flurophore addition and proteins were subsequently conjugated to RanGAP1. Activity was measured at five different substrate concentrations (0, 5, 20, 50 and 100mM) and at 25nM enzyme concentration. Reactions were stopped after intervals indicated above each lane in minutes with SDS loading buffer and analyzed by gel electrophoresis. Top panel, b, graphic representation of substrate concentration (□M) vs. velocity (□M min^{-1}) at time intervals 0, 5, 15, 40 and 80 minutes. Bottom panel, c, kinetic coefficients K_m, k_{cat} and k_{cat}/K_m obtained from data in b for RGS1 and RGS1mut.

Loop1 SENP6/7 Is Responsible For SUMO Specificity

Structure of Loop1

In a previous work by Lima and Reverter the proteolytic activity of the four sequence insertions located in the catalytic domain of SENP7 (named Loop1 to Loop4) was partially characterized and we have recapitulated this with SENP6. Of special interest was the Loop1 insertion, which is composed of 8 residues including four prolines, two glycines and a lysine residue in the center of the loop. Loop1 is structured in the crystal structure of SENP7 and its deletion produced important defects in the proteolytic activity of SENP7. Loop1 is unique to the SENP6 and SENP7 subclass, and sequence alignment displays a high degree of sequence identity with respect to SENP6, with only one single amino acid substitution (Thr690 for Ala) (Figure 89). A structural feature of Loop1 is the presence of a short stretch of four proline residues, forming a poly-proline helix structure. A poly-proline helix is a type of secondary structure that restrains conformational flexibility of Loop1, despite its lack of interactions with the core of the protease.

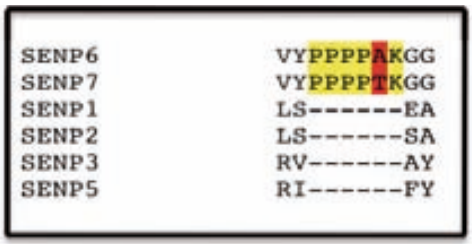

Figure 9. Sequence alignment of the SENPS at Loop1 region. Residues in Loop1 are *highlighted* and SENP6/7 amino alanine for threonine substitution is shown in *red*.

Mutagenic Analysis of SENP7 Loop1

To determine the structural basis for the Loop1 role in the proteolytic activity, we designed several mutant constructs of Loop1 of SENP7 (Figure 10). The first construct contained the substitution of the four consecutive prolines residues by glycines. The SENP7 (4Pto4G) mutant will assess the role of Loop1 in the activity of the protease by disrupting its spatial conformation. The introduction of four glycines increases the flexibility of the main chain of Loop1 and could lead to a non-productive interaction with the SUMO substrates in activity assays. Loop1 contains only one prominent charge residue at the center of it, Lys691, which could be relevant by establishing polar interactions with SUMO substrates. We have designed two single point mutants, Lys691 to Glu, in order to invert its charged properties, and Lys691 to Ala, which removes both the basic ε-amino group and the aliphatic side chain.

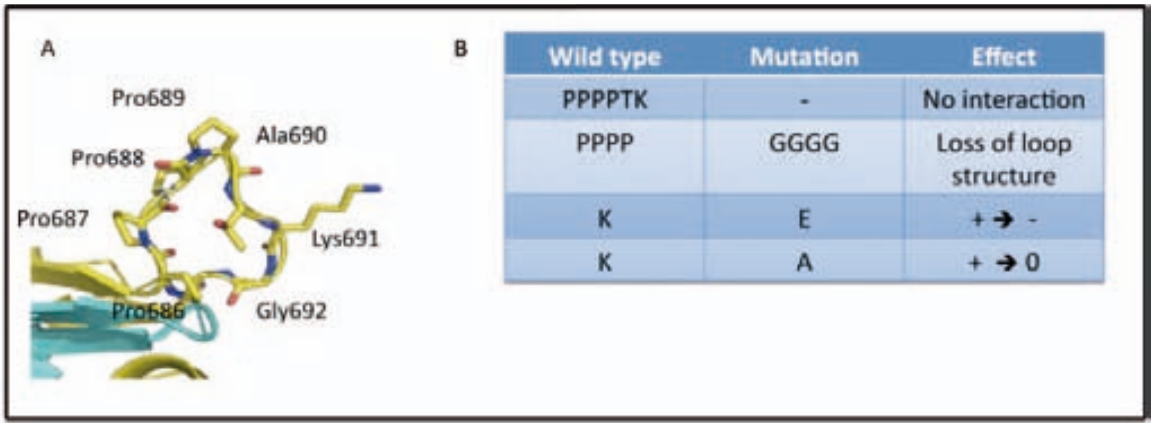

Figure 10. Summary of Loop1 mutations. Top panel, A, structure of SENP7Loop1. Residues are *labeled* and shown in *stick* configuration. Top panel, B, table of wild type and mutated residues in SENP7Loop1 and presumed effect on charge and structure.

SENP7 Loop1 mutants were tested against diSUMO2 and polySUMO2 chains substrates by using time course deconjugation analysis (Figure 11A and B). Deletion of Loop1 seriously compromises the proteolytic activity of SENP7, as previously described. The SENP7 Loop1 mutant construct of four prolines to glycines (SENP7 4Pto4A in Figure 10), which would increase the flexibility of Loop1, reduces the proteolytic activity of SENP7 as much as deletion of the whole Loop1 does. SENP7 single point mutant of lysine 691 to glutamic acid (SENP7 K691E in Figure 10) also dramatically reduces the proteolytic activity of the protease. Finally, the SENP7 single point mutant of lysine 691 to alanine (SENP7 K691A in Figure 10) has a reduction of the proteolytic activity to a lesser degree compared to the other constructs. In order to estimate the differences in the activity, initial rate velocities were measured for the diSUMO2 deconjugation reaction at 0.5nM of final enzyme concentration (Figure 10C & D). Deconjugation

rates for SENP7 wild type are approximately 10 to 20-fold faster than SENP7-ΔLoop1, SENP7 (K691E) and SENP7 (4Pto4G), whereas for SENP7 (K691A) the activity reduction is not so marked compared to the other mutant constructs.

These biochemical analyses with the SENP7 mutant constructs reveal that both the spatial conformation of Loop1 and the charge properties of Lys691 are important for a productive interaction of SENP7 with SUMO2, and thus for the correct cleavage of SUMO substrates. It is worth noting that Loop1 only represents a small region of the total interface of SENP7 with SUMO and that it is not present in the other members of the mammalian SENP family. Loop1 interaction with SUMO has not been described before and our data indicate that it can enhance the proteolytic activity for SENP6 and SENP7. Our next step was to figure out the putative surface region in SUMO that directly interacts with Loop1 of SENP6 and SENP7.

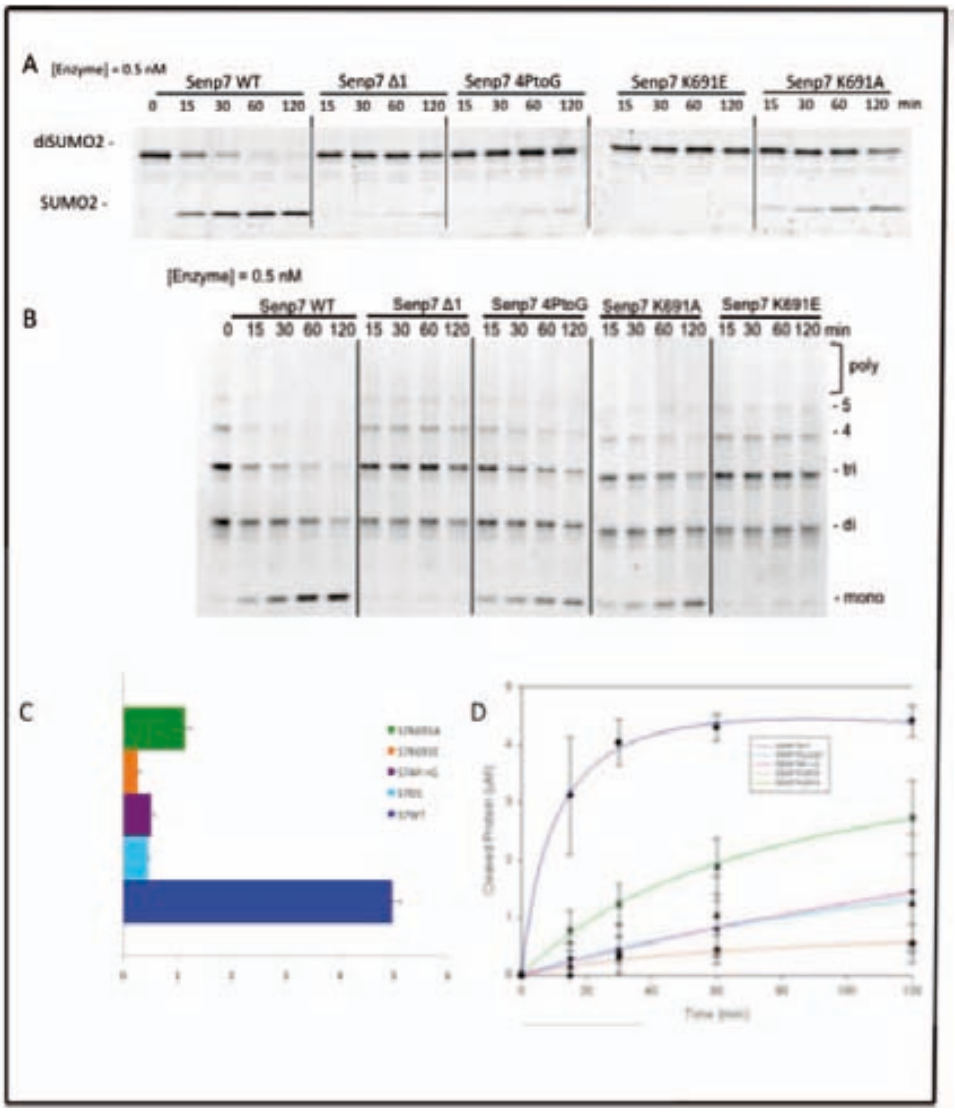

Figure 11. Deconjugation of diSUMO2 and polySUMO2 chains by SENP7 and associated mutants (next page). Top panel, A, time-course assay of SENP7WT, SENP7Δ1, SENP74PG, SENP7K691A and SENP7K691E against diSUMO2. Top panel, B, time-course assay of SENP7WT, SENP7Δ1, SENP74PG, SENP7K691A and SENP7K691E against polySUMO2. Reactions were run at 0.5nM enzyme concentration and time intervals are indicated above each lane in minutes. Reactions were stopped at each respective interval with SDS loading buffer and analyzed by PAGE. Proteins in both assays were detected by staining with SYPRO (Bio-Rad). Bottom panel, C, bar representation of approximate initial rate velocities for deconjugation of diSUMO2 determined within a linear range from data obtained from *D*. Bottom panel, D, kinetic analysis of deconjugation of diSUMO2 by SENP7 and associated mutants taken at 0, 15, 30, 60 and 120 min. *Axes* are labeled and *error bars* were obtained by conducting assays in triplicate.

Loop1 SENP7 Interaction with SUMO2

Based on previous structures of the complexes of SENP2 with either SUMO1 or SUMO2 we have predicted a region on the SUMO surface that is located close to Loop1 of SENP6 and SENP7 (Reverter and Lima, 2006; Shen et al 2006). Crystal structures of the complex between SENP1, SENP2 or ULP1 with SUMO indicate that the main residues involved in the interface and in the catalysis are conserved for all members of the SENP/ULP protease family. Thus, despite the lack of a crystal structure of the complex, we assume that the extended quilt-like interface observed between SUMO and SENP2 is going to be conserved for the SENP6 and SENP7 complexes. Our structural model indicates that a slight conformational move can place Loop1 close to a SUMO surface region. This surface seems to be more negatively charged for the SUMO2 isoform compared to SUMO1 (Figure2A and B). Thus, the disruption of this interface would be responsible for the SENP7 proteolytic defects described in Figure 10.

In order to investigate this region we have produced a single point mutation in SUMO2 of Asp71 for lysine, which could interfere with the positive charge created by the side chain of Lys691 of Loop1 of SENP7. D71 is one of the residues proposed to confer SUMO2/3 specificity in the previous swapping experiments. We were able to synthesize diSUMO2 with SUMO2 (D71K) as a substrate for deconjugation assays. Time-course proteolytic cleavage of diSUMO2 (D71K) substrate shows a decrease in the proteolytic activity for all SENP7 constructs tested, including the wild type form (Figure 12A). Time course deconjugation reactions were run at 5 nM final enzyme concentrations, one order

of magnitude higher than the experiments in Figure 11A. Particularly interesting is the loss of proteolytic activity in SENP7 wild type that becomes as defective as all Loop1 mutant constructs (Figure 11A & B). It is worthwhile to mention that just a single change of charge, Asp71 for lysine, on the surface of SUMO2 distant from the cleavage site can produce marked defects in the proteolytic activity of SENP7, with an approximate 20-fold loss with respect to the diSUMO2 wild type reaction (compare to Figure 11). These results support the formation of this novel and more extended interface between Loop1 and SUMO2.

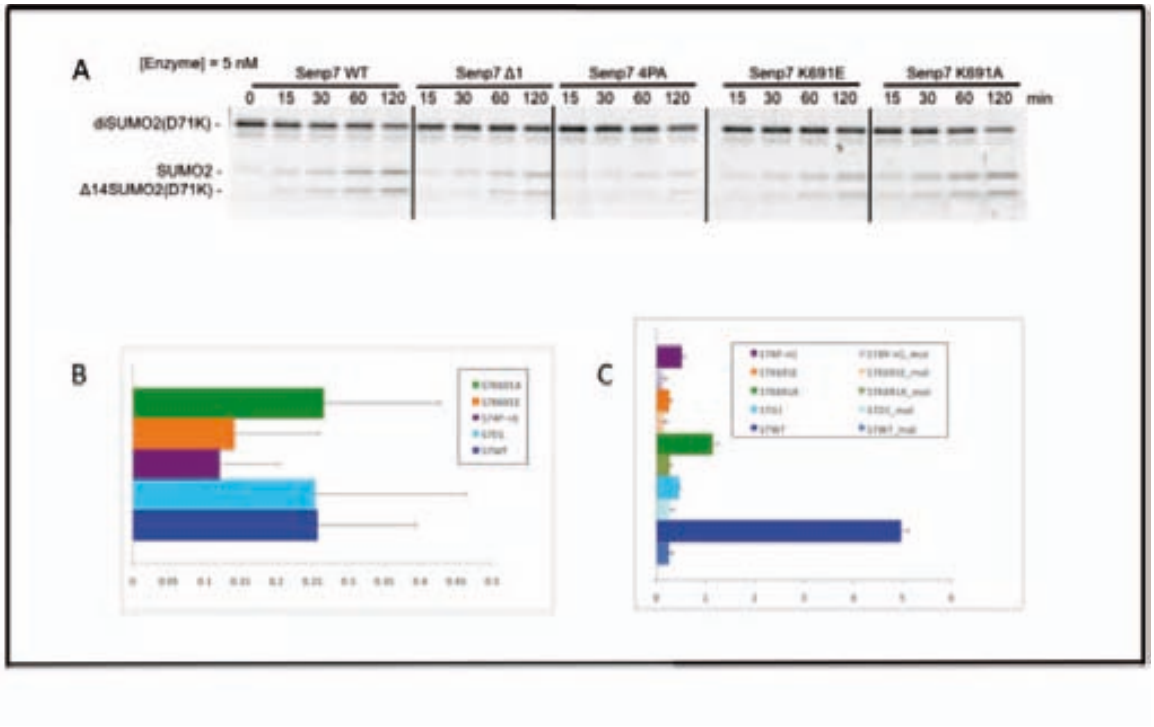

Figure 12. Deconjugation of diSUMO2(D71K) by SENP7 and associated mutants. Top panel, A, time-course assay of SENP7WT, SENP7Δ1, SENP74PG, SENP7K691A and SENP7K691E against diSUMO2 (D71K). Reactions were run at 5nM enzyme concentration and time intervals are indicated above each lane in minutes. Reactions were stopped at each respective interval with SDS loading buffer and analyzed by PAGE. Proteins in both assays were detected by staining with SYPRO (Bio-Rad). Bottom panel, C, kinetic analysis of deconjugation of diSUMO2 by SENP7 and associated

mutants taken at 0, 15, 30, 60 and 120 min. Bottom panel, B, bar representation of approximate initial rate velocities for deconjugation of diSUMO2(D71K) determined within a linear range from data obtained from *C*. Bottom panel, C, merge of initial rate velocities for deconjugation of diSUMO2 and diSUMO2(D71K) determined within a linear range from data obtained from Figure 10A and 11A). *Axes* are labeled and *error bars* were obtained by conducting assays in triplicate.

SENP2 Loop1 insertion is highly reactive against diSUMO2

Based on the aforementioned biochemical studies it can be concluded that SENP6/7 Loop1 is utile especially in the deconjugation of SUMO2 from diSUMO or multiSUMOylated species. We showed that complete removal of Loop1 from either SENP6 or SENP7 resulted in complete ablation of activity of either enzyme against diSUMO2 and mutation of Loop1 residues that compromised the structural and/or charge integrity of Loop1 affected the ability of SENP6 and SENP7 to deconjugate diSUMO2. In order to prove that Loop1 in and of itself if at least somewhat responsible for the ability of these enzymes to effectually cleave diSUMO2 we introduced Loop1 into the catalytic domain of SENP2 and studied the effects the insertion had on diSUMO2 deconjugation. We used sequence and structure-based comparisons between SENP7 catalytic domain and SENP2 in complex with RanGAP1-SUMO2 to the pinpoint the region within the SENP2 catalytic domain that would correspond to the Loop1 insertion in SENP6 and SENP7 (Figure 8 and 9). Residues 658-665 (PPPPAKGG) of SENP6, which differ from the SENP7 sequence by only one amino acid substitution were substituted C-terminal to residue 392 of SENP2 (Figure 13).

Figure 13. SENP6 Loop1 insertion in SENP2. Sequence alignment of SENP6 and SENP2 to show Loop1 insertion in SENP2. Inserted residues are shown in *red*. Structural alignment to show spatial arrangement of Loop1 in relation to SENP2 can be seen in Figure 9.

Time course deconjugation assays were performed with diSUMO2 as the substrate and the wild type SENP2 catalytic domain and the SENP2 catalytic domain containing the Loop1 insert as the enzymes (Figure 14). Reactions were run at 0.5nM enzyme concentration.

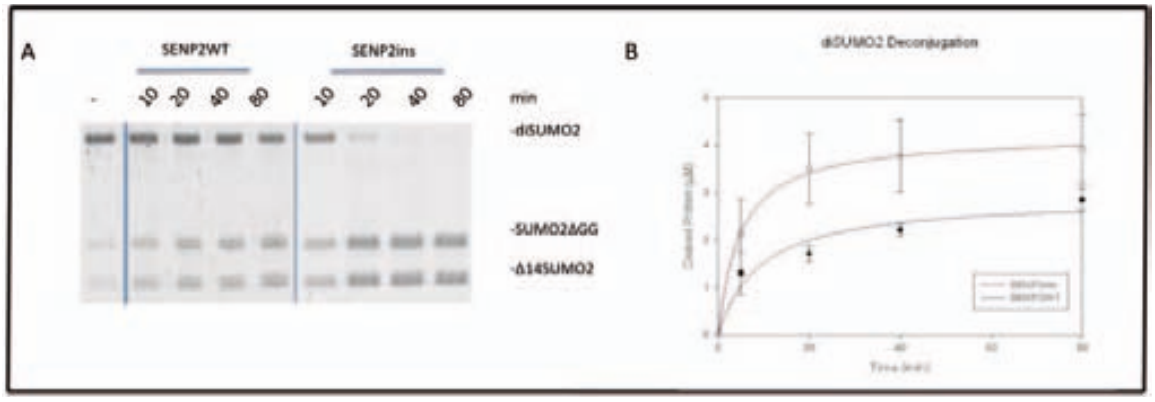

Figure 14. Deconjugation of diSUMO2 by SENP2 and SENP2ins. Top panel, A, time-course assay of SENP2 and SENP2ins against diSUMO2. Reactions were run at 0.5nM enzyme concentration and time intervals are indicated above each lane in minutes. Reactions were stopped at each respective interval with SDS loading buffer and analyzed by PAGE. Proteins were detected by staining with SYPRO (Bio-Rad). Top panel, B, kinetic analysis of deconjugation of diSUMO2 by SENP2 and SENP2ins taken at 0, 5, 20, 40 and 80 min. *Axes* are labeled and *error bars* were obtained by conducting assays in triplicate.

Similar to the time course assays performed in Figure 5, wild type SENP2 showed activity comparable to that of SENP6 and SENP7 with approximately 56% of diSUMO2 cleaved after the assayed 80 minutes. SENP2 containing the Loop1 insert however, showed an increase of 25% over the wild type with an average of 81% of diSUMO2 cleaved after the assayed 80 minutes. These results indicate that the Loop1 insertion at the indicated position is able to augment the already heightened SENP2 activity against diSUMO2 and that this increase is most likely due to the interaction between Loop1 and the tentative SUMO2 interaction surface on diSUMO2

Complexes With Substrates

Processing Complexes

In order to solidify the structural basis for our SENP6/7 isoform preference for multi-SUMOYlated SUMO2/3 species milligram amounts of active site mutants of SENP6 and various loop deletion mutants were made along with SUMO precursors, RanGAP1-SUMO2 and diSUMO2. While we were able to produce the entire catalytic domain of SENP6 (637-1112) in quantities sufficient for use in activity assays producing pure milligram amounts proved unfruitful. We opted instead to use SENP6 deletion mutants (SENP6Δ3 and SENP6Δ2Δ3) which were not only shown to be more active than the wild type construct but were able to be produced in milligram amounts. Both SENP6 isoforms eluted from gel filtration as single peaks consistent with their molecular weights (Figures 15 and 16). Due to the fact that both SENP6Δ2 and SENP6Δ3

showed catalytic activities in prior assays (Results) and that both enzymes behaved as expected it was assumed that they as well as the double deletion mutant SENP6□2□3CS showed no barriers in protein folding. A cysteine to serine mutant active site mutant was introduced into all proteases to (SENP6□3C1030S, SENP6□2□3C1030S and SENP2C548S) to render the enzymes inactive while at the same time stabilizing the enzyme-substrate complexes.

The structure of SENP2 was resolved both in a covalent thiohemiacetal transition-state complex and in the catalytically inert form in complex with SUMO precursors (Reverter and Lima, 2004 and 2006). We proved in *Results* that SENP6 was poor at activating SUMO precursors *in vitro* and when we attempted to form a stable complex via gel filtration we saw again that the SENP6-SUMO2GG interaction was not strong enough to elute as a single moiety and SENP6□3CS and SUMO2GG eluted at the elution volumes of the individual proteins (data not shown).

Deconjugation Complex with RanGAP1

The structure of SENP2 was also resolved in deconjugation complexes with RanGAP1-SUMO1 and RanGAP1-SUMO2 so our next step was to attempt to form a stable complex between SENP6 and RanGAP1-SUMO2, a substrate that from our activity assays was deconjugated by SENP6 at a fairly elevated rate (Reverter and Lima, 2006). This complex again did not form through gel filtration and SENP6□3CS and RanGAP1-SUMO2 eluted at their respective peaks

showing that these two proteins do no form a stable complex in solution (data not shown).

SENP6Δ3 Deconjugation Complex with diSUMO2

The same protocol was employed to make both SENP6-diSUMO2 complexes. ~7mg of SENP6Δ3CS (0.57μmol) and ~mg of diSUMO2 (0.57μmol) to a low salt buffer and incubated the mixture at room temperature for one hour before loading onto a HiLoad 20/60 Superdex200 column (GE Healthcare). SENP6Δ3CS has a molecular weight of ~35kDa and diSUMO2 has a molecular weight of 21kDa and individually SENP6Δ3CS elutes at around 223ml and diSUMO2 at 236ml (Figure 15A).

The SENP6Δ3CS-diSUMO2 complex elutes at 193.57ml resulting in a shift of ~29ml for SENP6Δ3CS and ~42ml for diSUMO2 (Figure 15A and B). The individual fractions were pooled and run on SDS-page and both SENP6Δ3CS and diSUMO2 eluted in the peak fractions at a near stoichiometrical ratio (taking into account the excess SENP6Δ3CS in the load fraction). On the HiLoad Superdex200 column a peak that elutes between 175 and 225ml corresponds to a protein of a molecular weight between 44 and 148kD and the SENP6Δ3CS-diSUMO2 complex elution at ~193ml corresponds with this approximation with a theoretical molecular weight of around 55kDa.

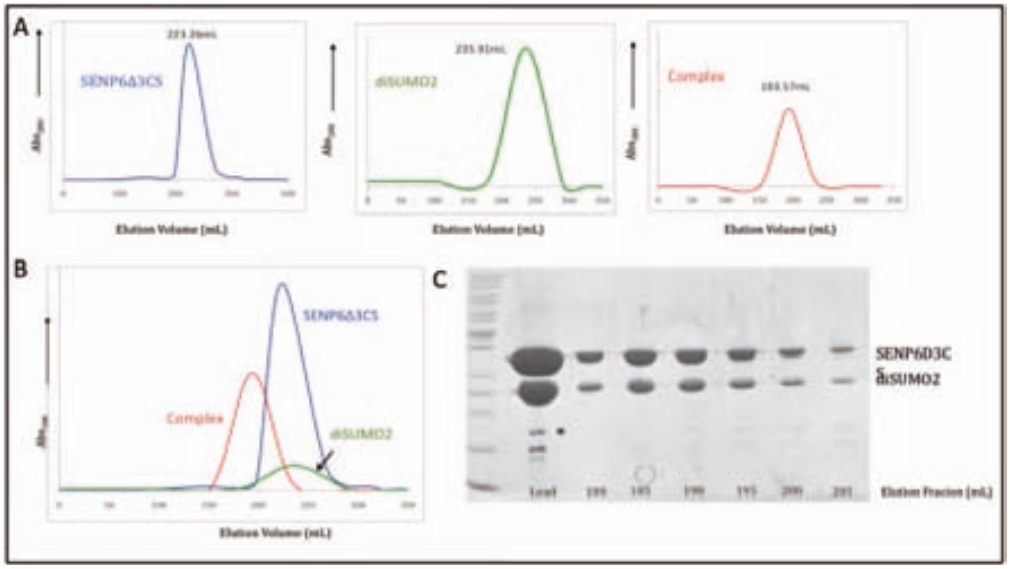

Figure 15. Gel chromatography of SENP6Δ3CS, diSUMO2 and complex. Top panel, A, chromatograms of SENP6Δ3CS (*blue*), diSUMO2 (*green*) and SENP2CS-diSUMO complex (*red*). Bottom panel, B, chromatogram of the merge of the SENP6Δ3CS, diSUMO2 and SENP6Δ3CS-diSUMO2 complex chromatograms found in *A*. All samples were run on a Superdex 200 gel filtration column (GE Healthcare) and peaks are *labeled* at the respective elution volumes. Bottom panel, C, collected fractions from gel filtration of SENP6Δ3CS -diSUMO2 analyzed by SDS-page. Elution fractions are *labeled* below each lane. Cleaved diSUMO2 (Δ14SUMO2 and SUMO2ΔGG) from active residual SENP2 is labeled with an *.

SENP6Δ2Δ3CS Deconjugation Complex with diSUMO2

Approximately 7mg of SENP6Δ2Δ3CS was also added to roughly the same number of milligrams of diSUMO2 and incubated for one hour at room temperature then loaded onto a HiLoad Superdex 200 gel filtration column (GE Healthcare). SENP6Δ2Δ3CS has a molecular weight of 33,250Da and elutes at around 226ml and as mentioned before diSUMO2 has an estimated molecular weight of 21,000Da and elutes at approximately 235ml (Figure 16A). Together the two proteins elute at ~212ml resulting a shift of 24ml for SENP6Δ2Δ3CS and 22ml for diSUMO2 (Figure 16 and B). The individual fractions were pooled and

analyzed by SDS-page (Figure 16C). Both proteins elute in the peak fraction (200 to 230ml) in a near 1:1 ratio at a molecular weight corresponding to between 30kDa and 60kDa which is consistent with the molecular weight of a SENP6Δ2Δ3CS-diSUMO2 complex which has the theoretical molecular weight of ~54.2kDa.

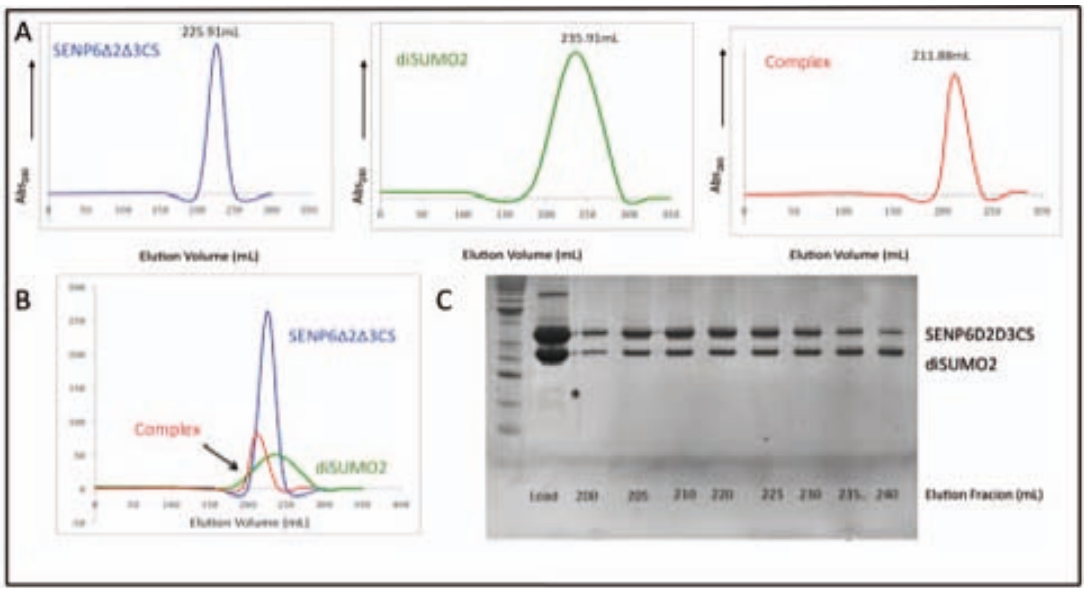

Figure 16. Gel chromatography of SENP6Δ2Δ3CS, diSUMO2 and complex. Top panel, A, chromatograms of SENP6Δ2Δ3CS (*blue*), diSUMO2 (*green*) and SENP6Δ2Δ3CS-diSUMO complex (*red*). Bottom panel, B, chromatogram of the merge of the SENP6Δ2Δ3CS, diSUMO2 and SENP6Δ2Δ3CS-diSUMO2 complex chromatograms found in *A*. All samples were run on a Superdex 200 gel filtration column (GE Healthcare) and peaks are *labeled* at the respective elution volumes. Bottom panel, C, collected fractions from gel filtration of SENP6Δ3CS -diSUMO2 analyzed by SDS-page. Elution fractions are *labeled* below each lane. Cleaved diSUMO2 (Δ14SUMO2 and SUMO2ΔGG) from active residual SENP2 is labeled with an *.

SENP6Δ2CS Deconjugation Complex with diSUMO2

A complex with SENP6Δ2CS with diSUMO2 was also attempted but in this case there was no complex formation. SENP6Δ2CS is a protein of around 53kDa and elutes at 194ml when run on a Superdex200 column. When incubated

with diSUMO2 and loaded on the gel filtration column, both proteins eluted at roughly their respective elution volumes (~192ml for SENP6ΔC2CS and 230ml for diSUMO2) indicating that there was no complex formation (Figure 17).

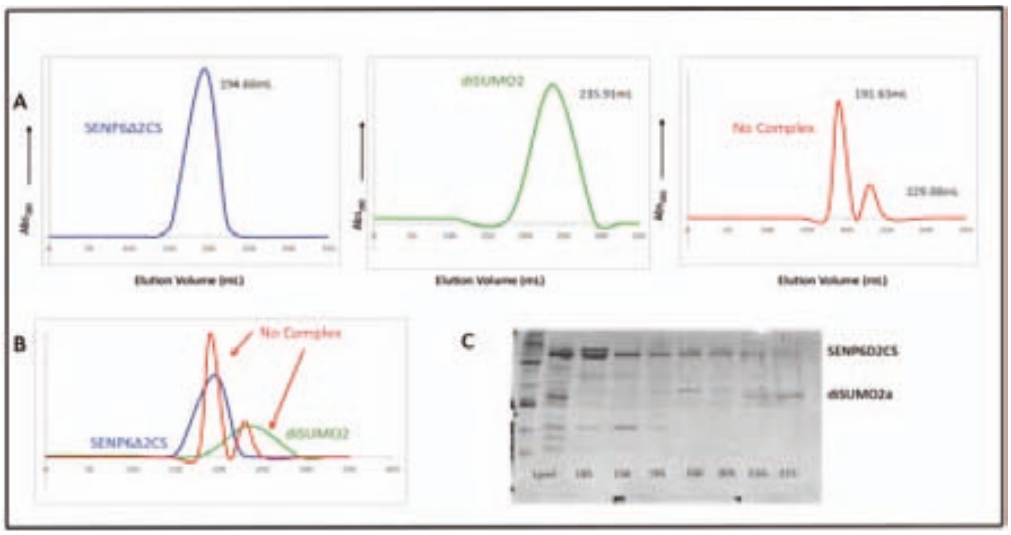

Figure 17. Gel chromatography of SENP6ΔC2CS, diSUMO2 and attempted complex. Top panel, A, chromatograms of SENP6ΔC2CS (*blue*), diSUMO2 (*green*) and SENP6ΔC2CS and complex attempted complex formation (*red*). Bottom panel, B, chromatogram of the merge of the SENP6ΔC2CS, diSUMO2 and attempted complex complex chromatograms found in *A* to show lack of complex formation. All samples were run on a Superdex 200 gel filtration column (GE Healthcare) and peaks are *labeled* at the respective elution volumes. Bottom panel, C, collected fractions from gel filtration of SENP6ΔC2CS and diSUMO2 attempted complex analyzed by SDS-page. Elution fractions are *labeled* below each lane.

SENP2CS Deconjugation Complex with diSUMO2

SENP2 and SENP6 were shown to have comparable rates in the deconjugation reaction against diSUMO so we tested both enzymes to see if they formed stable complexes within a gel filtration column. Six milligrams of SENP2CS (0.27μmol) and six milligrams (0.27μmol) of diSUMO2 were incubated on ice in a low salt buffer (100mM) for one hour before being loaded onto a

HiLoad 20/60 Superdex200 column (GE Healthcare), which has a molecular weight range of 10,000 to 600,000Da. SENP2CS has a molecular weight of approximately 19,000Da and diSUMO2 of 21,000Da. Individually SENP2CS elutes at ~252ml on the Superdex200 column and diSUMO2 elutes at ~235ml (Figure 14, A). SENP2CS-diSUMO2 eluted in a single peak at ~223ml showing a peak shift of around 29ml for SENP2 and 12ml for diSUMO2 (Figure 18). The individual peak fractions were pooled and run on SDS-PAGE. The major part of the complex eluted from the columns as fractions corresponding to molecular mass 30-45,000kDa which is consistent with the formation of a stable complex of SENP2CS-diSUMO2, which has a theoretical molecular weight of around ~40kDa. Due to the fact that SENP2CS and diSUMO2 are very similar in molecular weight it is difficult to ascertain whether the peak fractions contained an equimolar ratio of protease-to-substrate but what is clear is that there is a physical interaction between the two proteins causing a significant shift in molecular weight when loaded onto a gel filtration column.

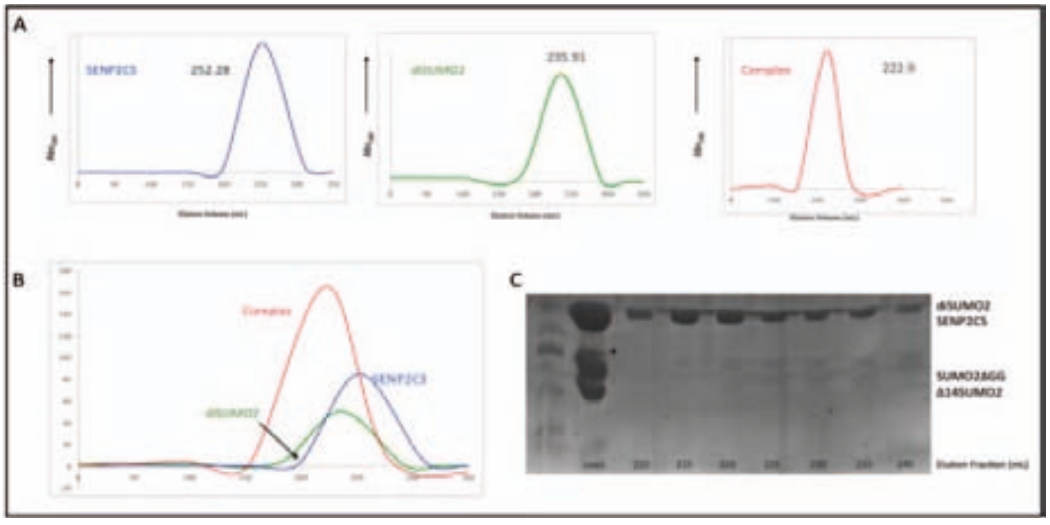

Figure 18. Gel chromatography of SENP2CS, diSUMO2 and complex. Top panel, A, chromatograms of SENP2CS (*blue*), diSUMO2 (*green*) and SENP2CS-diSUMO complex (*red*). Bottom panel, B, chromatogram of the merge of the SENP2CS, diSUMO2 and SENP2CS-diSUMO2 complex chromatograms found in *A*. All samples were run on a Superdex 200 gel filtration column (GE Healthcare) and peaks are *labeled* at the respective elution volumes. Bottom panel, C, collected fractions from gel filtration of SENP2CS-diSUMO2 analyzed by SDS-page. Elution fractions are *labeled* below each lane. Cleaved diSUMO2 (□14SUMO2 and SUMO2□GG) from active residual SENP2 is labeled with an *.

Characterization of SENP6 Loop3

In previous biochemical studies Loops 1, 2 and 3 were removed from the catalytic domain of both SENP6 and SENP7, the activity of the enzyme was effected in both positive and negative ways, depending on the loop. While Loop1 removal from both SENP6 and SENP7 showed stunted activity against all substrates tested Loop2 and Loop3 removal showed an overall increase the ability of the SENP6 and SENP7 to actively cleave both SUMO precursors and SUMO conjugated species (Reverter and Lima, 2008; Alegre and Reverter, 2011). As previously mentioned the structure of SENP7 catalytic domain was solved by Lima and Reverter and 2008. Though this provided insight into the rigidness of the poly-proline Loop1 and the unstructured nature of Loops 2 and 4, the structure of Loop3 proved elusive, presumably due to its unstructured or flimsy nature (Figure 19). Structural prediction programs predicted a very low percentage of secondary structural elements and no predicted tertiary structure (data not shown).

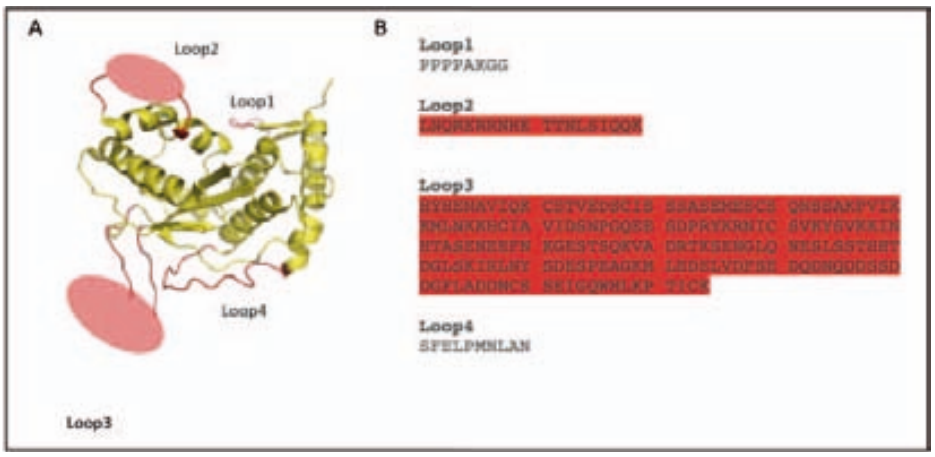

Figure 19. SENP6/7 Loop Insertions. Top panel, A, spatial arrangements of SENP7 Loop1, -2, -3 and -4 with respect to catalytic domain. Loops are shown in *red ribbon* and *labeled*. Areas where the loop structures are unknown are *shaded red*. Top panel, B, primary structure sequences of SENP6 Loop1, -2, -3 and -4 to compare segment sizes. Unknown structural regions in the corresponding SENP7 structures are *shaded red*.

In order to test whether this loop insertion in fact contained any structural elements we isolated and purified SENP6 Loop3 as a Smt3 fusion. Smt3 is the yeast form of SUMO and is occasionally used as a fusion protein in order to "chaperone" proteins, which otherwise might need help folding. The 184-residue Loop3 protein, weighing roughly 20.5kDa, eluted at 211ml on a Superdex200 gel filtration column (GE Healthcare), an accurate elution time for a protein that size (Figure 20). Smt3 cleavage did not prove a barrier to protein solubility as Loop3 was cleaved prior to addition to the gel filtration column, there was no accumulation to indicate protein aggregation and both proteins eluted at elution times indicative of their corresponding molecular weights. Peak fractions were pooled and concentrated to >15mg/ml and used for crystallography studies.

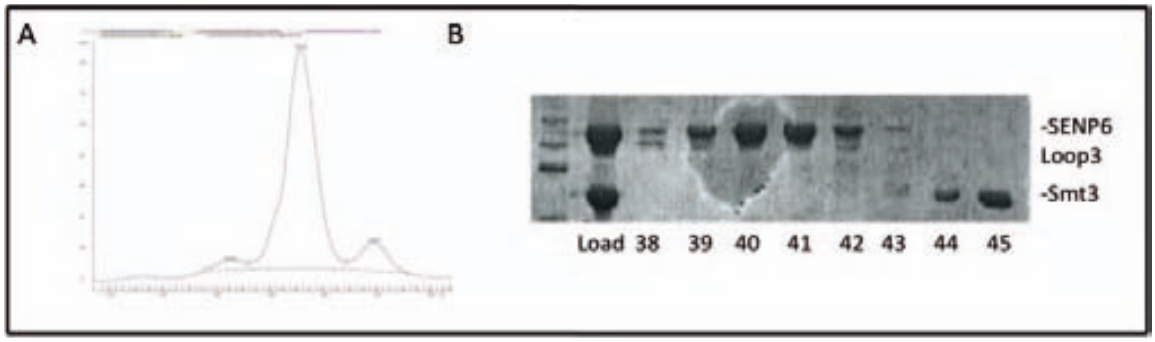

Figure 20. Gel chromatography of SENP6 Loop3. Top panel, A, chromatograms of SENP6 Loop3 taken from a Superdex 200 gel filtration column (GE Healthcare) and peaks are *labeled* at the respective elution volumes. Top panel, B, collected fractions from gel filtration of SENP6 Loop3 analyzed by SDS-page. Elution fractions are *labeled* below each lane.

Once we obtained milligrams amounts of SENP6 Loop3 the NMR analysis to determine if there were any tertiary structural elements. NMR is a technique that can utilize shifts in the inherent magnetic properties of atomic nuclei to determine if a protein contains any structural elements. SENP6 Loop3 was dissolved in TrisHCl and spectra were taken of the sample at 300K, 350K and again at 300K (Figure 21A, B and C). Spectral comparisons show no appreciable differences between 300 and 350K, which would confirm the absence of tertiary structure. The changes that are observed are reversible and disappear upon lowering the temperature from 350 to 300K. These changes can be explained by the presence of a partial or total loss of secondary structure due to the addition of heat.

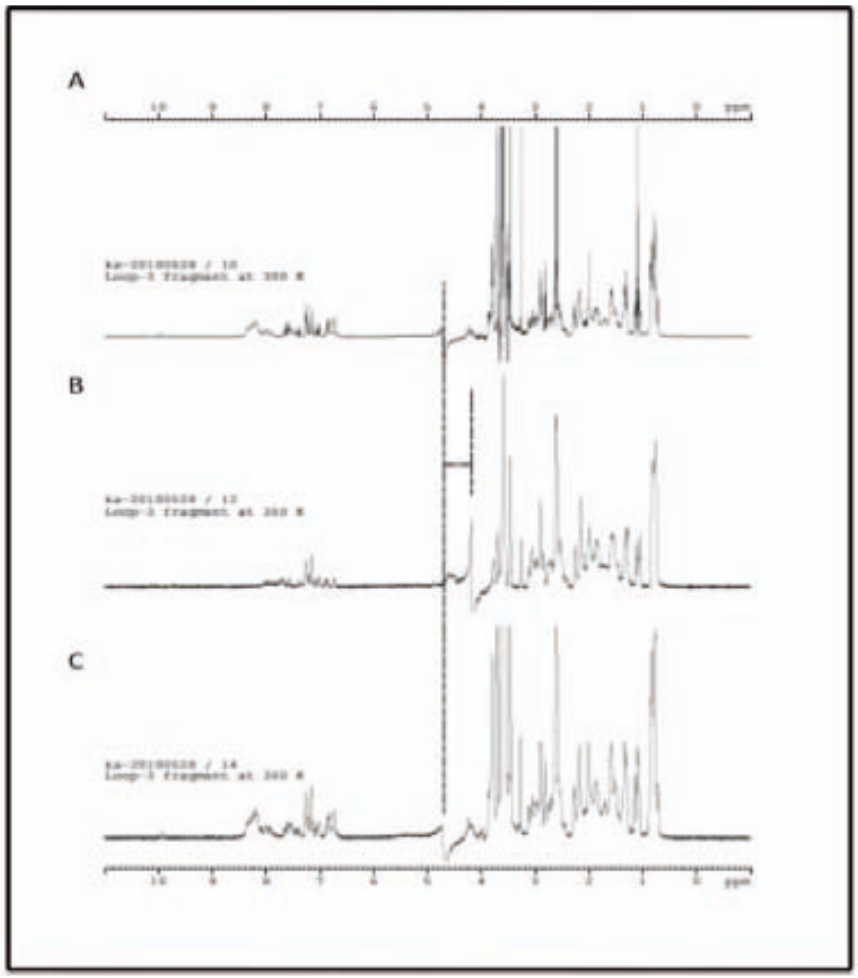

Figure 21. NMR analysis of SENP6 Loop3. Panels A, B and C 1-D 1-H NMR analysis of SENP6 Loop3 at 300, 350 and 300K, respectively.

Once we established that Loop3 contained no 3D structural elements we wanted to see if the loop contained any individual secondary structural elements, such as α helices or β sheets. The protein was analyzed via circular dichroism and Fourier Transform Infrared Analysis. Circular dichroism is a technique that can detect changes in a proteins secondary structure as a function of temperature or the concentration of denaturing agents, such as urea. A protein is exposed to light in the "far-UV" spectral region (190-250nm) at

different temperatures for example. Changes to the shape and magnitude of the CD spectra within this region with the varying temperature can be correlated with changes in the percentage of alpha helices, beta sheets and random coil structures within a protein. Loop3 was incubated at 20°, 60° and 90°C and subsequently analyzed via CD spectroscopy (Figure 22). The data indicated a decrease in molecular ellipticity at 220nm, indicative of a loss in alpha helix population upon temperature increase. No other loss of secondary structure was detected with this method.

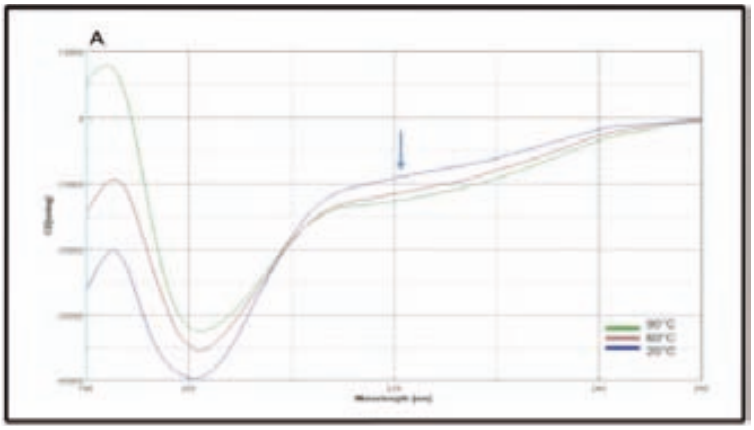

Figure 22. CD analysis of SENP6 Loop3. Top panel, A, Circular Dichroism analysis of SENP6 Loop3 showing the change in secondary structure as a function of heat. Temperatures are *labeled* and the wavelength depicting change in secondary structure is denoted by an *arrow*.

Fourier Transform Infrared Analysis is a technique that utilizes the fact that each protein has a unique set of absorption bands within its infrared spectrum. Amide bands are submitted to Fourier self deconvolution and subsequently a curve fitting procedure can be applied to estimate quantitatively

each component representing a type of secondary structure. The FTIR analysis further substantiated our suspicion about the existence of secondary structure by showing α-helical regions and some β-sheets at 1650 and 1630cm-1, respectively (Figure 23).

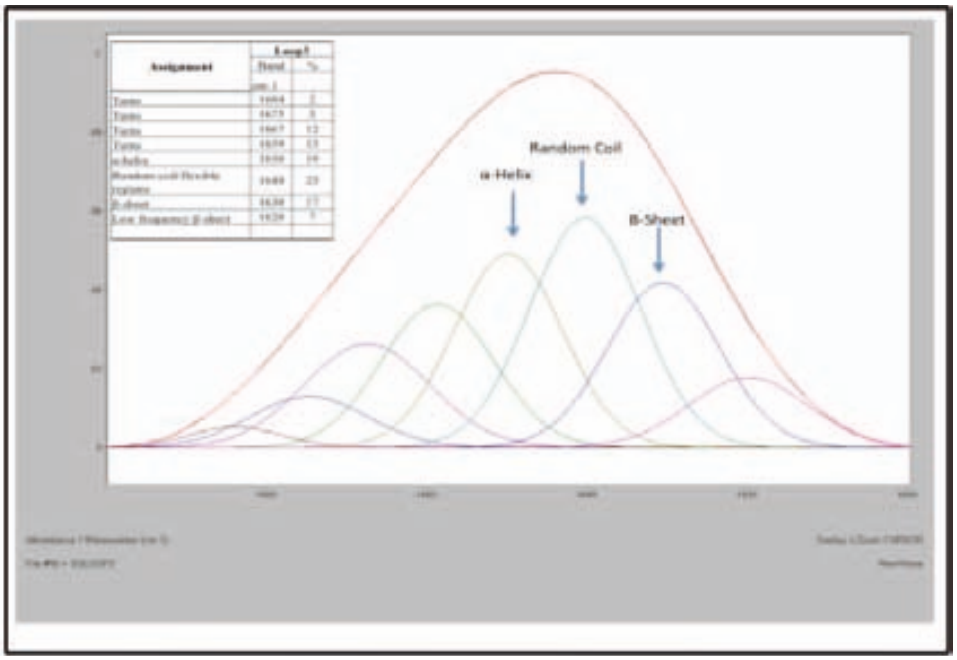

Figure 23 FTIR analysis SENP6 Loop3. Fourier Transform analysis of analysis of SENP6 Loop3 showing presence of secondary structural elements. α-helical regions were detected at 1650cm-, β-sheets at 1630cm-1 and random coil regions at 1640cm-1. Individual elements are *labeled* at corresponding wavelengths.

Thought both CD and FTIR pointed to a mainly unstructured loop, the presence of secondary structural elements prompted us to examine the loop further to determine where (if any) these structured regions existed. Limited proteolysis is a procedure in which a protein is exposed to an enzyme, which is specific for certain peptide bonds, in order to determine if there are any fragments within that are resistant to cleavage. When a protein is structured, or

globular, these regions will not be exposed to the enzyme and the region will be resistant to proteolysis. Chymotrypsin is a pancreatic enzyme, which preferentially cleaves amide bonds at tyrosine, tryptophan and phenylalanine residues. We exposed SENP6 Loop3 to various concentrations of chymotrypsin to determine if there was a stable region within the 184-residue loop. At a concentration of 10-3 chymotrypsin degraded Loop3 into several fragments, though one fragment of around 11kDa was prominent (Figure 24).

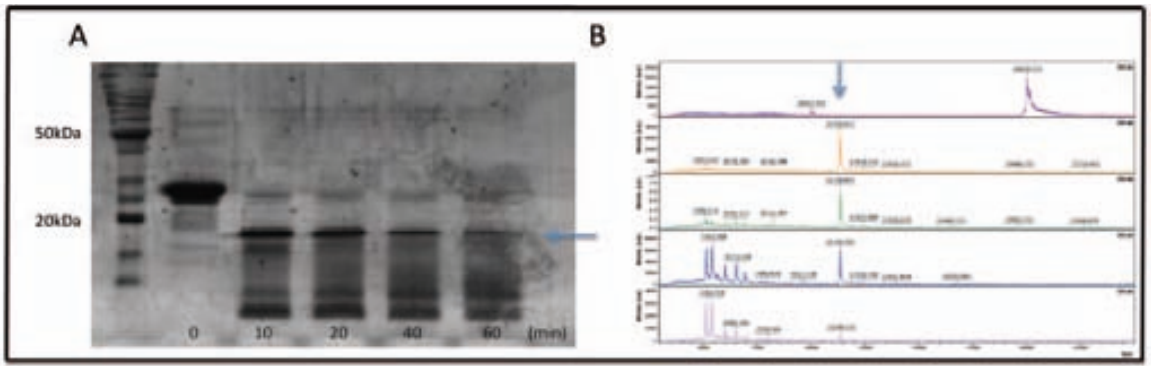

Figure 24. FTIR analysis SENP6 Loop3. Top panel, A, limited proteolysis of SENP6 Loop3 using chymotrypsin at 10-3 concentration. Fractions were taken at 0, 10, 20, 40 and 80 minutes and visualized by SDS-page. Time points are *labeled* below each fraction and fragment resistant to proteolysis is denoted by an *arrow*. Top panel, B, mass spectrometral analysis of fractions from *A*. Mass of resistant fragment is labeled with an arrow.

The reaction mixtures for mass spectrometry were incubated at 10-3 chymotrypsin concentration for time intervals T=0, 10, 20, 40 and 60 minutes at 37°C and one half of the sample was stopped using SDS loading buffer and the other half with TFA. The samples with SDS were then analyzed by gel electrophoresis (PAGE) for determination of fragment size and the samples containing TFA were sent for Mass Spectrometry (MALDI-TOF) analysis. The fractions from time points 10, 20 and 40 minutes all contained a fragment of

11,328 Daltons, which when exposed to this concentration of chymotrypsin, resisted cleavage (Figure 24). This fragment presumably contains structural elements that prevent enzyme access though whether these are individual secondary structural elements or whether they contain some tertiary structure elements is unknown. The decrease in the size of this fragment in the fractions from the time points taken at 40 and 80 minutes most likely points to the protein unfolding within solution and continued exposure to the enzyme after an extended time period. This can be further in the relative increase in the amount of smaller bands seen at those time points.

In order to separate and further analyze this stable fragment, we incubated ~5mg of SENP6 Loop3 with a concentration of 10-3 of chymotrypsin for 10 minutes and subsequently loaded the reaction mixture onto a Superdex75 column (GE Healthcare). In theory the chymotrypsin within the reaction mixture would be separated from the Loop3 fragments on the Superdex column without further causing any cleavage. The SENP6 Loop3 fragment eluted in a single peak at 197ml, an elution volume accurate for a protein of this molecular weight (Figure 25). The peak fractions were pooled and centrifuged to a final concentration of 15mg/ml and subsequently used in crystallography studies.

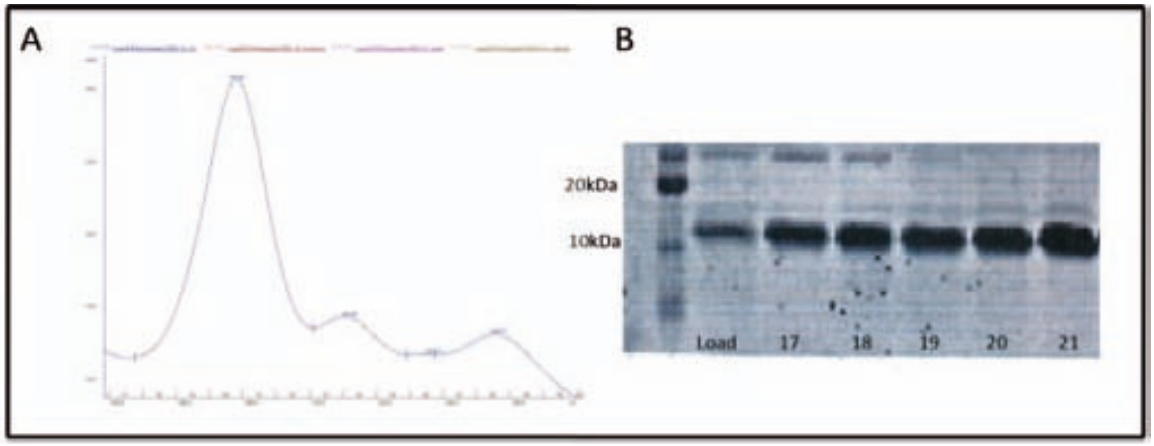

Figure 25. Gel chromatography of SENP6 Loop3 Fragment. Top panel, A, chromatogram of SENP6 Loop3 fragment taken from a Superdex75 gel filtration column (GE Healthcare). Peaks are *labeled* at the respective elution volumes. Top panel, B, collected fractions from gel filtration of SENP6 Loop3 analyzed by SDS-page. Elution fractions are *labeled* below each lane.

Discussion

As previously mentioned, the SUMO-specific SENP/Ulp family can be divided into two distinct subsets, those containing Ulp1 and those containing Ulp2. In the context of SENP6 and -7 this is evolutionarily interesting because the function of Ulp2 in yeast has been shown to be mechanistically equivalent to that of the corresponding enzymes in vertebrates in maintenance and regulation of SUMO chains (or Smt3 in the case of Ulp2)(Bylebyl et al., 2003). As SENP1 and -2 have been implicated in both the processing of immature SUMO and the deconjugation of SUMO from conjugated species (each with their own isoform specificity) the role of SENP6 and -7 appears to be more targeted solely toward the latter. Reverter and Lima showed in their paper published in 2006 that SENP6 and SENP7 were bad at processing SUMO precursors unless two glycine residues were inserted just C-terminal to the native C-terminal glycine residues, thus providing SENP6 and SENP7 with a homogenous set of C-terminal tails. Our data indicate that at a 5nM enzyme concentration both SENP6 and -7 are more active against the liberation of SUMO2 from RanGAP1 than in the processing of SUMO2 into the mature form and again this is only by integrating two additional C-terminal glycine residues. Both sets of data corroborate the fact that both enzymes show an isoform specificity toward SUMO2/3; in both the processing and deconjugation reactions, the dismantling of SUMO2 from conjugated substrates (in this case RanGAP1, diSUMO2) proceeds at rates almost

double (for RanGAP) and more than 20x (for diSUMO) that of the corresponding processing reactions containing SUMO1 (Alegre and Reverter, 2011).

The most striking difference between the sequences of SENP6 and SENP7 and the rest of the SENP family of proteases is the presence of four loop insertions within the catalytic domain that are unique to these two proteases. SENP6 and SENP7 are also the two SENPs most implicated in the dismantling of polySUMO2 chains. It is attractive thus to speculate that these loop insertions might play some role in the function of these two enzymes in this context (Mukhopadhyay, D et al 2006; Mukhopadhyay, D et al 2007; Lima and Reverter, 2008; Alegre and Reverter, 2011). Loop1 did prove integral to the function of the enzymes, as its removal substantially decreased the ability of the enzymes to deconjugate both diSUMO and polySUMO chains. Surprisingly however, at least for SENP6, there was an increase in activity when Loop2 and Loop3 were removed (Alegre and Reverter, 2011). Neither loop shows up in the crystal structure of the SENP7 catalytic domain, which leads one to speculate that the loops are disordered (Lima and Reverter, 2008). Structure prediction programs predict the same disorder for both regions and subsequent CD and FTIR experiments carried out in our lab further substantiated the claim that, at least in the case of SENP6, Loop3 is mainly unstructured. The increase in activity of the enzymes after removal of Loop2 and Loop3 implies that the enzymes, without these loops, are more efficiently able to either recognize or interact with the substrates. If these loops are indeed unstructured, reducing the entropy in the

system by removing these loops could explain the increase in activity of both enzymes, at least in this context. In fact, the expression of the full length SENP6 catalytic domain was so low 10L of fermentation in LB broth yielded <2mg of protein, while half the amount of LB produced >20mg of protein for the loop deletion mutants (SENP6Δ2Δ3 and SENP6Δ3). This lends nicely to the idea that removal of Loops -2 and -3 increased the solubility of the SENP6 catalytic domain by reducing the amount of unstructured protein. Even further, our complex formation experiments showed that SENP6Δ2Δ3 and SENP6Δ3 were able to form complexes with diSUMO2, while sole removal of Loop2 (SENP6Δ2) lead to no complex formation (Alegre and Reverter, 2011; data now shown). While the removal of SENP6 Loop2 augmented the ability of the enzyme to deconjugate diSUMO2 in activity assays on one hand, the presence of Loop3 seemed to hinder its ability to form a stable complex with diSUMO2 on the other hand. Thus SENP6 Loop3, while dispensable to the enzyme in terms of its ability to effectively deconjugate diSUMO2 in activity assays, seems to provide a transitory means for the enzyme by preventing it from stably "docking" onto a diSUMO2 molecule, even in the catalytically inactive form. It is attractive therefore to speculate that Loop3 might be implicated in providing the enzyme with some type of "shifting" mechanism, which could account for why these enzymes (SENP6 at least) are able to move along and hydrolyze polySUMO chains so rapidly and efficiently.

Interestingly in a paper published this year by Pinto et al it was shown that the catalytic domain of SENP6 was the most resistant to heat shock treatment compared with SENP1, SENP2, SENP5 and SENP7. Experiments were done which tested the ability of the enzymes to cleave SUMO substrates following heat shock treatment *in vivo* and which characterized the thermal stability of each SENP using fluorescence-based assays. SENP1, SENP2, SENP3, SENP5 and SENP7 all showed heat shock-induced decreases in the activity of their catalytic domains while SENP6 showed no deactivation. Additionally the melting temperature of SENP6 was determined to be 55.6°C, considerably higher than the 44.5 to 48.6°□C-temperature range of the other SENPs. This suggests some form of stability within the SENP6 catalytic domain, which renders the enzyme more resistant to heat-induced denaturation. Sequence (SENP1, -2, -3, -5, -6 and -7) and structural (SENP1, -2 and -7) alignments imply a shared core structure for all SENP proteins, which would logically imply a similar thermal stability for the proteases. It is therefore interesting to speculate whether the "non-core" structures or loops of SENP6 (more specifically Loop3) might contribute to its heightened thermal stability, perhaps by "anchoring" the protein in the folded form or by stabilizing the core by some other unknown mechanism we have yet to discover. Whatever its function, it will be interesting to see what role these loop insertions play in the context of the protease. More specifically Loop3, who in and of itself accounts for 40% and 20% of the catalytic domains of SENP6 and SENP7 respectively.

Structural examination of SENP7 superimposed on the previously resolved structure of SENP2 in complex with both RanGAP-SUMO2 and pre-SUMO2 revealed key residues which might be critical in the favored interaction between Loop1 of SENP6 and -7 and SUMO2/3. Mutational analysis revealed that two residues on SUMO1, N68 and D72, are partially responsible for the low favorability of SUMO1 interaction with Loop1. By substitution of these residues to the equivalent residues on SUMO2 the activity against both the processing and deconjugation reactions are recovered. The polar environment created by the Loop1 seems auspicious for the more polar resides on SUMO2 and -3 and it is probable this fact, combined with the fact that the corresponding residues on SUMO1 are unfavorable in said environment, is responsible for the isoformal partiality of SENP6 and -7 toward SUMO2 and -3.

Aside from providing a charge-conducive environment for SUMO2 residues, Loop1 also seems to provide a structural element, which contributes to the SENP7 Loop1-SUMO2 interaction. Removal of SENP7 Loop1 abrogates essentially all of the activity of the enzyme against SUMO2 substrates in deconjuation reactions but maintaining at the least the backbone of the Loop1 recovers some of the activity. We showed that maintaining the charge integrity of K691 on SENP7 Loop1 was essential to the activity of the enzyme. Though this residue lies C-terminal to the Loop1 poly-proline loop we speculate that the rigidity of this loop might maintain this positively charged lysine residue within range of the aspartic acid of a recipient SUMO2, thereby stabilizing the negative

charge. When SENP7 was assayed against a diSUMOD71K mutant where the mutant lysine would theoretically clash with the lysine residue of Loop1 the activity of the enzyme was seriously compromised, further proving that this charge stability contributes at least somewhat to the activity of the enzyme. Taken together, our results show that the activity of SENP7 is at least partially dependent on charge stabilization by residues on both SUMO and SENP7 and that a stable substrate-enzyme interaction is perpetuated when SUMO2 residues, not SUMO1, lie within the SENP7 Loop1 interface.

Hattersely et al also tested the isoform specificity of SENP6 and SENP7 by constructing diSUMO substrates containing two SUMO2s, one SUMO1 and one SUMO2 (both isoforms were used as both the "modifier" and the "substrate") and two SUMO1s. Their results coincide nicely with ours in that they showed that the minimum concentration of SENP6 required to cleave 50% of each substrate depended on whether SUMO1 or SUMO2 was in the acceptor and donor positions (Hattersly et al 2010). When SUMO2 was at both "modifier" and "substrate" positions SENP6 showed the highest activity and the activity gradually decreased when SUMO2 was replaced with SUMO1 at the "substrate" position, then at the "modifier" position and was the lowest when SUMO1 was at both positions. SENP6 activity against our diSUMO2 and diSUMO2/1 constructs show a similar pattern and altogether these results confirm that SENP6 is a protease specific for SUMO2/3 chains but also show that it exhibits activity toward mixed SUMO chains. SUMO1 has been shown to "cap"

polySUMO2/3 chains *in vivo* thus preventing further SUMO polymerization and polySUMO2/3 chains have been shown to take place in RNF4-mediated proteolysis, hence "capping" of SUMO2/3 chains by SUMO1 might modulate chain length and therefore dictate whether a protein could be targeted for degradation (Matic 2008). Our data suggest that though it has a preference for binding and cleaving SUMO2/3 moieties, SENP6 can still recognize and modify mixed SUMO1/2/3 chains and therefore could potentially influence the fate of polySUMOylated substrates. As previously mentioned i*n vivo* study of polySUMO2/3 chains is virtually impossible due to the transient nature of these SUMO2/3 multimers. The main hypothesis thus far has attributed this dynamicity to the rapid and incessant deconjugation by SENPs but the possibility of polySUMO chains being sequestered to the proteasome through RNF4-mediated SUMO recognition and subsequent protein ubiquitination might present an additional explanation for the lack of stable polySUMO moieties within the cell.

In vitro studies done by us and by Reverter and Lima in 2008 both show that not only is the presence of Loop1 detrimental to the activity of both SENP6 and SENP7 but that the structural integrity of the Loop1 is essential for active deconjugation of polySUMO moieties. Due to the lack of any structure that might confirm the structure of Loop1 or the interaction (if any) of Loop1 with SUMO, sequence comparisons combined with structure-based comparisons of SENP7 and SENP2 in complex with RanGAP1-SUMO2 were the only methods

available to try to elucidate the mechanisms by which these two proteins might interact. While biochemical methods proved fruitful in identifying possible interactors within the Loop1-SUMO interface we wanted to further show the utility of Loop1 in recognizing and deconjugating polySUMOylated species. Based on comparison of the aforementioned structures, a loop of eight residues protrudes into the SUMO interaction cleft which, based on sequence comparisons, and would correspond to the Loop1 position. We identified these eight residues of SENP6 Loop1 and inserted them directly in the SENP2 sequence at the corresponding site (SENP2ins). In all of our experiments we used SENP2 as the control enzyme due to the fact that it shows ubiquitous activity against all SUMO substrates, including diSUMO2 (Lima and Reverter, 2008; Alegre and Reverter; 2011). Though we tested SENP2 and SENP2ins against RanGAP1-SUMO1, RanGAP1-SUMO2 (data not shown) and diSUMO2 the only noticeable change in activity occurred when both enzymes were run against diSUMO2 (Figure 13). This evidence further validates our claim that this insertion facilitates recognition of polySUMOylated species, perhaps by providing an additional interaction surface specific to polySUMOylated species.

While the cellular functions of SENP6 and SENP7 have been studied in quite some detail, the mechanism by which these two proteases recognize target substrates remains unknown. It is an attractive theory to assume SENP6 and SENP7 share unique interaction surfaces with SUMO2/3 (more than SUMO1 at least) that dictate their isoformal bias but the main driving force for their

propensity for multi-SUMO2/3ylated species has yet to be elucidated. Bekes et al delved further into this issue by designing a novel SUMO monomer with a C-terminal proline to glycine substitution (Q90P) which could be recognized by SUMO machinery but whose proline-induced kink could not be accommodated by SENP proteases. They then designed an N- to C-terminal SUMO trimer integrating this SUMO2Q90P mutant in various combinations within the chain in order to determine the mechanism for polySUMO2 deconjugation. They purported that rather than deconjugating chains in a processive manner (starting at one end and moving down the chain in a stepwise fashion) SENPs were worked in a stochastic fashion, cleaving randomly within the chain and leaving various cleavage intermediates. SENP1 and SENP6, according to them, share this same stochastic mechanism for deconjugating polySUMO chains, and exert their specificity through recognition of single SUMO moieties. Our results are consistent with this hypothesis in that in our experiments SENP2, SENP6 and SENP7 were able to recognize and cleave all diSUMO substrates tested albeit at different rates. By manipulating the SUMO surface residues at the tentative Loop1 interaction site however we were able to adjust the effective ability of SENP6 and SENP7 to recognize and cleave SUMO1 and SUMO2 substrates, while the same mutations had no effect on SENP2. Thus polySUMO chain recognition and cleavage could additionally be regulated by the individual characteristics of each SENP, more specifically Loop1 of SENP6 and -7.

While RanGAP-SUMO has been used as the canonical model substrate to demonstrate SENP activity *in vitro*, it has not been shown to be an endogenous substrate of SENP6 and SENP7 *in vivo* (Lima and Reverter, 2008; Shen and Geoffrey, Alegre and Reverter, 2011). Due to the fact that ablation of either SENP6 or SENP7 results in the same accumulation of high molecular weight SUMO2/3 chains *in vivo* and that they have been shown to dismantle polySUMO2/3 chains *in vitro*, it seems more likely that these chains represent a natural substrate of these proteins and hence a more viable substrate to utilize in order to elucidate the activity and mechanism of SENP6 and -7. Our lab has utilized both a commercial version of polySUMO2/3 and a synthetic diSUMO substrate in order to demonstrate the deconjugation activities of SENP6 and SENP7 and overall we have seen that these two enzymes are most active against these two substrates compared to all the other substrates tested, including all SUMO1-containing substrates. This further supports our claim that SENP6 and SENP7 are SUMO2/3-specific and further that this specificity might contribute to their ability to recognize and regulate polySUMO2/3 chains within the cell (Alegre and Reverter, 2011; Lima and Reverter, 2008).

Being able to effectively model the interaction between SENP6 and -7 and a SUMO-conjugated substrate either through NMR studies or X-ray crystallography would solidify all the claims we have set forth here in regard to the actual (if any) interactions taking place between these two proteins. We were able to produce stable complexes between SENP6□2□3CS and SENP6□3CS

and diSUMO2 in milligram amounts (as well as the individual proteases) which were eventually used in crystallography studies. After initial trials using at least four crystal screens (each screen containing 96 different conditions), the complexes were replicated and variables such as final protein concentration (between 15mg/ml and 30mg/ml), final salt concentration (<20mM to 100mM NaCl) and plate incubation temperature (between 4°C and 18°C) were manipulated. Despite our tedious efforts we were not able to obtain any crystals that could be taken to the synchrotron for analysis and thus our study for the structure of the SENP6 protease and the complex of SENP6 with a SUMO substrate proved fruitless.

It is possible that our inability to produce any crystals of the diSUMO2 complexes was due to the fact that our diSUMO construct, while conceptionally correct, lacked the fine tuning that would produce a uniform batch of diSUMO molecules, which would be detrimental to crystal formation. Our "donor" molecule Δ14SUMO2 was constructed to exclude the N-terminal lysine residue thought to be the other major SUMOylation site (K11). Be removing this lysine we would in theory be preventing self-SUMOylation of the Δ14SUMO2 and funneling SUMOylation to the major SUMOylation site, K11, the "acceptor molecule", SUMO2ΔGG. This molecule is unable to act as a donor due to the fact that it lacks the two C-terminal glycines necessary for conjugation. Our *in vitro* SUMOylation reactions resulted in the formation of one predominant band corresponding to diSUMO2, though other bands, more specifically a band

corresponding to lower weight diSUMO2 and a band corresponding to a tri-SUMO moiety, were observed albeit to a lesser extent (Figure 26). While we were able to separate the diSUMO from all other elements of the reaction mixture for use in crystallography studies, it escaped our notice that the presence of the tri-SUMO moiety in and of itself was proof that the reaction was capable of SUMOylating at sites other than the expected major SUMOylation site. The self-SUMOylated diSUMO2 (two Δ14SUMO2 molecules, SUMOylated through an internal lysine residue) proved less troublesome due to the fact it was able to be separated from the desired diSUMO2 by application to anion exchange resin (Resource Q; GE Healthcare). Regardless the diSUMO we observed and purified, though technically "diSUMO" in all cases, was most likely a mixture of K5, K7, K11 and K24-linked diSUMO (the other predicted and proven SUMOylation sites)(Bekes *et al* 2011; Matic *et al* 2002; Pichler *et al* 2008). An interesting aspect of this is that while the diSUMO we used contained a mixture of different diSUMO molecules, this did not affect the ability of either SENP mutant from forming a complex with these diSUMOs. SENP6Δ2Δ3 and SENP6Δ3, to put it more clearly, did not distinguish from any of the diSUMOs within the mixture and equally formed stable complexes with all diSUMOs present. This could either be because the amount of errant diSUMOs was menial compared to the amount of the correct diSUMO moiety or because SENP6Δ2Δ3 and SENP6Δ3 show no bias toward forming complexes with diSUMO conjugated at different residues. In any case a new "acceptor" lysine has been constructed

which lacks K5 and K7 and mutational analysis of internal lysines will subsequently be carried out to prevent SUMOylation at these sites. Needless to say until a verifiably uniform diSUMO is achieved crystallography studies involving this molecule will be postponed.

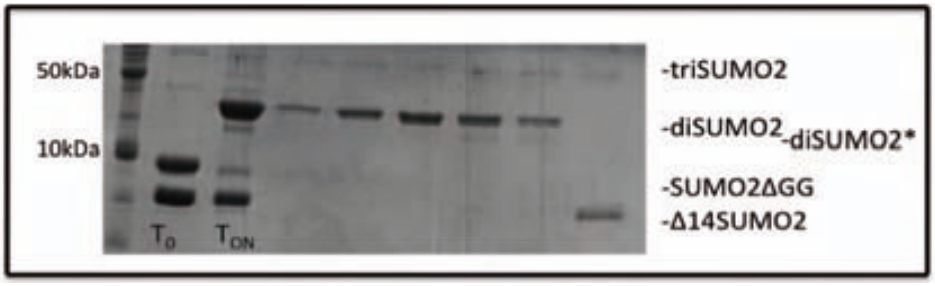

Figure 26. diSUMO2 formation. SDS-page analysis of diSUMO2 formation using Δ14SUMO2 as the donor and SUMO2ΔGG as the acceptor. Time zero and over night time points are *labeled* below respective lanes. Δ14SUMO2, SUMO2ΔGG, diSUMO2 and triSUMO two are *labeled*. diSUMO2* denotes diSUMO formed from two Δ14SUMO2 molecules instead of using SUMO2ΔGG as the acceptor.

While a SENP6 complex structure proved elusive, our attempts to recreate the role of Loop1, more specifically in the context of SUMO2 interaction, by inserting it into the SENP2 catalytic domain provided some hope for crystallography studies. Reverter and Lima were able to crystallize SENP2 in complex with SUMO2 and SUMO3 precursors in their paper published in 2006. Assuming our loop insertion of eight amino acids would not significantly alter the molecular packing of the crystals in the previous study it seems plausible that our SENP2ins in complex with SUMO2 and SUMO3 precursor might form crystals in similar conditions. Work is currently being carried out to determine if a crystal structure can be obtained that will effectively replicate the Loop1 interaction with SUMO2.

The characterization of Loop1 in the context of SUMO2 recognition, though useful in understanding at least one of the mechanisms SENP6 and SENP7 have in identifying and dismantling polySUMO chains, sheds light on only one of the loop insertions unique to these two enzymes. If an eight residue loop (Loop1) can play such an instrumental role in discriminating between two SUMO isoforms it is interesting to speculate that these other loop insertions (Loop2 being roughly twenty amino acids and Loop3 being forty amino acid in SENP7 and around one hundred amino acids in SENP6) might be integral to some other function of SENP6 and SENP7, either to the catalytic domain or to the whole protease itself. Spatially, the location of the loops suggests a mechanism for the enzymes to recognize or interact with more than one SUMO at a time, thus providing a scaffold for a polySUMO chain. Lima and Reverter purport in their paper published in 2008 that though Loop3 and Loop4 are too far from the SUMO interaction sites that correspond to both SUMO2 and RanGAP1 in the SENP2-RanGAP1SUMO2 structure, Loops1 and -2, which flank the SUMO binding site, could very well accommodate two adjacent SUMO molecules (Site A and Site B) (Figure 27A and B). Loops3 and -4 could therefore interact with additional SUMO molecules, as would be the case in a polySUMO chain (Site B and C). This theory however does not coincide with the previously mentioned theory by Bekes regarding SENPs use of a stochastic rather than processive mechanism to cleave polySUMO chains because recognition or interaction with a third SUMO moiety is not a necessary precursor for SUMO deconjugation in this

model (Figure 27C). They found comparable deconjugation rates regardless of the position of the accessible SUMO thus supporting their claim that the SUMO deconjugation machinery does not move sequentially from one SUMO moiety to the next in a chain but rather recognizes individual SUMO moieties resulting in cleavage anywhere within the chain (Bekes et al 2011).

The lack of polySUMO deconjugation intermediates renders the discovery to find the mechanism for the SENPs all the more difficult. While many studies have gone into exploring the functional and cellular aspects of the SENPs, less research has emerged regarding the structural significance of the catalytic domains since the characterization of the SENP1, SENP2 and SENP7 catalytic domain structures. This could be because the enzymes are assumed to be constitutively active and the structures available represent reliable and relevant representations of their catalytic domains. Complex structures of SENP1 and SENP2 with SUMO substrates support this theory by showing no evidence conformational rearrangement upon substrate binding. The structural and functional relevance of the SENP6 and SENP7 loops therefore must rely on speculative evidence, reinforced by molecular modeling and biochemical substantiation, until structural evidence is provided.

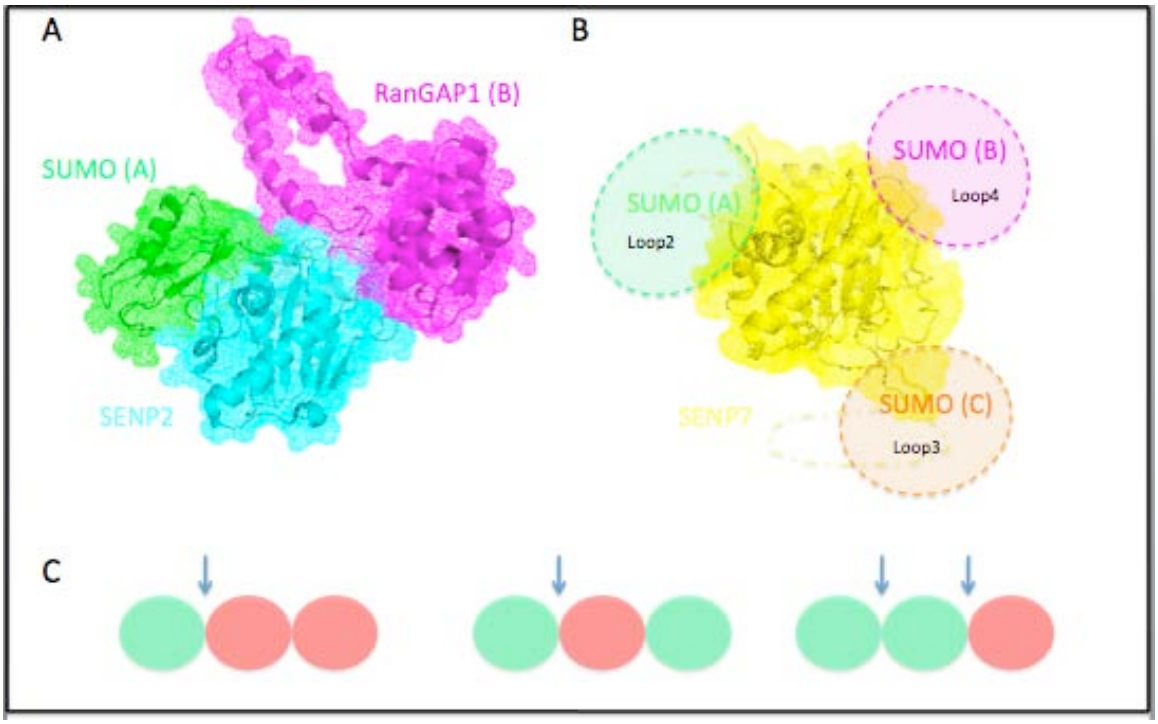

Figure 27. Structural models for SENP7 interaction with polySUMO. Top panel, A, the structure of SENP2 (*ribbon* and *mesh* representation) shown in *cyan* in complex with RanGAP1-SUMO2 (*ribbon* and *mesh* representation) shown in *magenta* and *green* respectively to indicate the position of sites A and B. Top panel, B, SENP7 (*ribbon* and *mesh* representation) shown in *yellow* depicted in similar orientation to SENP2 in *A* to highlight the positions of Loop2, Loop3 and Loop4 with respect to the putative SUMO interaction surfaces in sites A and B and site C. Bottom panel, C, a replication of Bekes et al 2011 experiment using a Q90P uncleavable by SENPs to show the "stochastic" model of SENP polySUMO cleavage. Cleavable SUMOs are represented by *green circles* and uncleavable SUMOs are represented by *red circles*. Arrows indicate SUMO cleavage sites.

Bibliography

Alegre, K.O., Reverter, D. (2011). Swapping small ubiquitin-like modifier (SUMO) isoform specificity of SUMO proteases SENP6 and SENP7 *J Biol Chem* 41, 36142-51.

Amerik, A.Y., Hochstrasser, M. (2004). Mechanism and function of deubiquitinating enzymes *Biochim Biophys Acta* 1-3, 189-207.

Andrews, E.A. et al. (2005). Nse2, a component of the Smc5-6 complex, is a SUMO ligase required for the response to DNA damage *Mol Cell Biol* 1, 185-96.

Armstrong, A.A., Mohideen, F., Lima, C.D. (2012). Recognition of SUMO-modified PCNA requires tandem receptor motifs in Srs2 *Nature* 7387, 59-63.

Ayaydin, G., Dasso, M. (2004). Distinct in vivo dynamics of vertebrate SUMO paralogues *Mol Biol Cell* 15, 5208-18

Azuma, Y. et al. (2001). Expression and regulation of the mammalian SUMO-1 E1 enzyme *FASEB* 10, 1825-7.

Azuma, Y., Araoutov, A., Dasso, M. (2003). *J Cell Biol SUMO-2/3 regulates topoisomerase II in mitosis* 3, 477-87.

Baboshina, O.V., Haas, A.L. (1996) Novel multiubiquitin chain linkages catalyzed by the conjugating enzymes E2EPF and RAD6 are recognized by 26 S proteasome subunit 5. *J Biol Chem* 271, 2823-31.

Bachant, J., Alcasabas, A., Blat, Y., Kleckner, N., Elledge, S.J. (2002). The SUMO-1 isopeptidase Smt4 is linked to centromeric cohesion through SUMO-1 modification of DNA topoisomerase II *Mol Cell* 9, 1169-82.

Bailey, D., O'Hare, P. (2002). Characterization of the localization and proteolytic activity of the SUMO-specific protease SENP1 *J Biol Chem* 1, 692-703.

Barrett, A.J., Rawlings, N.D. (2001). Evolutionary lines of cysteine peptidases *Biol Chem* 382, 727-733.

Bawa-Khalfe T., Cheng, J., Wang, Z., Yeh, ET. (2007). Induction of the SUMO-specific protease 1 transcription by the androgen receptor in prostate cancer cells *J Biol Chem* 52, 37341-9.

Bekes, M. et al. (2011). The dynamics and mechanism of SUMO chain deconjugation by SUMO-specific proteases. *J Biol Chem* 12, 10238-47.

Bernardi, R. et al. (2006). PML inhibits HIF-1alpha translation and neoangiogenesis through repression of mTOR *Nature* 7104, 779-85.

Bernier-Villamor et al. (2002). Structural basis for E2-mediated SUMO conjugation revealed by a complex between ubiquitin-conjugating enzyme Ubc9 and RanGAP1 *Cell* 108, 345-356.

Best, J.L. et al. (2002). SUMO-1 protease-1 regulates gene transcription through PML *Mol Cell* 10, 843-55.

Borden, K.L. and Freemont, P.S. (1996). The RING finger domain: a recent example of a sequence-structure family *Curr Opin Struct Biol* 3, 395-401.

Borer, R.A., Lehner, C.F., Eppenberg, H.M., Nigg, E.A. (1989). Major nucleolar proteins shuttle between nucleus and cytoplasm *Cell* 56, 379-90

Bossis, G., Melchior, F. (2006). Regulation of SUMOylation by reversible oxidation of SUMO conjugating enzymes *Mol Cell 21,* 349-57.

Brasch, K., Ochs, R.L. (1992). Nuclear bodies (NBs): a newly "rediscovered" organelle. *Exp Cell Res 2,* 211-23.

Briggs, M.S., Roder, H. (1992). Early hydrogen-bonding events in the folding reaction of ubiquitin *Proc Natl Acad Sci USA* 89, 2017-21.

Bruderer, R., Hay, R.T. et al. (2011). Purification and identification of endogenous polySUMO conjugates *EMBO Rep* 2, 142-48.

Brzovic, P.S. et al. (2001). Structure of BRCA1-BARD1 heterodimeric RING-RING complex *Nat struct Biol* 10, 833-7.

Bylebyl, G.R., Belichenko, I., Johnson, E.S. (2003). The SUMO isopeptidase Ulp2 prevents accumulation of SUMO chains in yeast. *J Biol Chem* 278, 4413-20.

Cai, Q., Robertson, E.S. (2010). Ubiquitin/SUMO Modification Regulates VHL Protein Stability and Nucleocytoplasmic Localization *PLos 9.*

Capili, A.D., Lima, C.D. (2007). Structure and analysis of a complex between SUMO and Ubc9 illustrates features of a conserved E2-Ubl interaction *J Mol Biol 3, 608-18.*

Chau V. et al. (1989). Editing of ubiquitin conjugates by an isopeptidase in the 26S proteasome *Science Nature* 4989, 1576-83.

Cheng, J. Bawa, T., Lee, P., Gong, L., Yeh, E.T. (2006). Role of desumoylation in the development of prostate cancer *Neoplasia* 8, 667-76.

Cheng, J., Wang, D., Wang, Z., Yeh, E.T. (2004). SENP1 enhances androgen receptor-dependent transcription through desumoylation of histone deacetylase 1 *Mol Cell Biol* 24, 6021-28.

Cheng, J., Kang, X., Zhang, S., Yeh, E.T. (2007). SUMO-specific protease 1 is essential for stabilization of HIF1alpha during hypoxia *Cell* 3, 584-95.

Choi, S.J. et al. (2006). Negative modulation of RXRalpha transcriptional activity by small ubiquitin-related modifier (SUMO) modification and its reversal by SUMO-specific protease SUSP1 *J Biol Chem* 41, 30669-77.

Comerford, K.M. et al. (2003). Small ubiquitin-related modifier-1 modification mediates resolution of CREB-dependent responses to hypoxia. *Proc Natl Acad Sci USAI 3, 986-91.*

Di Bacco, A. et al. (2006). The SUMO-specific protease SENP5 is required for cell division *Mol Biol Chem* 26, 4489-98.

Di Bacco, A., Gill, G. (2006). SUMO-specific proteases and the cell cycle. An essential role for SENP5 in cell proliferation *Cell Cycle* 20, 2310-3.

Di Bacco, A., Ouyang, J., Lee, H.Y., Catic, A. Ploegh, H., Gill, G. (2006). The SUMO-specific protease SENP5 is required for cell division. *Mol Cell Biol* 12, 4489-98.

Drag, M., Salvesen, G.S. (2008). DeSUMOylating enzymes--SENPs *IUBMB Life 60, 734-42.*

Duda, D.M. et al. (2007). Structure of a SUMO-binding-motif mimic bound to Smt3p-Ubc9p: conservation of a non-covalent ubiquitin-like protein-E2 complex as a platform for selective interactions within a SUMO pathway *J Mol Biol* 369, 619-30.

Duprez, E. et al. (1999). SUMO-1 modification of the acute promyelocytic leukaemia protein PML: implications for nuclear localisation. *J Cell Sci* Pt3, 381-93.

Etlinger, J.D., Goldberg, A.L. (1977). A soluble ATP-dependent proteolytic system responsible for the degradation of abnormal proteins in reticulocytes *Proc Natl Acad Sci USA* 74, 54-58.

Freesmont, P.S. (2000). RING for destruction? *Curr Biol* 2, R84-7.

Gan-Erdene, T. et al. (2003). Identification and characterization of DEN1, a deneddylase of the ULP family *J Biol Chem* 31, 28892-900.

Girdwood, D. et al. (2003). P300 transcriptional repression is mediated by SUMO modification Mol Cell 4, 1043-54.

Goldknopf, I.L., Busch, H. (1977). Isopeptide linkage between nonhistone and histone 2A polypeptides of chromosomal conjugate-protein A24 *Proc Natl Acad Sci USA* 74, 864-868.

Gong, L., Millas, S., Maul, G.G., Yeh, E.T. (2000). Differential regulation of sentrinized proteins by a novel sentrin-specific protease *J Biol Chem* 275, 3355-59.

Gong, L., Yeh, E.T. (2006). Characterization of a family of nucleolar SUMO-specific proteases with preference for SUMO-2 or SUMO-3 *J Biol Chem* 23, 15869-77.

Guo, D. et al. (2004). A functional variant of SUMO4, a new I kappa B alpha modifier, is associated with type 1 diabetes *Nat Genet* 8, 837-41.

Guterman, A., Glickman, M.H. (2004). Deubiquitinating enzymes are IN/(trinsic to proteasome function) *Curr Protein Sci* 3 201-11.

Haindl, M., Harasim, T., Eick, D., Muller, S. (2008). The nucleolar SUMO-specific protease SENP3 reverses SUMO modification of nucleophosmin and is required for rRNA processing *EMBO Rep* 3, 273-9.

Hamilton, K.S., et al. (2001). Structure of a conjugating enzyme-ubiquitin thiolester intermediate reveals a novel role for the ubiquitin tail *Structure* 10, 897-904

Han, Y. et al. (2010). SENP3-mediated de-conjugation of SUMO2/3 from promyelocytic leukemia is correlated with accelerated cell proliferation under mild oxidative stress *J Biol Chem* 17, 12906-15.

Hang, J., Dasso, M. (2002). Association of the human SUMO-1 protease SENP2 with the nuclear pore *J Biol Chem 277, 19961-66.*

Hass, A.l., Rose, I.A. (1982). The mechanism of ubiquitin activating enzyme. A kinetic and equilibrium analysis *J Biol Chem* 17, 10329-37.

Hass, A.L., Warms, J.V., Hershko, A., Rose, I.A. (1982). Ubiquitin-activating enzyme. Mechanism and role in protein-ubiquitin conjugation *J Biol Chem* 5, 2543-8.

Hattersley, N., Shen, L., Jaffray, E.G., Hay, R.T. (2011). The SUMO protease SENP6 is a direct regulator of PML nuclear bodies *Mol Biol Cell* 1, 78-90.

Hecker, C., Rabiller, M., Haglung, K., Bayer, P., Dikic, I. (2006). Specification of SUMO1- and SUMO2-interacting motifs *J Biol Chem* 435, 979-982.

Herscko, A., Heller, H., Elias, S., Ciechanover, A. (1983). Components of ubiquitin-protein ligase system. Resolution, affinity purification, and role in protein breakdown *J Biol Chem* 13, 8206-14.

Hochstrasser, M. (2001). SP-RING for SUMO: new functions bloom for a ubiquitin-like protein *Cell* 1, 5-8.

Hoege, C., Pfander, B., Moldovan, G.L., Pyrowalakis, G., Jentsch, S. (2002). RAD6-dependent DNA repair is linked to modification of PCNA by ubiquitin and SUMO *Nature* 419, 135-141.

http://www.nobelprize.org/nobel_prizes/chemistry/laureates/2004/

Huang, C. et al. SENP3 is responsible for HIF-1 transactivation under mild oxidative stress via p300 de-SUMOylation *EMBO J 18, 2748-62.*

Huang, D.T., Miller, D.W., Mathew, R., Cassell, R., Holaton, J.M., Roussel, M.F., Schulman, B.A. (2004). A unique E1-E2 interaction required for optimal conjugation of the ubiquitin-like protein NEDD8 *Nat Struct Mol Biol* 10, 927-935.

Huang, D.T., Schulman, B.A. (2005). Expression, purification and characterization of the E1 for human NEDD8, the heterodimeric APPBP1-UBA3 *Methods Enzymol* 398, 9-20.

Huang, D.T. et al. (2007). Basis for a ubiquitin-like protein thioester switch toggling E1-E2 affinity *Nature* 7126, 394-8.

Huang, L., Kinnucan, E., Wang, G., Beaudenon, S., Howldy, P.M., Huibregtse, J.M., Pavletich, N.P. (1999). Structure of an E6AP-UbcH7 complex: insights into ubiquitination by the E2-E3 enzyme cascade *Science* 286, 1321-26

Hunt, L.T. and Dayhoff, M.O. (1977). Amino-terminal sequence identity of ubiquitin and the nonhistone component of nuclear protein A24 *Biochem Biophys Res Commun* 74, 650-55.

Ibarr-Molero, B., Loladze, V.V., Makhatadze, G.I., Sanchez-Ruiz, J.M. (1999). Thermal versus guanidine-induced unfolding of ubiquitin. An analysis in terms of the contributions from charge-charge interactions to protein stability *Biochemistry* 38, 8138-49.

Itahana, Y., Yeh, E.T., Zhang, Y. (2006). Nucleocytoplasmic shuttling modulates activity and ubiquitination-dependent turnover of SUMO-specific protease 2 *Mol Cell Biol* 12, 4675-89.

Jackson, P.K. (2001). A new RING for SUMO: wrestling transcriptional responses into nuclear bodies with PIAS family E3 SUMO ligases *Genes, Dev* 23, 3053-8.

Jacobs, J.J., van Lohuizen, M. (2002). Polycomb repression: from cellular memory to cellular proliferation and cancer *Biochim Biophys Acta 2, 151-61.*

Jiang, M., Chiu, S.Y., Hsu, W. (2011). SUMO-specific protease 2 in Mdm2-mediated regulation of p53 *Cell Death Differ* 6, 1005-15.

Johnson, E.S. (2004). Protein modification by SUMO *Annu Rev Biochem* 73, 355-82.

Johnson, E.S., Gupta, A.A. (2001). An E3-like factor that promotes SUMO conjugation to the yeast septins *Cell 106*, 735-44.

Kagey, M.H., Melhuish, T.A., Wotton, D. (2003). The polycomb protein Pc2 is a SUMO E3 *Cell* 1, 127-37.

Kalman, P.B. et al. (2002). Identification of a multifunctional binding site on Ubc9p required for Smt3p conjugation *J Biol Chem* 277, 47938-45.

Kang, X. et al. (2010). SUMO-specific protease 2 is essential for suppression of polycomb group protein-mediated gene silencing during embryonic development *Mol Cell* 38, 191-201.

Kannouche, P.L., Wing, J., Lehmann, A.R. (2004). Interaction of human DNA polymerase eta with monoubiquitinated PCNA: a possible mechanism for the polymerase switch in response to DNA damage *Mol Cell* 14, 491-500.

Khorasanizadeh, S., Peter, I.D., Butt, T.R., Roder, H. (1993). Folding and stability of a tryptophan-containing mutant of ubiquitin *Biochemistry* 32, 7054-63.

Kim, K.I. et al. (2000). A new SUMO-1-specific protease, SUSP1, that is highly expressed in reproductive organs *J Biol Chem* 19, 14102-6.

Kim, Y.H. et al. (2005). Desumoylation of homeodomain-interacting protein kinase 2 (HIPK2) through the cytoplasmic-nuclear shuttling of the SUMO-specific protease SENP1 *FEBS Lett* 27, 6272-78.

Kim, Y.H., Choi, C.Y., Kim, Y. (1999). Covalent modification of the homeodomain-interacting protein kinase 2 (HIPK2) by the ubiquitin-like protein SUMO-1 *Proc Natl Acad Sci USA 22, 12350-5.*

Kotaja, N. et al. (2002). PIAS proteins modulate transcription factors by functioning as SUMO-1 ligases *Mol Cell Biol* 14, 5222-34.

Kuo, M.L., den Besten, W., Thomas, M.C., Sherr, C.J. (2008). Arf-induced turnover of the nucleolar nucleophosmin-associated SUMO-2/3 protease Senp3 *Cell Cycle* 21, 3378-87.

Kurepa, J. et al. (2003). The small ubiquitin-like modifier (SUMO) protein modification system in Arabidopsis. Accumulation of SUMO1 and -2 conjugates is increased by stress *J Biol Chem* 278, 6862-72.

Kurt, MB et al. (2004). A M55V Polymorphism in a Novel SUMO Gene (SUMO-4) Differentially Activates Heat Shock Transcription Factors and Is Associated with Susceptibility to Type I Diabetes Mellitus *J Bio Chem 26, 27233-38.*

Lake, M.W., Wuebbens, M.M., Rajagopalan, K.V., Schindelin, H. (2001). Mechanism of ubiquitin activation revealed by the structure of a bacterial MoeB-MoaD complex *Nature* 414, 325-9.

Lee, M.H. et al. (2011). NF-κB induction of the SUMO protease SENP2: A negative feedback loop to attenuate cell survival response to genotoxic stress *Mol Cell* 2, 180-91.

Li, I., Schindelin, H. (2008). Strcutural insights into E1-catalyzed ubiquitin activation and transfer to conjugating enzymes *Cell*, 2, 268-778.

Li, S.J., Hochstrasser, M.. (2003). The Ulp1 SUMO isopeptidase: distinct domains required for viability, nuclear envelope localization, and substrate specificity *J Cell Biol* 160, 1069-81.

Li, T., Fung, J., Mullern, J.F., Brill, S.J. (2007). The yeast Slx5-Slx8 DNA integrity complex displays ubiquitin ligase activity *Cell Cycle* 22, 2800-09.

Li, W. et al. (2008). Genome-wide and functional annotation of human E3 ubiquitin ligases identifies MULAN, a mitochondrial E3 that regulates the organelle's dynamics and signaling *PLoS ONE* 137, 133-45.

Liew, C.W., Sun, H., Hunter, T., Day, C.L. (2010). RING domain dimerization is essential for RNF4 function *Biochem J* 1, 23-9.

Lim, S.D. et al. (2005). Increased Nox1 and hydrogen peroxide in prostate cancer *Prostate* 2, 200-7.

Lima, C.D., Reverter, D. (2008). Structure of the human SENP7 catalytic domain and poly-SUMO deconjugation activities for SENP6 and SENP7 *J Biol Chem* 46, 32045-55.

Lois, L.M., Lima, C.D. (2005). Structures of the SUMO E1 provide mechanistic insights into SUMO activation and E2 recruitment to E1 *EMBO J* 3, 439-51.

Magori, S., Citovsky, V. (2011). Hijacking of the HOST SCF Ubiquitin Ligase Machinery by Plant Pathogens *Front Plant Sci* 2:87.

Mahajan, R., Delphin, C., Guan, T., Gerace, L., Melchior, F. (1997). A small ubiquitin-related polypeptide involved in targeting RanGAP1 to nuclear pore complex protein RanBP2 *Cell* 1, 97-107.

Maison C. et al. (2012). The SUMO protease SENP7 is a critical component to ensure HP1 enrichment at pericentric heterochromatin *Nat Struct Mol Biol* 4, 458-60.

Martin, N. et al. (2009). PARP-1 transcriptional activity is regulated by sumoylation upon heat shock *EMBO J* 22, 3534-48.

Matic, I. et al. (2008). In vivo identification of human small ubiquitin-like modifier polymerization sites by high accuracy mass spectrometry and an in vitro to in vivo strategy *Mol Cell Proteomics* 1, 132-44.

Matunis, M.J., Coutavas, E., Blobel, G. (1996). A novel ubiquitin-like modification modulates the partitioning of the Ran-GTPase-activating protein RanGAP1 between the cytosol and the nuclear pore complex *J Cell Biol* 135, 1457-70.

Matunis, M.J., Wu, J., Blobel, G. (1998). SUMO-1 modification and its role in targeting the Ran GTPase-activating protein, RanGAP1, to the nuclear pore complex *J Cell Biol* 3, 499-509.

Meulmeester, E., Kunze, M., Hsiao, H.H., Urlaub, H., Melchior, F. (2008). Mechanism and consequences for paralog-specific sumoylation of ubiquitin-specific protease 25 *Mol Cell* 30, 610-19

Miyauchi, Y., Yogosawa, S., Honda, R., Nishida, T., Yasuda, H. (2002). Sumoylation of Mdm2 by protein inhibitor of activated STAT (PIAS) and RanBP2 enzymes *J Biol Chem* 51, 5013-6.

Moldavan, G.L., Pfander, B., Jentsch, S. (2006). PCNA controls establishment of sister chromatid cohesion during S phase *Mol Cell* 23, 723-32.

Moraes, T.F., Edwards, R.A., McKenna, S., Pastushok, L., Xiao, W., Glover, J.N., Ellison, M.J. (2001). Crystal structure of the human ubiquitin conjugating enzyme complex, hMms2-hUbc13 *Nat Struct Biol* 8, 669-673.

Mukhopadhyay, D., Arnaoutov, A., Dasso, M. (2010). The SUMO protease SENP6 is essential for inner kinetochore assembly *J Cell Biol* 5, 681-92.

Mukhopadhyay, D., Dasso, M. (2007). Modification in reverse: the SUMO proteases *Trends Biochem Sci* 32, 286-95.

Mukhopadhyay, D et al. (2006). SUSP1 antagonizes formation of highly SUMO2/3-conjugated species *J Cell Biol* 174, 939-49.

Nagamalleswari, K. et al. (2010). Distribution and paralogue specificity of mammalian deSUMOylating enzymes *Biochem J* 430, 335-44.

Nakamura, S., Roth, J.A., Mukhopadhyay, T. (2002). Multiple lysine mutations in the C-terminal domain of p53 interfere with MDM2-dependent protein degradation and ubiquitination *Oncogene* 16, 2605-10.

Negorev, D., Maul, G.G. (2001). Cellular proteins localized at and interacting within ND10/PML nuclear bodies/PODs suggest functions of a nuclear depot *Oncogene* 49, 7234-42.

Nijman, S.M. et al. (2005). A genomic and functional inventory of deubiquitinating enzymes *Cell* 5, 773-86.

Nishida, T. et al. (2000). A novel mammalian Smt3-specific isopeptidase 1 (SMT3IP1) localized in the nucleolus at interphase *Eur J Biochem* 267, 6423-27.

Nishida, T., Kaneko, F., Kitagawa, M., Yasuda, H. (2001). Characterization of a novel mammalian SUMO-1/Smt3-specific isopeptidase, a homologue of rat axam, which is an axin-binding protein promoting beta-catenin degradation *J Biol Chem* 276, 39060-6.

Nishikawa, S. (2004). Mass spectrometric and mutational analyses reveal Lys-6-linked polyubiquitin chains catalyzed by BRCA1-BARD1 ubiquitin ligase *J Biol Chem* 279, 3916-24.

Novatchkova, M. et al. (2004). SUMO conjugation in plants *Planta* 220, 1-8.

Ouyang, J., Shi, Y., Valin, A., Xuan, Y., Gill, G. (2009). Direct binding of CoREST1 to SUMO-2/3 contributes to gene-specific repression by the LSD1/CoREST1/HDAC complex *Mol Cell* 34, 145-54.

Owerbach, D., McKay, E.M., Yeh, E.T., Gabbay, K.H., Bohren, K.M. (2005). Owerbach, D, McKay, EM, Yeh, ET, Gabbay, KH, Bohren, KM, Biochem Biophys Res Commun, 2005, 337, 517-20 *Biochem Biophys Res Commun* 337, 517-20.

Papouli, E. et al. (2005). Crosstalk between SUMO and ubiquitin on PCNA is mediated by recruitment of the helicase Srs2p *Mol Cell* 19, 122-33.

Pfander, B., Moldovan, G.L., Sacher, M., Hoege, C., Jentsch, S. (2005). SUMO-modified PCNA recruits Srs2 to prevent recombination during S phase *Nature* 436, 428-33.

Pichler, A., Gast, A., Seeler, J.S., Dejean, A., Melchior, F. (2002). The nucleoporin RanBP2 has SUMO1 E3 ligase activity *Cell* 108, 109-120.

Pichler, A., Knipscheer, P., Saitoh, H., Sixma, T.K., Melchior, F. (2004). The RanBP2 SUMO E3 ligase is neither HECT- nor RING-type *Nature Struct, Mol Biol* 11, 984-991.

Poukka, H., Karvonen, U., Janne, O.A., Palvimo, J.J. (2000). Covalent modification of the androgen receptor by small ubiquitin-like modifier 1 (SUMO-1) *Proc Natl Acad Sci USA* 26, 14145-50.

Prudde, J., Pebernard, S., Raffa, G., Slavin, D.A., Perry, J.J., Tainer, J.A. (2007). SUMO-targeted ubiquitin ligases in genome stability *EMBO J* 18, 4089-101.
Ramage, R., Green, J., Muir, T.W., Ogunobi, O.M., Love, S., Shaw, K. (1975). Synthetic, structural and biological studies of the ubiquitin system: the total chemical synthesis of ubiquitin *Proc Natl Acad Sci USA* 72, 11-5.

Reverter, D., Lima C.D. (2004). A basis for SUMO protease specificity provided by analysis of human Senp2 and a Senp2-SUMO complex *Structure (Camb)* 12, 1519-1531.

Reverter, D., Lima, C.D. (2006). Structural basis for SENP2 protease interactions with SUMO precursors and conjugated substrates *Nat Struct Mol Biol* 12, 1060-8.

Reverter, D., Lima, C.D. (2005). Insights into E3 ligase activity revealed by a SUMO-RanGAP1-Ubc9-Nup358 complex *Nature* 435, 687-92.

Ringose, L. (2007). Polycomb comes of age: genome-wide profiling of target sites *Curr Opin Cell Biol* 3, 290-7.

Rodriguez, M.S., Dargemont, C., Hay, R.T. (2001). SUMO-1 conjugation in vivo requires both a consensus modification motif and nuclear targeting *J Biol Chem* 276, 12654-9.

Ross, S., Best, J.L., Zon, L.I., Gill, G. (2002). SUMO-1 modification represses Sp3 transcriptional activation and modulates its subnuclear localization *Mol Cell* 10, 831-42.

Rotin, D., Kumar, S. (2009). Physiological functions of the HECT family of ubiquitin ligases *Nat Rev Mol Cell Biol* 6, 398-409.

Rytinki, M.M. et al. (2009). PIAS proteins: pleiotropic interactors associated with SUMO *Cell Mol Life Sci* 66, 3029-41.

Saeki, Y., Tayama, T., Toh-e, A., Yokosawa, H. (2004). Definitive evidence for Ufd2-catalyzed elongation of the ubiquitin chain through Lys48 linkage *Biochem Biophys Res Commun* 320, 840-5.

Saitoh, H., Hinchey, J.(2000). Functional heterogeneity of small ubiquitin-related protein modifiers SUMO-1 versus SUMO-2/3 *J Biol Chem* 275, 6252-6258.

Salomoni, P., Pandolfi, P.P. (2002). The role of PML in tumor suppression *Cell* 108, 165-70.

Sampson, D.A., Wang, M., Matunis, M.J. (2001). The small ubiquitin-like modifier-1 (SUMO-1) consensus sequence mediates Ubc9 binding and is essential for SUMO-1 modification *J Biol Chem* 276, 21664-69.

Sapetschnig, A. et al. (2002). Transcription factor Sp3 is silenced through SUMO modification by PIAS1 *EMBO J* 19, 5206-15.

Satijn, D.P. et al. (1997). RING1 is associated with the polycomb group protein complex and acts as a transcriptional repressor *Mol Cell Biol* 7, 4105-13.

Schelsinger, D.H., Goldstein, G. (1975). Molecular conservation of 74 amino acid sequence of ubiquitin between cattle and man *Nature* 5507, 42304.
Schlesinger, D.H., Goldstein, G., Niall, H.D. (1975). The complete amino acid sequence of ubiquitin, an adenylate cyclase stimulating polypeptide probably universal in living cells *Biochemistry* 10, 2214-8.

Schuettengruber, B. et al. (2007). Genome regulation by polycomb and trithorax proteins *Cell* 4, 735-45.

Sehat B. et al. (2010). SUMOylation mediates the nuclear translocation and signaling of the IGF-1 receptor *Sci Singal* 108, ra10.

Shen, L. et al. (2006). SUMO protease SENP1 induces isomerization of the scissile peptide bond *Nat Struct Mol Biol 12, 1069-77.*

Shen, L.N. et al. (2006). The structure of SENP1-SUMO-2 complex suggests a structural basis for discrimination between SUMO paralogues during processing *Biochem J* 397, 279-88.

Shen, T.H. et al. (2006). The mechanisms of PML-nuclear body formation *Mol Cell* 24, 331-9.

Shuai, K. (2000). Modulation of STAT signaling by STAT-interacting proteins *Oncogene 21, 2638-44.*

Sobko, A., Ma, H., Firtel, R.A. (2002). Regulated SUMOylation and ubiquitination of DdMEK1 is required for proper chemotaxis *Dev Cell* 6, 745-56.

Spence, J., Gali, R.R., Dittmar, G., Sherman, F., Karin, M., Finley, D. (2000). Cell cycle-regulated modification of the ribosome by a variant multiubiquitin chain *Cell* 102, 67-76.

Stelter, P., Ulrich, H.D. (2003). Control of spontaneous and damage-induced mutagenesis by SUMO and ubiquitin conjugation *Nature* 425, 188-91.

Sundquist, W.I., Schubert, H.L., Kelly, B.N., Hill, G.C., Holton, J.M., Hill, C.P. (2004). Ubiquitin recognition by the human TSG101 protein *Mol Cell* 13, 783-89.

Takahashi, Y., Strunnikov, A. (2008). In vivo modeling of polysumoylation uncovers targeting of Topoisomerase II to the nucleolus via optimal level of SUMO modification *Chromosoma* 2, 189-98.

Takahashi, Y., Toh-e, A., Kickuchi, Y. (2003). Comparative analysis of yeast PIAS-type SUMO ligases in vivo and in vitro *J Biochem* 133, 415-22.

Tatham, M.H. et al. (2001). Polymeric chains of SUMO-2 and SUMO-3 are conjugated to protein substrates by SAE1/SAE2 and Ubc9 *J Biol Chem 276, 35368-74.*

Tatham, M.H. et al. (2008). RNF4 is a poly-SUMO-specific E3 ubiquitin ligase required for arsenic-induced PML degradation *Nat Cell Biol* 10, 538-46.

Tong, H., Hateboer, G., Perrakis, A., Bernards, R., Sixma, T.K. (1997). Crystal structure of murine/human Ubc9 provides insight into the variability of the ubiquitin-conjugating system *J Biol Chem* 34, 21381-7.

Ulrich, H.D. (2002). Degradation or maintenance: actions of the ubiquitin system on eukaryotic chromatin *Eukaryotic Cell* 1, 7051-58.

Uzunova, K. et al. (2007). Ubiquitin-dependent proteolytic control of SUMO conjugates *J Biol Chem* 282, 34167-75.

Vertegaal, A.C. et al. (2006). Distinct and overlapping sets of SUMO-1 and SUMO-2 target proteins revealed by quantitative proteomics *Mol Cell Prot* 5, 2298-310.

Vijay-Kuman, S., Bugg, C.E., Cook, W.J. (1987). Structure of ubiquitin refined at 1.8 A resolution *J Mol Biol* 194, 8138-8149.

Walden, H. et al. (2003). The structure of the APPBP1-UBA3-NEDD8-ATP complex reveals the basis for selective ubiquitin-like protein activation by an E1 *Mol Cell* 12, 1427-37.

Walsh, C.T., Garneau-Tsodikova, S., Gatto, G.J. (2005). Protein posttranslational modifications: the chemistry of proteome diversifications *Angew Chem Int Ed Engl* 45, 7242-72.

Wang, G., Xi, J., Begley, T.P., Nicholson, L.K. (2001). Solution structure of ThiS and implications for the evolutionary roots of ubiquitin *Nat Stuc Bio*. 8, 47-51.

Wang, Z., Jones, G.M., Prelich, G. (2006). Genetic analysis connects SLX5 and SLX8 to the SUMO pathway in Saccharomyces cerevisiae *Genetics* 172, 1499-1509.

Wilkinson, K.D., Urban, M.K., Haas, A.L. (1980). Ubiquitin is the ATP-dependent proteolysis factor I of rabbit reticulocytes J Biol Chem 255, 7529-7532.

Wu, H. et al. (1995). Interaction of the erythropoietin and stem-cell-factor receptors *Nature* 6546, 242-6.

Wu, K. et al. (2003). DEN1 is a dual function protease capable of processing the C terminus of Nedd8 and deconjugating hyper-neddylated CUL1 *J Biol Chem* 31, 28882-91.

Xie, Y., Kersher, O., Kroetz, M.B., McConchie, H.G., Sung, P., Hochstrasser, M. (2007). The yeast Hex3.Slx8 heterodimer is a ubiquitin ligase stimulated by substrate sumoylation *J Biol Chem* 282, 34176-84.

Xu, Z., Au, S.W. (2005). Mapping residues of SUMO precursors essential in differential maturation by SUMO-specific protease, SENP1 *Biochem J* 386, 325-30.

Yang, Y. et al. (2007). SIRT1 sumoylation regulates its deacetylase activity and cellular response to genotoxic stress *Nat Cell Biol* 11, 1253-62.

Yao, T., Cohe, R.E. (2002). A cryptic protease couples deubiquitination and degradation by the proteasome *Nature* 6905, 403-7.

Yeh, E.T., Gong, L, Kamitani, T. (2000). Ubiquitin-like proteins: new wines in new bottles *Gene* 248, 1-14.

Yukita, A. et al. (2004). XSENP1, a novel sumo-specific protease in Xenopus, inhibits normal head formation by down-regulation of Wnt/beta-catenin signallin *Genes Cells* 9, 723-36.

Yun, C. et a. (2008). Nucleolar protein B23/nucleophosmin regulates the vertebrate SUMO pathway through SENP3 and SENP5 proteases *J Cell Biol* 4, 589.

Zhang, H., Saitoh, H., Matunis, M.J. (2002). Enzymes of the SUMO modification pathway localize to filaments of the nuclear pore complex *Mol Cell Biol* 22, 6498-6508.

Zhang, X.D. et al. (2008). SUMO-2/3 modification and binding regulate the association of CENP-E with kinetochores and progression through mitosis *Cell* 29, 729-41.

Zheng, N., Wang, P., Jeffrey, P.D., Pavletich, N.P. (2000). Structure of a c-Cbl-UbcH7 complex: RING domain function in ubiquitin-protein ligases *Cell* 102, 533-39.

Zheng, X.U. et al. (2006). Crystal structure of the SENP1 mutant C603S-SUMO complex reveals the hydrolytic mechanism of SUMO-specific protease *Biochem J* 398, 345-52.

Zunino, R., Braschi, E., Xu, L., McBride, H.M. (2009). Translocation of SenP5 from the nucleoli to the mitochondria modulates DRP1-dependent fission during mitosis *J Biol Chem* 26, 17783-95.

Conclusions

Conclusions

Processing vs. Deconjugation

1. SENP6 and SENP7 are both inefficient in processing preSUMO to the mature form.
2. SENP6 and SENP7 are both efficient at deconjugating SUMO2 from conjugated substrates.
3. SENP6 and SENP7 are both efficient at deconjugating polySUMO2/3 and diSUMO2 substrates.

SUMO1 vs. SUMO2

1. SUMO1 residues Ala68 and His 71, which lie within the tentative SENP6 and SENP7 Loop1 interaction site, are not conducive to the Loop1 environment.
2. SUMO2 residues Asn68 and Asp71 show a more favored environment to accommodate SENP6 and SENP7 Loop1 charges.

SENP6 and SENP7 Loop1

1. Loop1 is an essential element in both the isopeptidase and endopeptidase activities of SENP6 and SENP7.
2. The structural and charge integrity of Loop1 is integral to SENP6 and SENP7's ability to deconjugate SUMOylated species.
3. Insertion of Loop1 into SENP2 increases the activity of the protease against diSUMO2, in comparison to the wild type protein.

Complex Formations

1. SENP6□2□3CS, SENP6□3CS and SENP2CS are able to form stable complexes with diSUMO2.
2. SENP6□2CS is not able to form a stable complex with diSUMO2.

SENP6 Loop3

1. Loop3 is a mainly unstructured element in the SENP6 catalytic domain.

2. Removal of Loop3 enhances SENP6 performance in activity assays.
3. The presence of Loop3 prevents the formation of a stable complex with diSUMO2 in solution.

Appendix

THE JOURNAL OF BIOLOGICAL CHEMISTRY VOL. 286, NO. 41, pp. 36142–36151, October 14, 2011

Swapping Small Ubiquitin-like Modifier (SUMO) Isoform Specificity of SUMO Proteases SENP6 and SENP7[*][S]

Received for publication, June 6, 2011, and in revised form, August 24, 2011 Published, JBC Papers in Press, August 30, 2011, DOI 10.1074/jbc.M111.268847

Kamela O. Alegre[1] **and David Reverter**[2]

From the Departament de Bioquímica i Biologia Molecular, Institut de Biotecnologia i de Biomedicina, Universitat Autonoma de Barcelona, 08193 Barcelona, Spain

Background: The SENP/ULP family of SUMO proteases display different cleavage preference for SUMO isoforms.
Results: Insights into the structural determinants for the preference of SENP6 and SENP7 for the SUMO2/3 isoform.
Conclusion: A novel interface between SENP6 or SENP7 and SUMO determines the SUMO isoform preference.
Significance: This may be the first time that the cleavage preference between SUMO1 and SUMO2/3 was swapped by single point mutagenesis.

SUMO proteases can regulate the amounts of SUMO-conjugated proteins in the cell by cleaving off the isopeptidic bond between SUMO and the target protein. Of the six members that constitute the human SENP/ULP protease family, SENP6 and SENP7 are the most divergent members in their conserved catalytic domain. The SENP6 and SENP7 subclass displays a clear proteolytic cleavage preference for SUMO2/3 isoforms. To investigate the structural determinants for such isoform specificity, we have identified a unique sequence insertion in the SENP6 and SENP7 subclass that is essential for their proteolytic activity and that forms a more extensive interface with SUMO during the proteolytic reaction. Furthermore, we have identified a region in the SUMO surface determinant for the SUMO2/3 isoform specificity of SENP6 and SENP7. Double point amino acid mutagenesis on the SUMO surface allows us to swap the specificity of SENP6 and SENP7 between the two SUMO isoforms. Structure-based comparisons combined with biochemical and mutagenesis analysis have revealed Loop 1 insertion in SENP6 and SENP7 as a platform to discriminate between SUMO1 and SUMO2/3 isoforms in this subclass of the SUMO protease family.

The small ubiquitin-like modifier (SUMO)[3] belongs to the Ubl (ubiquitin-like) protein family, which is attached to protein substrates via an isopeptidic bond between their C-terminal glycine and a lysine residue on the substrate (1). After ubiquitin, SUMO is the second best characterized member of the Ubl family (2). SUMO is attached to target proteins by an enzymatic cascade analogous to ubiquitin (3). The SUMO pathway comprises a cascade of three enzymatic steps that leads to the formation of the isopeptidic bond on the target protein (4). The process can be reversed by the action of the SUMO proteases, which cleave off SUMO from the target protein. Thus, the abundance of SUMO substrates in the cell is regulated by a balance of conjugation by the SUMO enzymatic cascade and deconjugation by the SENP/ULP protease family (5).

The human SUMO protein family consists of four members, SUMO1, SUMO2, SUMO3, and SUMO4. SUMO4 does not seem to participate in the formation of SUMO conjugates *in vivo* (6). After maturation of their C-terminal tail, SUMO2 and SUMO3 are 95% identical (thus referred as SUMO2/3 in the text), whereas SUMO1 shares only 43% identity to SUMO2 or SUMO3. Recent reports indicate that SUMO isoforms are non-redundant in the cell; some substrates can be exclusively modified by SUMO1 or SUMO2/3, whereas others can be modified by both SUMO isoforms (7–9). Interestingly, *in vivo* heat shock or oxidative stress experiments produce an accumulation of SUMO2/3 in the cell, whereas SUMO1 remains unaltered (10). Another important difference between both SUMO isoforms is that SUMO2/3 can form polySUMO2/3 chains through an N-terminal lysine residue (11–13). One function of the polySUMO2/3 chains might be the stabilization of PML nuclear bodies (14), which is also the signal for the ubiquitin-dependent degradation by the recruitment of the E3 ubiquitin ligase RNF4 (15, 16). A recent study has analyzed the dynamics of conjugation/deconjugation of polySUMO chains, highlighting in *Schizosaccharomyces pombe* the role of deconjugation for the correct homeostasis of the cell (17).

In humans, the SENP/ULP protease family is comprised of seven members; six are SUMO-specific proteases (SENP1, SENP2, SENP3, SENP5, SENP6, and SENP7), whereas one is specific for another ubiquitin-like protein, Nedd8 (SENP8, also named DEN1 or NEDP1) (5). All SENPs share a conserved C-terminal domain of ~220 amino acid residues, containing the catalytic triad (His-Asp-Cys) characteristic of the cysteinyl proteases. Several crystal structures have been reported for the catalytic domains of some members of the family, in the apo form or in complex with SUMO substrates (18–23). All structures of the catalytic domains reveal a similar three-dimensional structure with conserved elements required for the correct proteolytic activity. Two different proteolytic activities can be performed by the SENP/ULP protease family, maturation of the SUMO precursor (processing) and hydrolysis of the isopep-

* This work was supported by Ministerio de Educacion y Ciencia Grant BFU2008-0364 and European Community Grant MIRG-CT-2007-200346.
[S] The on-line version of this article (available at http://www.jbc.org) contains supplemental Figs. 1 and 2.
1 Supported by a scholarship from the Ministerio de Educacion y Ciencia.
2 To whom correspondence should be addressed: Universitat Autonoma de Barcelona, 08193 Bellaterra, Barcelona, Spain. Tel.: 93-5868955; Fax: 93-581-2011; E-mail: david.reverter@uab.cat.
3 The abbreviation used is: SUMO, small ubiquitin-like modifier.

tidic bond (deconjugation). Structural and functional analysis has revealed a preferential cleavage of the isopeptidic bond over the cleavage of the peptidic bond in deconjugation and processing reactions, respectively (24). Recent studies indicate that the members of the SENP/ULP family show preferential roles in the cleavage of SUMO substrates. For example, SENP2 exhibits a clear SUMO isoform preference in the processing reaction depending on the SUMO C-terminal tail, but the deconjugation reaction is faster and does not discriminate between SUMO1 and SUMO2/3 substrates (19). SENP6 and SENP7 showed lower processing activities compared with deconjugation of SUMO substrates, but in all instances, they show a clear isoform preference for SUMO2/3 (24–27). SENP3 and SENP5 have also been reported to possess an isoform preference for SUMO2/3 (25, 28, 29).

SENP/ULP family members are localized in different regions inside of the cell, most being nuclear. Cellular localization is controlled by the distinct N-terminal extensions of the SENP/ULP family members, and it has been proposed that these regions regulate the activity of the protease. For example, SENP2 is localized to filaments of the nuclear pore complex (30), but differential splicing produces SENP2 protease variants that can shuttle between the cytoplasm and the nucleus (31). SENP3 and SENP5 have been localized in the nucleolus (30). SENP6 and SENP7 are localized in the nucleoplasm, and SENP6 has been recently shown to be implicated in the assembly of the inner kinetochore during mitotic progression (32).

SENP6 and SENP7 are the most divergent members within the SENP/ULP family (5, 25) with a catalytic domain displaying a lower sequence similarity and conserved sequence insertions in distinct loop regions. Biochemical and structural studies of the SENP7 catalytic domain suggested a role for the Loop 1 insertion in the proteolytic activity of the enzyme, whereas Loop 2 and Loop 3 insertions were dispensable (26). In the present study, we have further investigated the structural determinants of Loop 1 insertion in the proteolytic activity of SENP6 and SENP7 and have identified a novel and more extensive interface between SUMO and this subclass of SUMO proteases. Furthermore, we show that the region of SUMO involved in the interface with Loop 1 is responsible for the isoform preference displayed by SENP6 and SENP7 for SUMO2/3. Single point mutagenesis on the SUMO surface allows SENP6 and SENP7 to swap their SUMO2/3 isoform specificity for SUMO1. In conclusion, we disclose a novel and more extended substrate-enzyme interface between SUMO and the SENP6 and SENP7 subclass of SUMO proteases.

EXPERIMENTAL PROCEDURES

Protein Mutagenesis and Purification—The catalytic domains of human SENP2-(364–589), SENP6-(637–1112), and SENP7-(662–984) were produced in *Escherichia coli* and purified as described (19, 26). All SUMO1 and SUMO2 constructs, including precursors, double glycine insertions at the C terminus, and mature forms, were produced in *E. coli* as described before (19, 20). Conjugation and purification of RanGAP1-SUMO substrates were produced as described previously (33).

Single point mutations were introduced into the SUMO1 (A72N, H75D, S9C, and C52S), SUMO2 (N68A, D71H, and K11C) and SENP7 (K691E, K691A) coding regions using the QuikChange mutagenesis kit (Stratagene). The SENP7 four mutant construct P686G/P687G/P688G/P689G was constructed by PCR. PCR was used to construct SENP6 deletion mutants by fusing amino acids 656–664 (Loop-1 SENP6-Δ657–663), substituting two glycine residues for the loop between residues 720 and 735 (Loop 2 SENP6-Δ721–734), and fusing amino acids 874 to 973 (Loop 3 SENP6-Δ875–972) of SENP6 and by fusing amino acids 683–692 (Loop 1 SENP7-Δ682–691) of SENP7. All constructs were confirmed by DNA sequencing. SENP6 deletion mutants were purified by metal affinity chromatography and gel filtration (as described before for SENP7) (26) and concentrated to 1 mg/ml in a buffer containing 25 mM Tris-HCl (pH 8.0), 350 mM NaCl, and 1 mM β-mercaptoethanol.

To prepare the diSUMO2 dimer, Δ14-SUMO2 was produced as SUMO donors, and SUMO2ΔGG (deletion of the C-terminal di-Gly motif) was produced as SUMO acceptor. Both proteins were produced and purified in *E. coli* as described before for the wild type (19). DiSUMO2 was formed overnight at 37 °C in a reaction mixture containing 20 mM HEPES (pH 7.5), 5 mM $MgCl_2$, 0.1% Tween, 50 mM NaCl, 1 mM dithiothreitol, 2 mM ATP, 150 nM SAE1/SAE2 (E1), 100 nM Ubc9 (E2), IR1 (E3), 32 mM Δ14-SUMO2, and 16 mM SUMO2ΔGG in MilliQ water; and purified by gel filtration (Superdex75, GE Healthcare). The diSUMO2(N68A/D71H) double point mutant and diSUMO2(D71K) were prepared as the wild type form, but instead of using Δ14-SUMO2 as the SUMO donor, a triple single point mutant with a deletion of the first eight amino acid residues, Δ8-SUMO2(K11C/N68A/D71H), and Δ14-SUMO2(D71K) were utilized.

Biochemical and Kinetic Assays—Titration of the carboxyl-terminal hydrolase activity (processing) was measured by incubating preSUMO1GGG_1G_2-*X*, preSUMO1GGG_1G_2-*X*(A72N/H75D), preSUMO2GGG_1G_2-*X* and preSUMO2GGG_1G_2-*X*(N68A/D71H) (-*X* represents the natural C-terminal tail sequence for each SUMO isoform, and G_1 represents the glycine insertions) precursor proteins (5 μM) with purified SENP6, SENP7, and SENP2 at three different enzyme concentrations (0.5, 5, and 50 nM) at 37 °C in a buffer containing 25 mM Tris-HCl (pH 8.0), 150 mM NaCl, 0.1% Tween 20, and 2 mM dithiothreitol. Reactions were stopped after 25 min with SDS loading buffer and analyzed by gel electrophoresis (PAGE). Proteins were detected by staining with SYPRO (Bio-Rad).

Identical experimental conditions were used to assay the deconjugation activities for SENP2, SENP6 wild type and deletion mutants, and SENP7 at 0.5, 5, 50 nM using RanGAP1-SUMO1, RanGAP1-SUMO1(A72N/H75D), RanGAP1-SUMO2, and RanGAP1-SUMO2(N68A/D71H) substrates at 3 mM. Deconjugation activities using diSUMO2 substrates at 3 μM were performed using enzyme concentrations at 0.05, 0.5, and 50 nM. For the titration analysis, the reactions were stopped after 25 min with SDS loading buffer and analyzed by PAGE. Proteins were detected by staining with SYPRO (Bio-Rad). Products were quantified by detecting fluorescence under UV illumination using a Gel-Doc apparatus with associated integration software (Quantity One; Bio-Rad).

Processing and deconjugation time course reactions were performed with similar buffer conditions as for the end point reactions. SENP6 and SENP2, at 5 and 1 nM respectively, were incubated with RanGAP1-SUMO1, RanGAP1-SUMO1(A72N/H75D), RanGAP1-SUMO2, and RanGAP1-SUMO2(N68A/D71H) substrates at 3 μM. Reactions were run at 37 °C and stopped at 5, 20, 40, and 80 min with SDS loading buffer and analyzed by PAGE. The same buffer conditions were used for the time course reactions using diSUMO2 and diSUMO2(N68A/D71H) mutant with SENP2, SENP6, and SENP7 at 0.5 nM and diSUMO2 and diSUMO2(D71K) with SENP7, SENP7-ΔLoop 1, SENP7(K691E), SENP7(K691A), and SENP7(P686G/P687G/P688G/P689G) at 0.5 nM with reactions stopped at 15, 30, 60 and 120 min.

Initial reaction velocities were measured for SENP6-ΔLoop 3 at 1 nM and SENP7 and associated mutants at 0.5 nM in a buffer containing 25 mM Tris-HCl (pH 8.0), 150 mM NaCl, 0.1% Tween 20, and 2 mM dithiothreitol at 37 °C. Substrates used for the processing and deconjugation reactions were prepared at 5 μM. Reactions were stopped at indicated time intervals with SDS loading buffer and analyzed by PAGE. Products were quantified by detecting fluorescence using a Gel-Doc apparatus with associated integration software (Quantity One; Bio-Rad). All data points were fitted to a hyperbolic curve. All assays were conducted in triplicate. *Error bars* indicate ±1 S.D.

Michaelis-Menton steady-state kinetics was performed for SENP6 by introduction of S9C and C52A point mutants into SUMO1 and SUMO1(A68N/H71D) to allow for fluorophore addition. SUMO1(S9C/C52C) and SUMO1(S9C/C52C/A68N/H71D) were used for labeling with Alexa Fluor 488 fluorophore (Invitrogen) and were subsequently conjugated to RanGAP1. Initial deconjugation velocities were measured at eight different substrate-labeled concentrations (0, 0.25, 1, 2, 6, 20, 50, and 100 μM) for a SENP6 concentration at 25 nM. Reactions were stopped after 0, 5, 15, 40, and 80 min with SDS loading buffer and analyzed by SDS gel electrophoresis. Fluorescence signal was followed and measured by using Versadoc apparatus with associated integration software (Quantity One, Bio-Rad). Kinetic constants were obtained from the graph representation substrate concentration (μM) *versus* initial velocity (μM min^{-1}). All assays were conducted in triplicate.

RESULTS

Mutagenic Analysis of Loop 1 Insertion in SENP7—In a previous work, we partially characterized the proteolytic activity of the four sequence insertions located in the catalytic domain of SENP7 (named Loop 1 to Loop 4) (26). Of special interest is the Loop 1 insertion, which is composed of eight residues, including four prolines, two glycines, and a lysine residue in the center of the loop (Fig. 1). Loop 1 is structured in the crystal structure of SENP7, and its deletion produced important defects in the proteolytic activity of SENP7 (26). Loop 1 is unique to the SENP6 and SENP7 subclass, and the sequence alignment displays a high degree of sequence identity with respect to SENP6, with only one single amino acid substitution (Thr-690 for Ala) (Fig. 1*C*). A structural feature of Loop 1 is the presence of a short stretch of four proline residues, forming a poly-proline helix structure. A poly-proline helix is a type of secondary structure that restrains conformational flexibility of Loop 1, despite its lack of interactions with the core of the protease.

To determine the structural basis for the Loop 1 role in the proteolytic activity, we designed several mutant constructs of Loop 1 of SENP7. The first construct contained the substitution of the four consecutive prolines residues by glycines. The SENP7 (P686G/P687G/P688G/P689G) mutant will assess the role of Loop 1 in the activity of the protease by disrupting its spatial conformation. The introduction of four glycines increases the flexibility of the main chain of Loop 1 and could lead to a non-productive interaction with the SUMO substrates in activity assays. Loop 1 contains only one prominent charge residue at the center of it, Lys-691, which could be relevant by establishing polar interactions with SUMO substrates. We have designed two single point mutants, Lys-691 to Glu, to invert its charged properties, and Lys-691 to Ala, which removes both the basic ε-amino group and the aliphatic side chain.

SENP7 Loop 1 mutants were tested against diSUMO2 and polySUMO2 chains substrates by using time course deconjugation analysis (Fig. 1, *D* and *G*). Deletion of Loop 1 seriously compromises the proteolytic activity of SENP7 as described previously (26). The SENP7 Loop 1 mutant construct of four prolines to glycines (Fig. 1, SENP7, P686G/P687G/P688G/P689G), which would increase the flexibility of Loop 1, reduces the proteolytic activity of SENP7 as much as deletion of the whole Loop 1 does. SENP7 single point mutant of Lys-691 to glutamic acid (SENP7(K691E) in Fig. 1) also dramatically reduces the proteolytic activity of the protease. Finally, the SENP7 single point mutant of Lys-691 to alanine (SENP7(K691A) in Fig. 1) has a reduction of the proteolytic activity to a lesser degree compared with the other constructs. To estimate the differences in the activity, initial rate velocities were measured for the diSUMO2 deconjugation reaction at 0.5 nM of final enzyme concentration (Fig. 1, *E* and *F*). Deconjugation rates for SENP7 wild type are −10–20-fold faster than SENP7-ΔLoop 1, SENP7(K691E), and SENP7(P686G/P687G/P688G/P689G), whereas for SENP7(K691A), the activity reduction is not so marked compared with the other mutant constructs.

These biochemical analyses with the SENP7 mutant constructs reveal that both the spatial conformation of Loop 1 and the charge properties of Lys-691 are important for a productive interaction of SENP7 with SUMO2 and thus for the correct cleavage of SUMO substrates. It is worth noting that Loop 1 only represents a small region of the total interface of SENP7 and SENP6 with SUMO and that it is not present in the other members of the mammalian SENP family. Loop 1 interaction with SUMO has not been described previously, and our data indicate that it can enhance the proteolytic activity for SENP6 and SENP7. Our next step was to figure out the putative surface region in SUMO that directly interacts with Loop 1 of SENP6 and SENP7.

Loop 1 SENP7 Interaction with SUMO2—Based on previous structures of the complexes of SENP2 with either SUMO1 or SUMO2 (19, 20), we have predicted a region on the SUMO surface that is located close to Loop 1 of SENP6 and SENP7. Crystal structures of the complex between SENP1, SENP2, or ULP1 with SUMO indicate that the main residues involved in

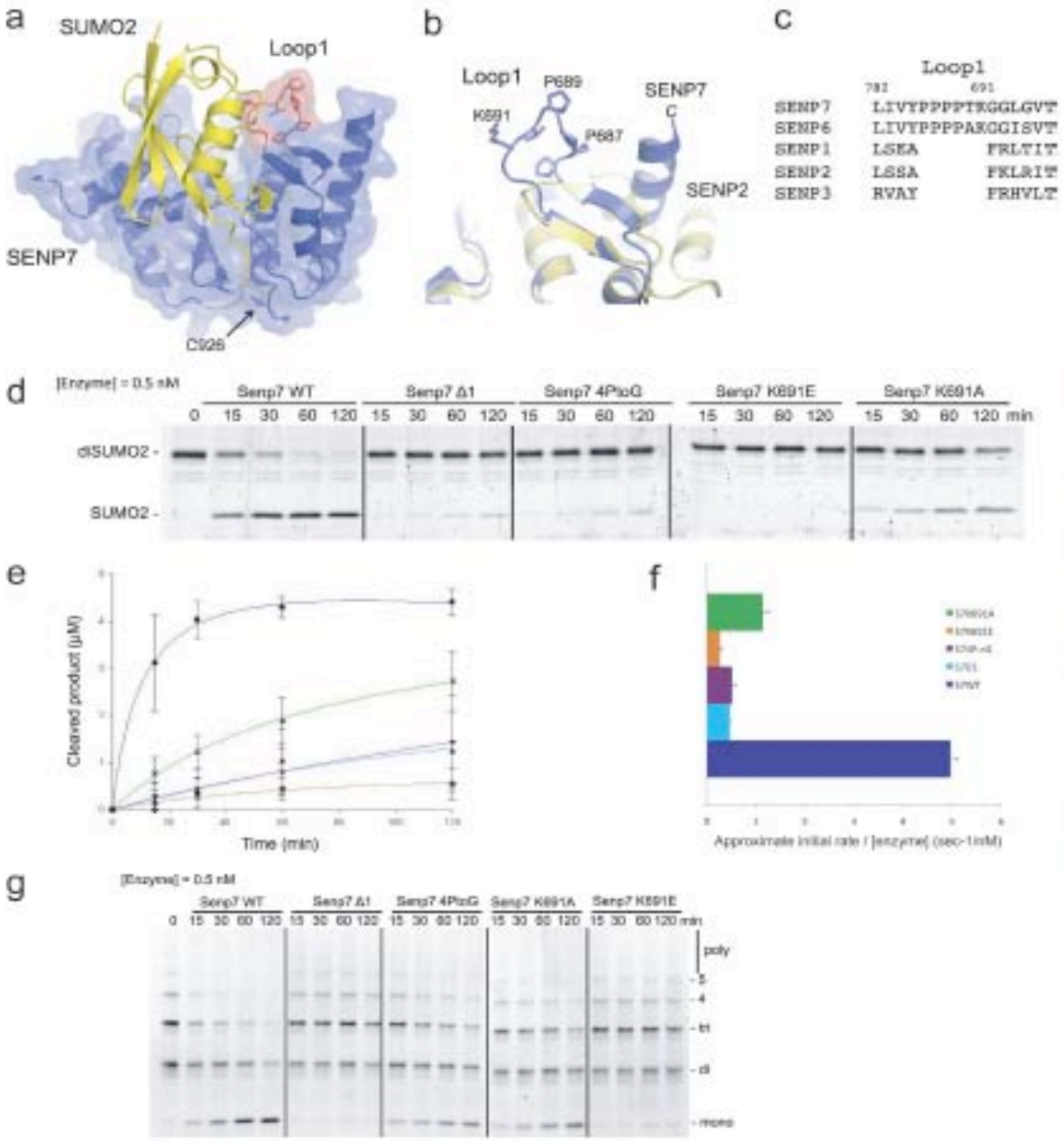

FIGURE 1. **Deconjugation analysis of Loop 1 mutant constructs in SENP7.** *a* and *b*, superposition of SENP2 and SENP7 catalytic domains in pink and blue, respectively. The position of SUMO2 is indicated schematically based on SUMO2 in complex with SENP2 (Protein Data Bank code 2IO0). SENP7 Loop 1 is indicated in red to highlight the relative position in respect to the entire protease. Key residues are highlighted in stick representation and labeled accordingly. *c*, sequence alignment of SENP proteases based on structural similarity highlighting Loop 1 insertion in SENP6 and -7. *d* and *g*, deconjugation assays of SENP7 and associated mutants at 0.5 nM enzyme concentration against diSUMO2 and polySUMO2, respectively. Assays were run were run at time intervals indicated above each lane in minutes. *e*, kinetic analysis of deconjugation of diSUMO2 by SENP7 and associated mutants taken at 0, 15, 30, 60, and 120 min. *f*, bar representation of approximate initial rate velocities for deconjugation of diSUMO2 determined within a linear range from data obtained from *e*. Axes are labeled, and error bars were obtained by conducting assays in triplicate.

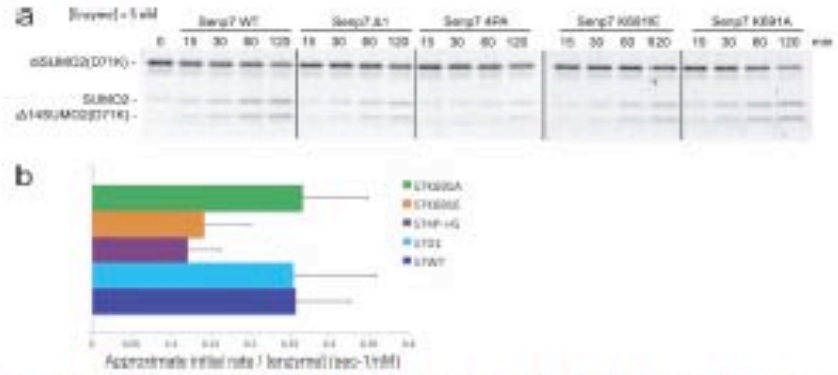

FIGURE 2. **Deconjugation of diSUMO2(D71K) with SENP7 Loop 1 mutant constructs.** *a*, deconjugation assays of SENP7 and associated mutants against diSUMO2(D71K). Assays were run at 5 nM enzyme concentration, and time intervals are indicated *above each lane* in minutes. *b*, bar representation of approximate initial rate velocities for deconjugation of diSUMO2(D71K) determined within a linear range based on data obtained from kinetic analysis taken at 0, 15, 30, 60, and 120 min (not shown). *Axes* are labeled, and *error bars* were obtained by conducting assays in triplicate.

the interface and in the catalysis are conserved for all members of the SENP/ULP protease family. Thus, despite the lack of a crystal structure of the complex, we assume that the extended quilt-like interface observed between SUMO and SENP2 is going to be conserved for the SENP6 and SENP7 complexes. Our structural model indicates that a slight conformational move can place Loop 1 close to a SUMO surface region. This surface seems to be more negatively charged for the SUMO2 isoform compared with SUMO1 (see Fig. 3, *A* and *B*). Thus, the disruption of this interface would be responsible for the SENP7 proteolytic defects described in Fig. 1.

To investigate this region, we have produced a single point mutation in SUMO2 of Asp-71 for lysine, which could interfere with the positive charge created by the side chain of Lys-691 of Loop 1 of SENP7. We were able to synthesize diSUMO2 with SUMO2(D71K) as a substrate for deconjugation assays. Time course proteolytic cleavage of diSUMO2(D71K) substrate shows a decrease in the proteolytic activity for all SENP7 constructs tested, including the wild type form (Fig. 2*A*). Time course deconjugation reactions were run at 5 nM final enzyme concentrations, one order of magnitude higher than the experiments in Fig. 1*D*. Particularly interesting is the loss of proteolytic activity in SENP7 wild type that becomes as defective as all Loop 1 mutant constructs (Fig. 2, *A* and *B*). It is worthwhile to mention that just a single change of charge, Asp-71 for lysine, on the surface of SUMO2 distant from the cleavage site can produce marked defects in the proteolytic activity of SENP7, with an approximately loss of 20-fold with respect to the diSUMO2 wild type reaction (see supplemental Fig. 1). These results support the formation of this novel and more extended interface between Loop 1 and SUMO2.

Deconjugation Analysis of SUMO Isoform Preference for SENP6 and SENP7—Different groups have reported a preferential proteolytic activity of SENP6 and SENP7 subclass for SUMO2/3 isoform (25–29, 34). We have predicted a novel interface involving Loop 1, unique to the SENP6 and SENP7 subclass, and SUMO, with different residues involved depending on the SUMO isoform type. We already showed that the Loop 1 interaction improves the catalytic activity for SENP6 and SENP7, and our next assessment was to check whether Loop 1 also had a role for the SUMO2/3 isoform preference. Based on a model of the complex between SENP7 and SUMO2, we analyzed the chemical nature of the residues of SUMO1 and SUMO2/3 in contact with Loop 1 of SENP7. We observed that the SUMO2/3 amino acid residues involved in the interface have a more polar nature when compared with the analogous SUMO1 residues, more specifically, Asp-71 (His in SUMO1) and Asn-68 (Ala in SUMO1) (Fig. 3, *A* and *B*). We wanted to investigate whether these residues could account for the SUMO2/3 isoform preference showed by SENP6 and SENP7 (26).

To test our hypothesis, we first produced SUMO2 with two point mutations, Asn-68 for Ala and Asp-71 for His, making a version of SUMO2 that resembles the SUMO1 interface with Loop 1 of SENP7. Similarly, we also produced SUMO1 with equivalent single point mutation positions used for SUMO2 double point mutant to revert the trend of the proteolytic reaction. Double point mutant SUMO2(N68A/D71H) and SUMO1(A72N/H75D) behaved similarly to wild type SUMO1 or SUMO2 during gel filtration and anion exchange purification, indicating that the two SUMO double mutants did not appear to present a barrier to protein folding. We also conjugated SUMO2(N68A/D71H) and SUMO1(A72N/H75D) to RanGAP1 to generate the canonical model substrate used in our deconjugation assays. The conjugation of double point SUMO mutants to RanGAP1 behaved similarly to the conjugation of wild type SUMO1 and SUMO2 (data not shown).

SENP6, SENP7, and SENP2 were first compared in deconjugation assays using wild type and double point mutants as substrates, namely RanGAP1-SUMO1, RanGAP1-SUMO2, RanGAP1-SUMO1(A72N/H75D), and RanGAP1-SUMO2(N68A/D71H) (Fig. 3*C*). Three different enzyme concentrations were used in the titration assays (0.5, 5, and 50 nM) in the presence of 3 μM of each RanGAP1-SUMO substrate. As observed in Fig. 3*C*, SENP2 is more active and does not discriminate between wild type and double point mutants of SUMO1 and SUMO2. However, in the case of SENP6, there is a noticeable reduction of activity for the SUMO2 double point mutant and an increase of activity for SUMO1 double point mutant. For SENP7, the

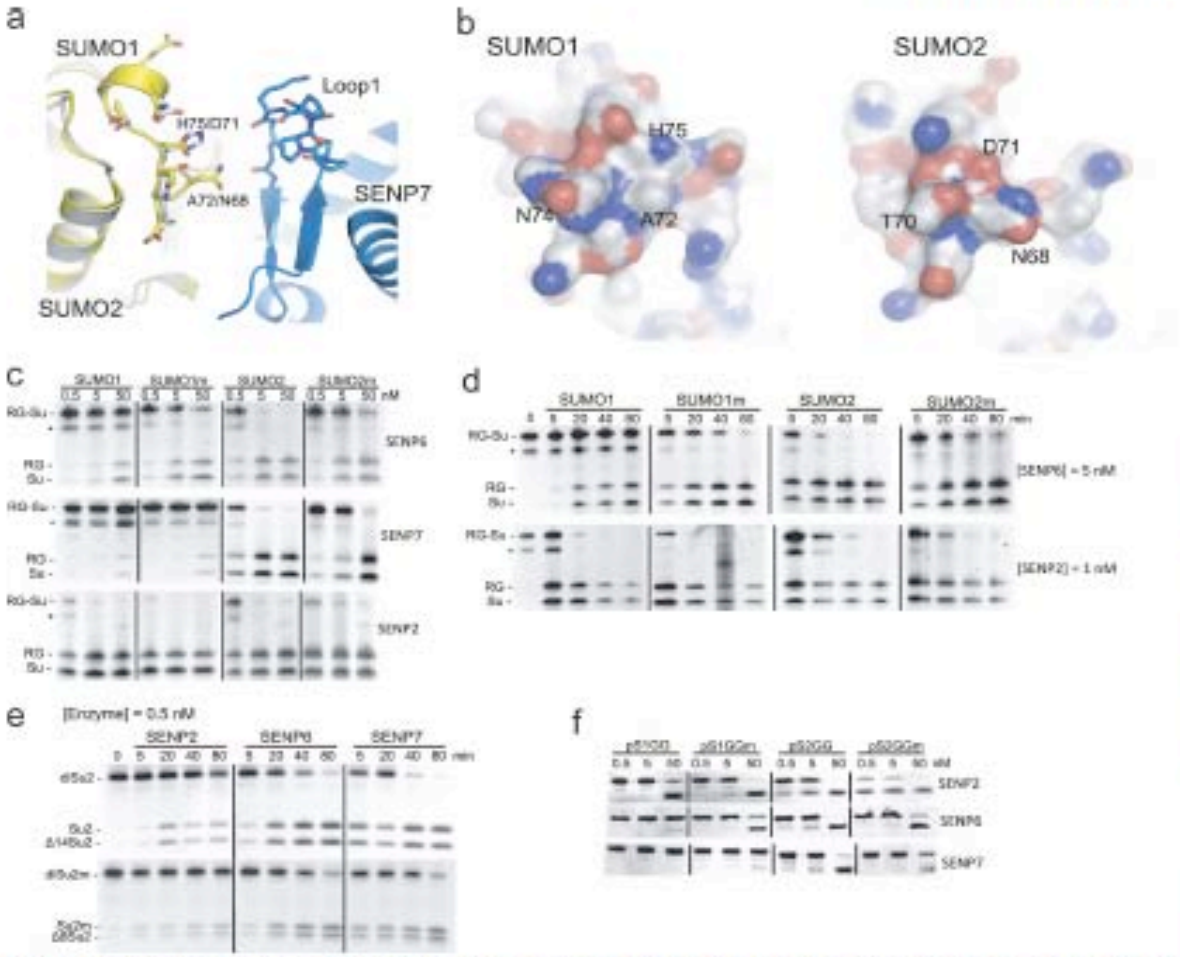

FIGURE 3. **SENP7-SUMO interaction models, processing and deconjugation activities of SUMO isoform mutants.** *a*, structural model of potential interaction sites between SENP7 (*blue ribbon*) and SUMO1 (*gray ribbon*) and SUMO2 (*yellow ribbon*). The positions of SUMO1 and SUMO2 are based on SUMO1 and -2 in complex with SENP2 (Protein Data Bank codes 1TH2 and 2IO0). Key residues in the SUMO-protease interface are indicated in stick representation and labeled according to their position and side chain composition in both SUMO and SENP7. *b*, electrostatic potential surface representation of SUMO1 and -2 to highlight differences within SENP7 Loop-1 possible interaction sites. All images were modified and represented using the respective Protein Data Bank codes in PyMOL (36). *c* and *d*, activity and time course assays, respectively, of deconjugation of SENP2, SENP6, and SENP7 against RanGAP1-SUMO1 (*RG-Su*), RanGAP1-SUMO1(A72N/H75D), RanGAP1-SUMO2, and RanGAP1-SUMO2(N68A/D71H). An *asterisk* indicates RanGAP1-SUMO degradation products. *e*, time course assay of deconjugation of SENP2, -6, and -7 against diSUMO2 (*di*Su2) and diSUMO2(N68A/D71H) (*di*Su2m). *f*, activity assay of processing of preSUMO1GGG$_1$G$_2$-*X*, preSUMO1GGG$_1$G$_2$-*X* (A72N/H75D), preSUMO2GGG$_1$G$_2$-*X*, and preSUMO2GGG$_1$G$_2$-*X*(N68A/D71H). Activity assays were run at 0.5, 5, and 50 nM enzyme concentration against 5 μM substrate concentration at 37 °C and stopped after 25 min with SDS loading buffer and analyzed via PAGE. Time course assays were run at 0.5 nM enzyme concentration, and time intervals are indicated *above each lane* in minutes. Proteins were detected by staining with SYPRO (Bio-Rad).

decrease in the activity of SUMO2 double point mutant is also appreciated, whereas for SUMO1 no activity is detected, as reported previously by different groups (28–29, 34). These differences are better appreciated in a time course deconjugation reaction, where all RanGAP1-SUMO constructs were substrates in pulse-chased reactions with either SENP2 at 1 nM or SENP6 at 5 nM (Fig. 3*D*). Time course results with SENP6 confirmed the reduction of proteolytic activity for RanGAP1-SUMO2(N68A/D71H) and the increase of activity for RanGAP1-SUMO1(A72N/H75D). In contrast SENP2, despite having a proteolytic activity one order of magnitude faster than SENP6, showed basically no differences between the wild type substrates and the double point mutants. As mentioned above, SENP2 does not contain the Loop 1 insertion in its sequence; thus, the unaltered SENP2 activities between SUMO isoforms could be explained by the lack of the interface between Loop 1 and SUMO.

As stated previously (25–27), SENP6 shows a low degree of proteolytic activity against SUMO1 substrates, in contrast to SUMO2/3, which is preferentially cleaved by the SENP6 and SENP7 family members. Interestingly, a gain of the SENP6 proteolytic activity with RanGAP1-SUMO1(A72N/H75D) com-

pared with RanGAP1-SUMO1 wild type is totally opposed to the loss of activity observed for RanGAP1-SUMO2(N68A/D71H) double point mutant (Fig. 3, *C* and *D*). SENP6 proteolytic activity against RanGAP1-SUMO1(A72N/H75D) is almost as efficient as with RanGAP1-SUMO2 wild type substrate, a striking result for a protease with a reported isoform preference for SUMO2/3 substrates. Thus, in addition to the enhancement of the proteolytic activity in the SENP6 and SENP7 subclass, the unique Loop 1 insertion has a prominent role in the discrimination between the two SUMO isoforms by these proteases.

SENP6 and SENP7 have been suggested to posses a major proteolytic activity for deconjugation of poly-SUMO2 chain substrates (24, 26), with an improved hydrolysis of the isopeptidic bond formed between SUMO2 Lys-11 and the C-terminal Gly-93 from the next SUMO2. We have designed a version of diSUMO2 where the donor SUMO2 contains the two mutations (N68A/D71H) and the acceptor SUMO2 contains a deletion of the C-terminal di-glycine motif to keep off poly-SUMO chain formation. In Fig. 3*E*, a time course deconjugation analysis has been run using SENP2, SENP6, and SENP7 at 0.5 nM. A trend similar to the RanGAP1-SUMO substrates is observed, and the differences between the proteolytic activity for diSUMO2 and diSUMO2(N68A/D71H) are also noticeable, with an activity reduction for the double point mutant of diSUMO2 for SENP6 and SENP7.

Processing Analysis of SUMO Isoform Preference for SENP6 and SENP7—Some groups have reported that the SENP6 and SENP7 subclass displayed poor proteolytic activities in the formation of the mature form of SUMO from their precursors (25–27). However, as described previously (26), addition of two glycine residues after the Gly-Gly motif improved maturation rates substantially for SENP7, minimizing the inhibitory effect of the C-terminal tail observed in the processing reaction (19). Thus, the substrates tested in the processing reactions were preSUMO1GGG$_1$G$_1$-*X*, preSUMO1GGG$_1$G$_1$-*X*(A72N/H75D), preSUMO2GGG$_1$G$_1$-*X*, and preSUMO2GGG$_1$G$_1$-*X*(N68A/D71H). (-*X* represents the natural C-terminal tail sequence for each SUMO isoform, and G$_1$ represents the glycine insertions.) Although the processing is not as efficient as the deconjugation reaction, differences between the wild type forms and the double point mutants can be appreciated in the titration analysis for SENP6 and SENP7 (Fig. 3*F*). A gain of proteolytic activity is observed for the maturation of the SUMO1 double point mutant precursor and a corresponding loss of activity for the SUMO2 double point mutant precursor, compared with their wild type forms. These results support the formation of similar enzyme-substrate complexes between SENP6 and SENP7 with the precursor forms of SUMO1 and SUMO2, and as observed for the deconjugation reaction, a prominent role for the Loop 1 insertion is observed. Interestingly, as observed in the deconjugation reactions, the processing activity for the maturation of SUMO1 precursor in SENP7 is much lower compared with SENP6, as previously stated (25, 26, 34).

SENP6 Loop-insertion Deletion Mutants—To further characterize the catalytic domain of SENP6, we produced three different constructs of SENP6 lacking the equivalent loop insertion sequences observed in the crystal structure of SENP7 (26), namely SENP6-ΔLoop 1, SENP6-ΔLoop 2, and SENP6-ΔLoop 3 (see "Experimental Procedures" for further sequence details). The amino acid sequence of Loop 1 from SENP6 is identical to the corresponding Loop 1 from SENP7, whereas for Loop 2 and Loop 3, the amino acid sequences between SENP6 and SENP7 are not homologous. Interestingly, SENP6 Loop 3 is ~150 residues long compared with SENP7 Loop 3, which is only 50 residues long. In the SENP7 crystal structure, Loop 2 and Loop 3 were disordered, and their removal did not produce any change in the proteolytic activity for all the substrates tested, in contrast to the SENP7 Loop 1 (Fig. 1).

We tested all SENP6 deletion mutants with our canonical model substrates, RanGAP1-SUMO (including the wild type and the double point mutant). In the titration analysis shown in Fig. 4*A* and supplemental Fig. 2, the SENP6-ΔLoop 1 mutant displays a loss of activity for all substrates under these conditions, whereas SENP6-ΔLoop 2 and SENP6-ΔLoop 3 mutants show a similar or higher activity with respect to the wild type form (compare with Fig. 3*C*). Particularly interesting is the increase in the proteolytic activity observed for the SENP6-ΔLoop 3 deletion mutant, which was not observed for SENP7 (26). This gain of proteolytic activity by deleting Loop 3 of SENP6 might be explained by a decrease in the total entropy of the system by removing an insertion of 150 amino acid residues, which is presumably not ordered in the SENP6 structure and could interfere in the correct binding of the substrate.

SENP6 deletion mutants were also run against RanGAP-SUMO1 and RanGAP-SUMO2 double point mutant substrates (Fig. 4*A*). SENP6-ΔLoop 2 and SENP6-ΔLoop 3 deletion mutants show the same trend in the proteolytic activity with the SUMO double point mutant substrates as observed for the SENP6 wild type form (Fig. 3), with an increase and a decrease in the proteolytic activity for SUMO1 and SUMO2 double point mutant, respectively. As stated before, the SENP6-ΔLoop 1 deletion mutant showed a reduced proteolytic activity with either the wild type or any of the double point mutant substrates tested. These results with SENP6 correlate well with the deletion mutant results for SENP7 (26), and support the role of the Loop 1 insertion in the enhancement of the proteolytic activity by the formation of an extended interface with SUMO.

Initial Rate Measurements for SENP6-ΔLoop 3 Mutant—To obtain a more quantitative assessment for the proteolytic differences between the SUMO substrates, initial rate velocities were measured using SENP6-ΔLoop 3 as the protease in both processing and deconjugation reactions. The SENP6-ΔLoop 3 deletion mutant was chosen due to the higher activity level compared with the wild type SENP6, as observed in Fig. 4*A*. Deconjugation assays were pulse chased up to 80 min using RanGAP1-SUMO1, RanGAP1-SUMO1(A72N/H75D), RanGAP1-SUMO2, and RanGAP1-SUMO2(N68A/D71H) substrates. Similarly, processing reactions were analyzed using preSUMO1GGG$_1$G$_1$-*X*, preSUMO1GGG$_1$G$_1$-*X*(A72N/H75D), preSUMO2GGG$_1$G$_1$-*X*, and preSUMO2GGG$_1$G$_1$-*X*(N68A/D71H) substrates (Fig. 4*B*). The enzyme concentration for the deconjugation and processing reaction was 1 and 5 nM, respectively. Enzyme concentrations were optimized in each instance to better estimate the initial rate velocities for each proteolytic reaction.

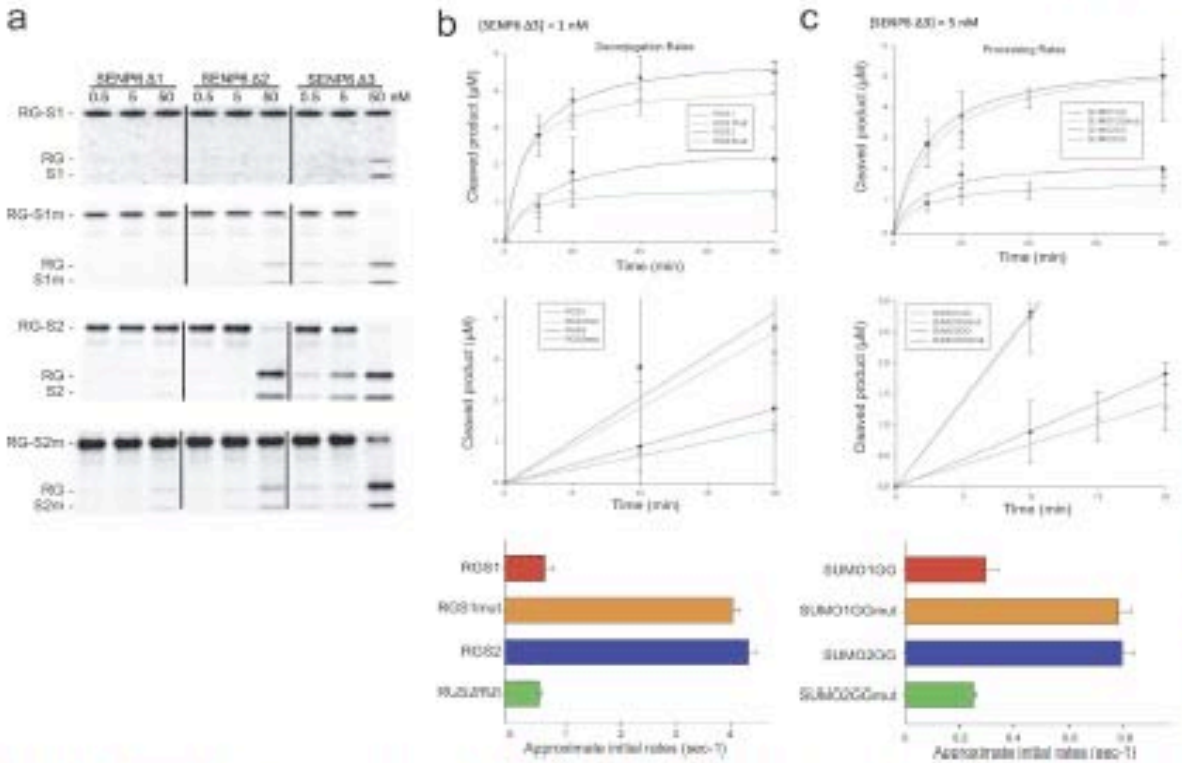

FIGURE 4. **Kinetic analysis for processing and deconjugation of SENP6 deletion mutants.** *a*, deconjugation reaction of RanGAP-SUMO1, RanGAP1-SUMO1(A72N/H75D), RanGAP1-SUMO2, and RanGAP1-SUMO2(N68A/D71H) by SENP6-ΔLoop 1, -ΔLoop 2, and -ΔLoop 3. Activity assays were run at 0.5, 5, and 50 nM enzyme concentration against 5 μM substrate concentration at 37 °C and stopped after 25 min with SDS loading buffer and analyzed via PAGE. Proteins were detected by staining with SYPRO (Bio-Rad). *b* and *c*, deconjugation and processing activity, respectively, of SENP6-ΔLoop 3, were taken at 0, 10, 20, 40, and 80 min; deconjugation and processing initial rate activity of SENP6-ΔLoop 3 were taken at 0, 10, 15, and 20 min; bar representation of initial rate velocities for deconjugation and processing of SENP6-ΔLoop 3 were determined within a linear range from data obtained from *b*. Axes are labeled, and error bars were obtained by conducting assays in triplicate.

As observed in Fig. 4*B*, the SUMO1(A72N/H75D) double point mutant increases the proteolytic activity of SENP6-ΔLoop 3 by an approximate order of 3- and 5-fold in both processing and deconjugation reactions, respectively. In contrast, the SUMO2(N68A/D71H) double point mutant decreases its proteolytic activity by an order of 4- and 6-fold in the processing and deconjugation reaction, with respect to the wild type SUMO2. Interestingly, the initial rates velocities measured for the SUMO1(A72N/H75D) double point mutant are quite similar to the initial rates velocities displayed by the SUMO2 wild type. These results confirm our previous data and indicate that the SUMO isoform preference displayed by SENP6 for SUMO2/3 can be modulated by swapping two single amino acid residues between SUMO1 and SUMO2/3.

Steady-state Kinetic Analysis of SUMO1 Mutants—To estimate the kinetic parameters of the contribution of this novel surface of SUMO to the proteolytic activity of SENP6 and SENP7 subclass, we developed a more quantitative activity assay using deconjugation substrates that are chemically modified with a fluorophore (Alexa Fluor 488). The maleimide group of Alexa Fluor 488 reacts covalently with cysteine residues. To develop this reagent we have produced a double mutant of SUMO1 with the substitutions of Ser-9 for cysteine and Cys-52 for alanine. SUMO1 (S9C/C52A) is modified with the fluorophore at the flexible N-terminal tail at position 9, which is not essential for activity. Although SUMO1 contains a cysteine residue buried in the hydrophobic core (Cys-52), it has been replaced by alanine to avoid a potential modification by the fluorophore that could affect the catalytic properties of the SUMO proteases. SUMO1 (S9C/C52A) was tested in conjugation assays and compared with SUMO1 wild type to assess that they both have similar catalytic properties (data not shown).

Deconjugation time-course reactions were run using fluorogenic RanGAP1-SUMO1 and RanGAP1-SUMO1(A72N/H75D) substrates with SENP2 and SENP6 at 1 and 25 nM, respectively (Fig. 5). As shown in previous results (Figs. 3 and 4), there is a clear gain of proteolytic activity for the SUMO1(A72N/H75D) double point mutant compared with SUMO1 wild type for SENP6, in contrast to SENP2 where the proteolytic activities for both substrates displayed only minor differences. A Michaelis-Menten representation of the initial velocities measured for a range of substrate concentration varying from 0.25 to 100 μM, displayed hyperbolic curves that allowed us to estimate the catalytic constants of the reaction (Fig. 5, *B* and *C*). Michaelis-Menten

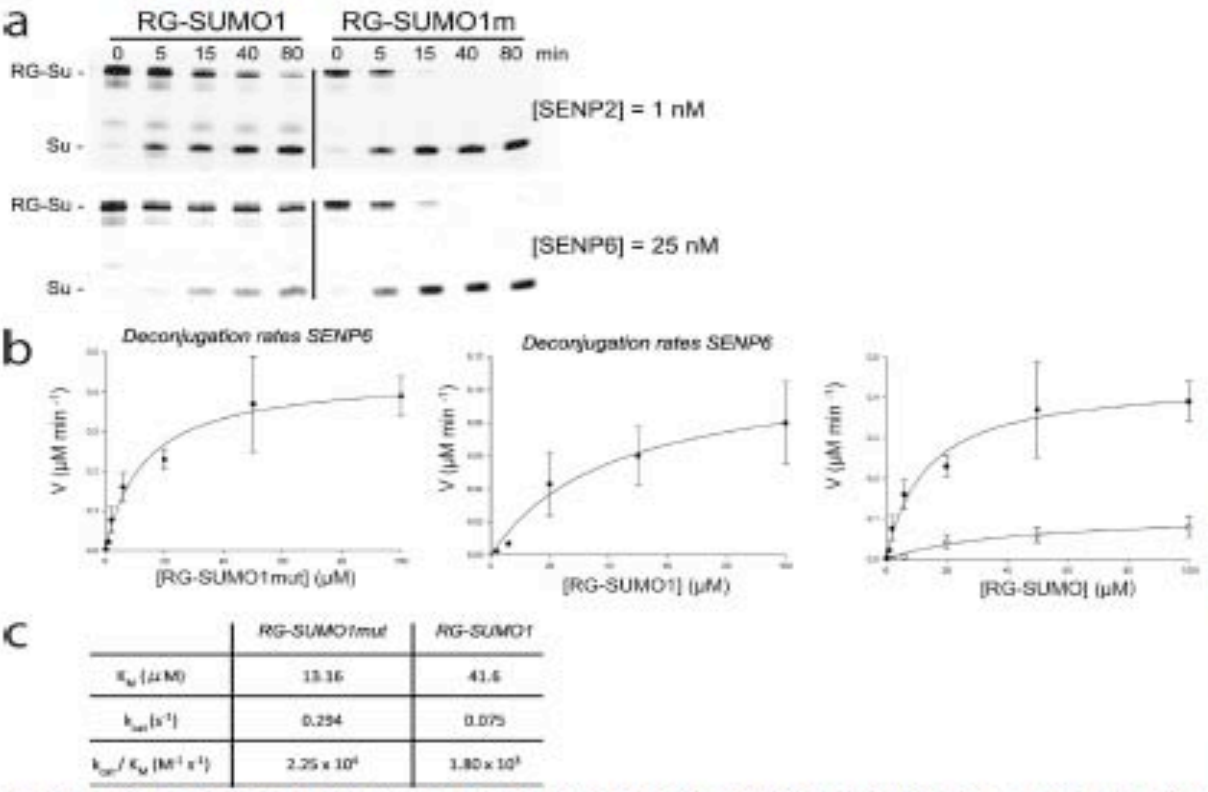

c

	RG-SUMO1mut	RG-SUMO1
K_M (μM)	13.16	41.6
k_{cat} (s^{-1})	0.294	0.075
k_{cat}/K_M ($M^{-1} s^{-1}$)	2.25×10^4	1.80×10^3

FIGURE 5. **Steady-state kinetics of the deconjugation reaction for RanGAP1-SUMO1 and RanGAP1-SUMO1mut by SENP6.** a, Deconjugation activity against RanGAP1-SUMO1 and RanGAP1-SUMO1(A72N/H75D) (RG-SUMO1m) with SENP6 and SENP2 at 25 and 1 nM concentrations, respectively. Both substrates are labeled with Alexa Fluor 488, and the kinetics was followed with a VersaDoc apparatus (Bio-Rad). b, Michaelis-Menten graphic representation of substrate concentration (μM) versus velocity (μM min^{-1}) at time intervals 0, 5, 15, 40, and 80 min for RanGAP1-SUMO1mut (*left*) and RanGAP1-SUMO1 (*middle*). *The right panel* depicts a comparison of the two graphs. Initial rate deconjugation activities were measured at five different substrate concentrations (0, 0.25, 1, 2, 6, 20, 50, and 100 μM) and at 25 nM SENP6 concentration. Reactions were stopped after intervals indicated above each lane in minutes with SDS loading buffer and analyzed by gel electrophoresis. c, table of the kinetic coefficients K_m, k_{cat}, and k_{cat}/K_m obtained from data in b for RanGAP1-SUMO1 and RanGAP1-SUMO1mut.

constants K_m were 41.6 and 13.16 μM for SUMO1 and SUMO1(A72N/H75D) substrates, respectively; whereas the catalytic constant k_{cat} were 0.075 and 0.294 s^{-1} for SUMO1 and SUMO1(A72N/H75D) substrates, respectively. The total gain of proteolytic activity by the SUMO1 double point mutant is ~12.5-fold, as estimated by the k_{cat}/K_m catalytic efficiency of the enzyme. Based on these results, this novel interface between Loop 1 of SENP6 and SENP7 and SUMO affects both the binding and the catalytic properties of the enzyme.

DISCUSSION

SENP6 and SENP7, the most divergent SUMO proteases of the SENP/ULP family with respect to the catalytic domain, contain sequence insertions in the catalytic domain whose removal compromises the proteolytic activity of the enzyme. In particular, deletion of the Loop 1 insertion in SENP6 and SENP7 results in a diminished activity in both processing and deconjugation reactions, whereas deletion of Loop 2 and Loop 3 display similar or even higher activities with respect to the wild type form (as observed for SENP6-ΔLoop 3). Biochemical and mutagenesis analysis on Loop 1 insertion reveal that both the structural conformation of the loop and the charge properties of the side chain of Lys-691 are basic for the correct proteolytic activities showed in the SENP7 reactions. In particular, the putative interaction with the SUMO surface of the ε-amino group of Lys-691 seems fundamental for a correct formation of the enzyme-substrate complex, and this interaction seems only to occur with a particular structural conformation of Loop 1. This property is restricted to SENP6 and SENP7 family members, because for the other members of the SENP/ULP family, the Loop 1 sequence is not present, and at least for SENP1 and SENP2, this lack of sequence does not suppose a constraint for their proteolytic activity (19, 21, 25, 34). Thus, we predict a more extended interface for SENP6 and SENP7 in the complex with SUMO, including the Loop 1 insertion present only in this subclass of SUMO proteases.

Several groups have reported that SENP6 and SENP7 preferred SUMO2/3 as substrates in deconjugation and processing reactions (25–27). The specificity of the SENP family members for the different SUMO isoforms is largely based on contacts at

the interface of the SENP and SUMO structures. A structural model based on the crystal structure of the interaction of SENP2 with SUMO2 suggests a region of SUMO that could interact with the Loop 1 of SENP7. In particular, in our model, the locations of residues Asp-71 and Asn-68 in the structure of SUMO2 are in a short contact distance with Loop 1 of SENP7, presumably by establishing polar interactions. Substitution of these residues by the corresponding SUMO1 residues histidine and alanine, respectively, reduce the protease activity for all of the substrates tested. Interestingly, when we swap the corresponding SUMO1 residues with residues from SUMO2, a notable gain of proteolytic activity can be observed for all SUMO1 substrates tested, and in some instances becomes as active as with the SUMO2 substrate and thus reverts the isoform preference of SENP6 and SENP7.

This novel SUMO interface is only relevant for the SENP6 and SENP7 family members because these are the only SUMO proteases with a Loop 1 insertion in their catalytic domains. For the other members of the SENP/ULP protease family, SENP3 and SENP5 have also been reported to have a strong selectivity for SUMO2/3, but in this case, a different region in the SUMO surface may account for such activity. However, we cannot rule out the possibility of the formation of a similar Loop 1 structure due to the lack of structural information for SENP3 and SENP5 catalytic domains. This is in contrast to SENP1 and SENP2 catalytic domains, where SUMO isoform differences for the deconjugation reaction are minor (19, 21). In the SUMO maturation reaction, it has been reported that the two residues in the C-terminal tail immediately following the cleavage site were responsible for the SENP1 and SENP2 isoform preference (19, 21, 35). A recent study confirmed the different SUMO isoform specificities shown in the human SENP/ULP family by using SUMO-vinyl sulfone adducts for *in vivo* experiments and SUMO-amidomethyl coumarin as substrates (36). In this study, a similar SUMO2/3 isoform preference for the SENP6 and SENP7 catalytic domains is confirmed, and interestingly, it is suggested that the N-terminal domain of some SUMO proteases can influence their paralog specificity (34).

The SENP6 and SENP7 subclass of the SENP/ULP family are the most divergent with respect to their catalytic domain. In this study, we have identified a region in the SUMO surface that is responsible for the SUMO isoform preference for SUMO2/3 displayed by this subclass of SUMO proteases. Single point mutagenesis in this region can swap their SUMO isoform preference between SUMO2/3 and SUMO1. The disclosure of this region reveals important insights into the biochemical and structural biology of the SUMO deconjugation reaction, and it can lead to the development of valuable tools for studying the SUMO isoform specificity inside of the cell. Although additional structural work will be required to describe in detail the physical basis of this novel SUMO-SENP interface, our biochemical and mutagenesis experiments suggest how SENP6 and SENP7 are able to discern between SUMO1 and SUMO2/3 isoforms.

Acknowledgment—We acknowledge Christopher D. Lima for reagents and support.

REFERENCES

1. Hershko, A., and Ciechanover, A. (1998) *Ann. Rev. Biochem.* **67**, 425–479
2. Kerscher, O., Felberbaum, R., and Hochstrasser, M. (2006) *Annu. Rev. Cell Dev. Biol.* **22**, 159–180
3. Geiss-Friedlander, R., and Melchior, F. (2007) *Nat. Rev. Mol. Cell Biol.* **8**, 947–956
4. Johnson, E. S. (2004) *Annu. Rev. Biochem.* **73**, 355–382
5. Mukhopadhyay, D., and Dasso, M. (2007) *Trends Biochem. Sci.* **32**, 286–295
6. Owerbach, D. A., McKay, E. M., Yeh, E. T., Gabbay, K. M., and Soboeiro, K. M. (2005) *Biochem. Biophys. Res. Commun.* **337**, 517–520
7. Vertegaal, A. C., Andersen, J. S., Ogg, S. C., Hay, R. T., Mann, M., and Lamond, A. I. (2006) *Mol. Cell. Proteomics* **5**, 2298–2310
8. Ayaydin, F., and Dasso, M. (2004) *Mol. Biol. Cell* **15**, 5208–5218
9. Garcia, J., and Lima, C. D. (2011) *Nat. Rev. Mol. Cell Biol.* **12**, 861–871
10. Bossis, G., and Melchior, F. (2006) *Mol. Cell* **21**, 349–357
11. Knipscheer, P., and Sixma, T. K. (2007) *Curr. Opin. Struct. Biol.* **6**, 665–673
12. Mattic, I., van Hagen, M., Schimmel, J., Macek, B., Ogg, S. C., Tatham, M. H., Hay, R. T., Lamond, A. I., Mann, M., and Vertegaal, A. C. (2008) *Mol. Cell. Proteomics* **7**, 132–144
13. Tatham, M. H., Jaffray, E., Vaughan, O. A., Desterro, J. M., Botting, C. H., Naismith, J. H., and Hay, R. T. (2001) *J. Biol. Chem.* **276**, 35368–35374
14. Fu, C., Ahmed, K., Ding, H., Ding, X., Lan, J., Yang, Z., Miao, Y., Zhu, Y., Shi, Y., Zhu, J., Huang, H., and Yao, X. (2005) *Oncogene* **24**, 5403–5413
15. Tatham, M. H., Geoffroy, M. C., Shen, L., Plechanovova, A., Hattersley, N., Jaffray, E. G., Palvimo, J. J., and Hay, R. T. (2008) *Nat. Cell Biol.* **10**, 538–546
16. Békés, M., Prudden, J., Srikumar, T., Raught, B., Boddy, M. N., Salvesen, G. S. (2011) *J. Biol. Chem.* **286**, 10258–10267
17. Lallemand-Breitenbach, V., Jeanne, M., Benhenda, S., Nasr, R., Lei, M., Peres, L., Zhou, J., Zhu, J., Raught, B., and de Thé, H. (2008) *Nat. Cell Biol.* **10**, 547–555
18. Mossessova, E., and Lima, C. D. (2000) *Mol. Cell* **5**, 865–876
19. Reverter, D., and Lima, C. D. (2004) *Structure* **12**, 1519–1531
20. Reverter, D., and Lima, C. D. (2006) *Nat. Struct. Mol. Biol.* **13**, 1060–1068
21. Shen, L. N., Dong, C., Liu, H., Naismith, J. H., and Hay, R. T. (2006) *Biochem. J.* **397**, 279–288
22. Shen, L., Tatham, M. H., Dong, C., Zagórska, A., Naismith, J. H., and Hay, R. T. (2006) *Nat. Struct. Mol. Biol.* **13**, 1069–1077
23. Xu, Z., Chua, S. P., Lam, K. H., Chan, H. Y., Ng, T. B., and Au, S. W. (2006) *Biochem. J.* **398**, 345–352
24. Mukhopadhyay, D., Ayaydin, F., Kolli, N., Tan, S. H., Anan, T., Kamitani, A., Azuma, Y., Wilkinson, K. D., and Dasso, M. (2006) *J. Cell Biol.* **174**, 939–949
25. Mikolajczyk, J., Drag, M., Békés, M., Cao, J. T., Ronai, Z., and Salvesen, G. S. (2007) *J. Biol. Chem.* **282**, 26217–26224
26. Lima, C. D., and Reverter, D. (2008) *J. Biol. Chem.* **283**, 32045–32055
27. Shen, L. N., Geoffroy, M. C., Jaffray, E. G., and Hay, R. T. (2009) *Biochem. J.* **421**, 223–230
28. Di Bacco, A., Ouyang, J., Lee, H. Y., Catic, A., Ploegh, H., and Gill, G. (2006) *Mol. Cell. Biol.* **26**, 4489–4498
29. Gong, L., and Yeh, E. T. (2006) *J. Biol. Chem.* **281**, 15869–15877
30. Zhang, H., Saitoh, H., and Matunis, M. J. (2002) *Mol. Cell. Biol.* **22**, 6498–6508
31. Itahana, Y., Yeh, E. T., and Zhang, Y. (2006) *Mol. Cell. Biol.* **26**, 4675–4689
32. Mukhopadhyay, D., Arnaoutov, A., and Dasso, M. (2010) *J. Cell Biol.* **188**, 681–692
33. Reverter, D., and Lima, C. D. (2009) *Methods Mol. Biol.* **497**, 225–239
34. Kolli, N., Mikolajczyk, J., Drag, M., Mukhopadhyay, D., Moffatt, N., Dasso, M., Salvesen, G., and Wilkinson, K. D. (2010) *Biochem. J.* **430**, 335–344
35. Xu, Z., and Au, S. W. (2005) *Biochem. J.* **386**, 325–330
36. DeLano, W. L. (2010) *The PyMOL Molecular Graphics System*, version 0.99rc6, Schrödinger, LLC, New York

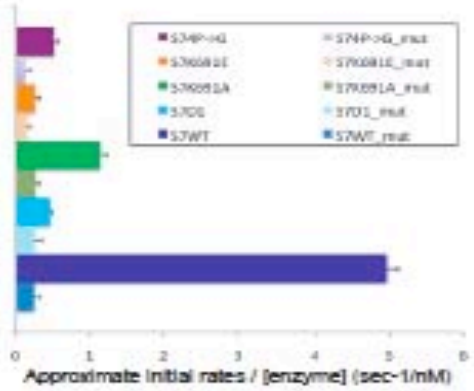

Supplementary figure 1. Bar table of the comparison of the approximate initial rates for the deconjugation reaction of the diSUMO2 and diSUMO2(D71K) with SENP7 wild type and mutants. This figure is based on results of figures 1F and 2B.

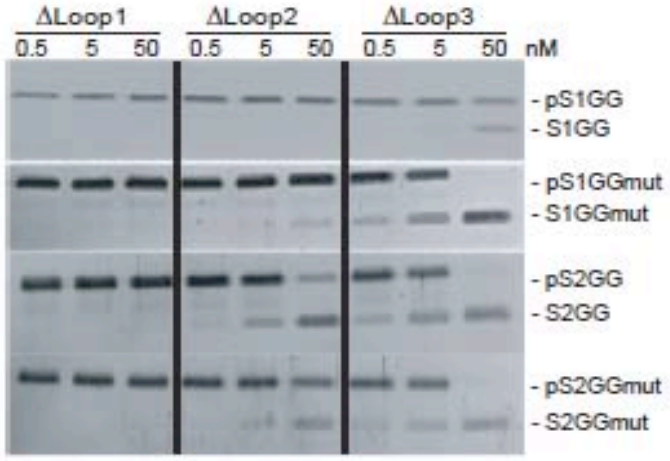

Supplementary figure 2. End point processing reaction for preSUMO1GG (pS1GG), preSUMO1GG(A72N/H75D) (pS1GGmut), preSUMO2GG (pS2GG) and preSUMO2GG (N68A/D71H) (pS2GGmut) with deletion loop mutants of SENP6 (ΔLoop1, ΔLoop2 and ΔLoop3). Reactions were run for 15 minutes at 37 C and stopped with SDS-PAGE loading buffer. Gel was stained with SYPRO.

Summary of SENP Activities

Table 1. Summary of observed catalytic activities of SENP2, SENP6 and SENP7

SENP isoform	S2/S2ins*	S6	S7
pS1GG	++++	-	-
pS1GGmut	+++	+/-	-
pS2GG	+++	+	+
pS2GGmut	+++	+/-	+/-
RGS1	++++	+/-	+/-
RGS1mut	++++	+	+
RGS2	++++	++	++
RGS2mut	++++	+	+
diSUMO2	++	++++	++++
diSUMO2	++++*	-	-
diSUMO2mut	++	++	++
diSUMO2/1	+	-	x

Table 2. Summary of observed catalytic activities of SENP6 deletion mutants

SENP isoform	S7	S7□1	S74P G	S7K691E	S7K691A
diSUMO2	++++	-	+/-	-	++
diSUMO2 (D71K)	+	-	-	-	+

polySUMO2	++++	-	+	-	+

SENP isoform	S7	S7Δ1	S74P G	S7K691E	S7K691A
diSUMO2	++++	-	+/-	-	++
diSUMO2 (D71K)	+	-	-	-	+
polySUMO2	++++	-	+	-	+

Table 3.

Summary of observed catalytic activities of SENP7 Loop1 mutants

Summary of Present Investigation in English

Swapping the SUMO Isoform Specificity of SENP6/7

SENP6 and SENP7 are the most divergent members in the SENP family of proteases and they are the only members that bear four loop insertions dispersed throughout their catalytic domains. The superposition of the SENP7 catalytic domain with the SENP2-SUMO complex revealed a tentative SENP7 Loop1-SUMO interface and upon further inspection, distinct residues on SUMO1 and SUMO2 were identified at the interface. A series of mutants were constructed bearing characteristics of both SUMOs and by swapping the residues from SUMO1 to SUMO2 and vice versus we were able to both decrease and increase the activity of the SENP6 and SENP7 toward these substrates.

Loop1 SENP6/7 Is Responsible For SUMO Interface Specificity

In addition to mutations on SUMO we constructed a series of mutations on SENP7-Loop1 within the tentative SENP7-Loop1-SUMO interface to determine the structural and functional roles of the residues that reside within this region. We were able to recover some of the activity lost by the removal of Loop1 by replacing the four prolines of Loop1 with glycines proving that Loop1 plays at least a structural role in SUMO recognition. We also identified Lys691 of Loop1 in SENP7 as indispensible to the activity of the enzyme. D71 is one of the residues proposed to confer SUMO2/3 specificity in the previous swapping experiments. We mutated this residue in diSUMO2 and saw a decrease in activity of SENP7. This could be explained by our theory that this region on SUMO is interacting with Loop1, more specifically K691, and the decrease in activity was caused by a charge clash between SUMO2 and SENP7 Loop1.

To further show the utility of Loop1 in deconjugation of multi-SUMOylated species we inserted the eight residues of SENP6 Loop1 into SENP2. We saw an overall increase in activity of SENP2 against diSUMO2 but not against any other substrate tested.

Complexes With Substrates

In order to see if SENP6 was able to form any stable complexes in solution, we produced milligram amounts of □3SENP6CS and □2□3SENP6CS (the two constructs of the protein that showed both good yields in protein

production and high performance in activity assay). We incubated each protease with SUMO precursors, RanGAP1-SUMO2 and diSUMO2 substrates. Of all the substrates tested, only diSUMO was able to form a stable complex with Δ3SENP6CS and Δ2Δ3SENP6CS. Δ2SENP6CS was also tested but there was no indication of any complex formation, leading to the hypothesis that SENP6 Loop3 was impeding, perhaps entropically, the ability of SENP6 to form a stable complex with diSUMO2.

SENP6 Loop3 Characterization

Loop3 takes up roughly 40% and 20% of the catalytic domains of SENP6 and SENP7 respectively. In our loop deletion experiments we saw an overall increase in the activity when Loop3 was not present and removal of Loop3 proved vital to the ability of the enzyme to form a stable complex with diSUMO2. In order to try to decipher what role this loop plays in the context of the protease, we isolated the 184 insert from SENP6 and produced and purified the protein. 1-H 1-D NMR pointed to an overall lack of tertiary structure within the loop but limited proteolysis and mass spectrometry analyses showed a stable fragment of around 11kDa. Further circular dichroism and Fourier Transform Infrared Spectroscopy suggested the presence of some secondary structural elements but overall characterization of SENP6 Loop3 showed a mainly unstructured loop.

Resumen de trabajo en español

Intercambiar la especifidad de las isoformas de SUMO1 y SUMO2/3 para SENP6/SENP7

SENP6 y SENP7 son los miembros más divergentes de la familia de proteasas SENP y los únicos miembros que llevan cuatro inserciónes o "loops" localizadas en su dominio catalítico. Al sobreponer el dominio catalítico de SENP7 sobre el complejo SENP2-SUMO podemos ver una posible interfaz entre el Loop1 de SENP7 y SUMO. También identificamos diferentes residuos de SUMO1 y SUMO2 que podrían formar parte de la interfaz. Diseñamos una serie de mutantes de SUMO1 y SUMO2 donde se intercambian entre ellos los residuos que forman parte de la interfaz. De esta manera fuimos capaces de intercambiar la actividad proteolítica de SENP6 y SENP7 hacia estos substratos.

El Loop1 de SENP6 y SENP7 es responsable de la especificidad de la interfaz entre los SUMOs y las SENP6/7

Diseñamos una serie de mutantes del Loop1 de SENP7 dentro de la posible interfaz entre el Loop1 de SENP7 y SUMO para determinar los papeles estructurales y funcionales de los residuos que están dentro de esta región. Los mutantes de SENP6/7 sin el Loop1 perdían gran parte de su actividad, esta se podía recuperar un poco al reemplazar las cuatro prolinas del Loop1 por glicinas. De esta manera probamos que el Loop1 tiene un papel por lo menos estructural en el reconocimiento de SUMO. También identificamos el residuo Lys691 del Loop1 de SENP7 como elemento indispensable en la actividad de la enzima ya que al mutar este residuo por un aspártico disminuye la actividad para sustratos con SUMO2. Por otra parte el residuo Asp71 de SUMO2 es uno de los residuos

propuestos para el reconocimiento de SUMO2/3. Cuando mutamos este residuo a lisina, vemos una bajada en la actividad de SENP7. Este hecho sugiere que Asp71 de SUMO2 está interaccionando con Loop1 y quizas con la Lys691, y que la bajada en la actividad es causada por una repulsión de cargas.

Por otro lado con el objectivo de estudiar el efecto de Loop1 en la desconjugación de especies SUMOyladas, insertamos los ocho residuos de SENP6 Loop en el dominio catalítico de SENP2. Esta inserción provoca un aumento de la actividad sustancial de SENP2 contra diSUMO en comparación con la forma wild type.

Complejos con substratos

Para ver si SENP6 es capaz de formar algún complejo estable, producimos cantidades en miligramos de los mutantes inactivos de Δ3SENP6C1030S y de Δ2Δ3SENP6C1030S. Incubamos cada proteasa con los precursors de SUMO, con RanGAP1-SUMO2 y con diSUMO2. De todos los substratos que probamos, diSUMO2 fue el único que podía formar un complejo estable con Δ3SENP6CS y Δ2Δ3SENP6CS por copurificación en una columna de gel fitración. Con Δ2SENP6CS no pudimos formar ningún complejo. Con esta información llegamos a la conclusión que el Loop3 de SENP6 reduce, quizá por razones de entropía, la capacidad de SENP6 de formar un complejo estable con diSUMO2.

Caracterización del Loop3 de SENP6

Para descifrar el papel que este loop tiene en el contexto de la proteasa, producimos y purificamos los 185 residuos de Loop3 de SENP6. Analysis 1-H 1-D RMN mostraba una falta de estructura terciaria dentro del loop, pero proteólisis limitada y espectroscopia de masas mostraban un fragmento estable de cerca de 11kDa. Dicroísmo circular y FTIR tambien sugieren la presencia de algunos elementos de estructura secundaria. Globalmente, la caracterización biofísica del Loop3 de SENP6 muestra que el loop es una proteína desestructurada.